SEPT.-DEC. 2004
Volume X Number III
ISSN 0859 144X

THE ASEAN JOURNAL OF RADIOLOGY

Published by The Radiological Society and
The Royal College of Radiologists of Thailand,
Bangkok, Thailand

Started through an educational grant from Bracco since 1995

THE IMAGE OF INNOVATION

SEPT.-DEC. 2004
Volume X Number III

ISSN 0859 144X

THE ASEAN JOURNAL OF RADIOLOGY

Published by The Radiological Society and
The Royal College of Radiologists of Thailand,
Bangkok, Thailand

Started through an educational grant from Bracco since 1995

www.bracco.com

Chief Editor

Professor Kawee Tungsubutra
Kaweevej Hospital, 318 Taksin Road, Dhonburi, Bangkok 10600, Thailand.

Asean Journal of Radiology.
Instructions for Authors.

1. The Asean Journal of Radiology publishes the papers on Radiological Sciences, such as research work, review articles, case reports, innovations in Medical Sciences related to all branches of Radiology, and letters to the editor. The aforementioned materials can be written in English only.

2. The authors have to submit 2 copies of the manuscript and a diskette: **to Prof. Dr. Kawee Tungsubuttra.** 318 Kaweevej Hospital, Taksin Road, Dhonburi, Bangkok 10600, Thailand.

3. The original copy to be submitted must be typed in a double space on one side of the page of 8.1/2" x 11.1/2" paper.

4. The format of the article must include :

a. Title page and address of the author (s)
b. Abstract
c. Introduction (Background)
d. Material and Method
e. Results and discussion (Tables and Illustrations)
f. Acknowledgement (if any)
g. References (Follow the Vancouver style developed by ICMJE)

5. We will provide 5 copies of reprints for the author (s) who submit (s) an article for publication in the Asean Journal.

6. The illustrations and tables must be clearly prepared with legends in English as they are the art works to be reproduced.

7. The authors are reponsible for the contents of the article as to its facts and findings.

8. Ethics.

Paper reporting studies which might be interpreted as human experimentation (e.g. controlled trials) should conform to the standards of the Declaration of Helsinki (see British Medical Journal 1964:2:177) and should indicate that, approval that such studies may proceed, has been granted by the local or hospital Ethics Committee.

When reporting experiments on animals indicate whether the institution's or the National Research Council's guide for, or any national law on, the care and use of laboratory animals was followed.

THE ASEAN JOURNAL OF RADIOLOGY

Volume X Number III SEPT.-DEC. 2004

CONTENTS

		Page
1.	INFECTIONS OF THE BRAIN AND NERVOUS SYSTEM AS DIAGNOSED BY CT. AND MRI. Vallop LOAPAIBUL, Kawee TUNGSUBUTRA	163-176
2.	CONGENITAL ANOMALY OF HEAD AND NERVOUS SYSTEM COMMONLY FOUND IN THAILAND Vallop LOAPAIBUL, Kawee TUNGSUBUTRA	177-184
3.	BRAIN TUMOURS SYSTEMIC CLASSIFICATION AND DIAGONSIS BY CT. AND MRI. Vallop LOAPAIBUL, Kawee TUNGSUBUTRA	185-198
4.	PITUICYTOMA; BENIGN SPINDLE CELL TUMOR OF POSTERIOR PITUITARY GLAND: A CASE REPORT Hungspreug, Phudhichareonrat, Leum-udom	199-204
5.	CHORDOID MENINGIOMA: A case report. Noppaklao ITTIPHANITPHONG	205-210
6.	CASE SERIES: COMPENSATED HYPOTHYROIDISM PRESENTED AS SIMPLE GOITRE Dr. M.A. Taher	211-212
7.	CASE SERIES: LIVER ABSCESSES MIMICKING NEOPLASMS AND RUPTURED INTO ANTERIOR ABDOMINAL WALL AND PLEURAL CAVITY Dr. M.A. Taher	213-215
8.	ACUTE ABDOMEN DUE TO DEAD WORM IN GALL BLADDER Dr. M.A. Taher	217-218
9.	ROLE OF ULTRASONOGRAPHY IN DIAGNOSIS OF INFANTILE HYPERTROPHIC PYLORIC STENOSIS-A PRELIMINARY WORK IN THE NORTHERN PART OF BANGLADESH Dr. Md.Murshed Ali, Dr. Md.Jafrul Hannan, Dr. Kazi Habibur Rahman, Dr. Md.Rezaul Karim	219-222

THE ASEAN JOURNAL OF RADIOLOGY

Volume X Number III SEPT.-DEC. 2004

CONTENTS

		Page
10.	ISOTOPE RENOGRAM IN ECTOPIC KIDNEY Dr. M.A. Taher	223-224
11.	ROLE OF PREOPERATIVE ULTRASONOGRAPHY IN IDENTIFYING POTENTIAL PROBLEMS IN LAPAROSCOPIC CHOLECYSTECTOMY. Dr. Md.Murshed Ali, Dr. Md.Jabed Akher	225-230
12.	A LARGE SEMINOMA ARISING IN ONE OF BILATERAL UNDESCENDED TESTES: A CASE REPORT Phuvitoo SUNGTONG	231-240
13.	A COMPARISON OF BONE SPECT IMAGE QUALITIES OBTAINED FROM OSEM AND FBP ALGORITHMS Chiraporn TOCHAROENCHAI, Surachai NGAMRATANAPAIBOON, Chulaluk KOMOLTRI	241-248

INFECTIONS OF THE BRAIN AND NERVOUS SYSTEM AS DIAGNOSED BY CT. AND MRI.

Vallop LOAPAIBUL[1] M.D.,
Kawee TUNGSUBUTRA[2] M.D., F.R.C.R. (ENGLAND)

ABSTRACT

Common Infections of the brain and nervous system found and diagnosed by CT. and MRI. or both, in the faculty of Medicine and Srinakarin hospital, Khon Kaen University will be presented and discussed as examples for their rontgenologic findings by CT, and/or MRI.

Category I	**Brain Abcess,** 2 cases
Category II	Inflammatory processes (involving) brain from pre-existing **pulmonary TB.** 1 case, **Cerebritis** and **Subdural Empyema.**
Category III	**Melioidosis** cerebral abscesses 1 case. (Bacteria: Pseudomonas Pseudomallei) **Melioidosis, Cerebritis and Subdural Empyema** 1 case
Category IV	**CNS, TB.: TB. Meningitis:** **TB. Meningitis** at **Basal Cistern** 3 cases. CNS, TB.: Tuberculoma, Rt. Occipital lobe. 1 case
Category V	**Cysticercosis**: **Calcified cerebral parenchyma** 6 cases.Cysticercus cellulose, larva of tape worm, calcified larva of tape worm in both cerebral hemispheres.
Category VI	**Virus Infection, Rabies.** 2 cases.
Category VII	**Protozoa,** Secondary to HIV Infection, **Toxoplasma Capsulatum.,** Toxoplasmosis 1case.
Category VIII	**HIV with Cryptococcosis.** **Cryptococcus neoforman** (Fungus infection)

CATEGORY I: Brain abscess or Abscesses with congenital anormally as underlying factor.

Brain abscess. Case I

Clinical: Female, girl age 4 years, having underlying **congenital anormaly, Tetralogy of Fallot**, with a present history of having high fever, 4 days before admission, he had a complaint of headache and projectile vomiting, blood culture showed mixed infections. CT. scan of the brain was done, both without contrast and with contrast enhancement.

[1] Department of Radiology, Faculty of Medicine, Khon Kaen University, Khon Kaen, THAILAND.

CATEGORY I: Case I

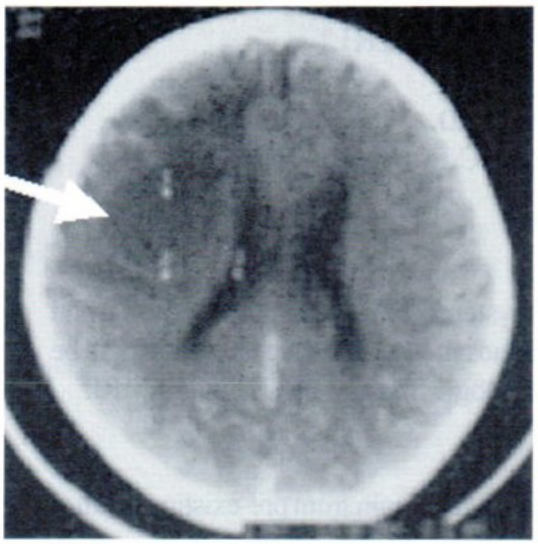

Fig. A NC.CT. (NON-CONTRAST CT.) an abcess can be seen in the frontal lobe Rt. side.

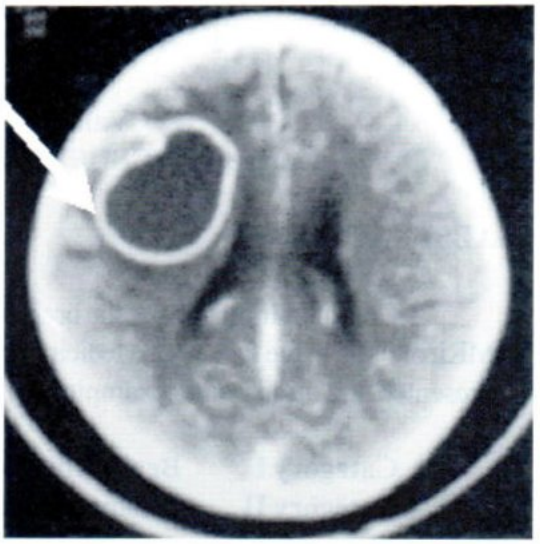

Fig.B CE.CT. (CONTRAST ENHANCEMENT CT.) rim ring enhanced wall.

Brain Abscess. Case II

Clinical: Male, boy 6 years, having **underlying Tetralogy of Fallot**, 7 days, before coming to the hospital, he had fever, headache, projectile vomiting, convulsion and periodic spasm of muscles of mouth and face, left side, with weakness of right, leg. CSF. culture. Anaerobes+ve

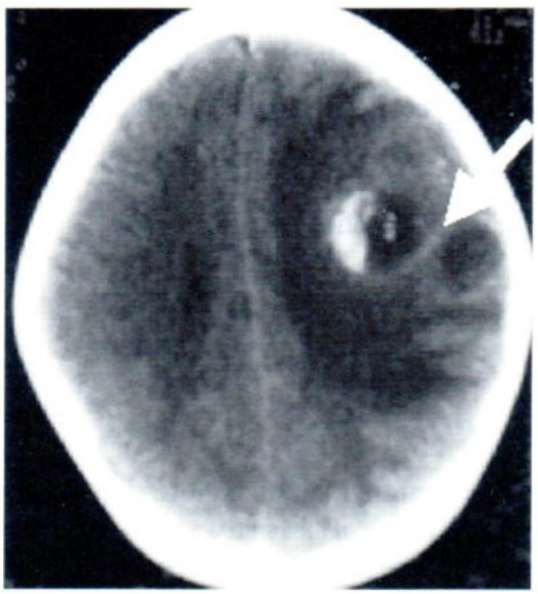

Fig A NC.CT.

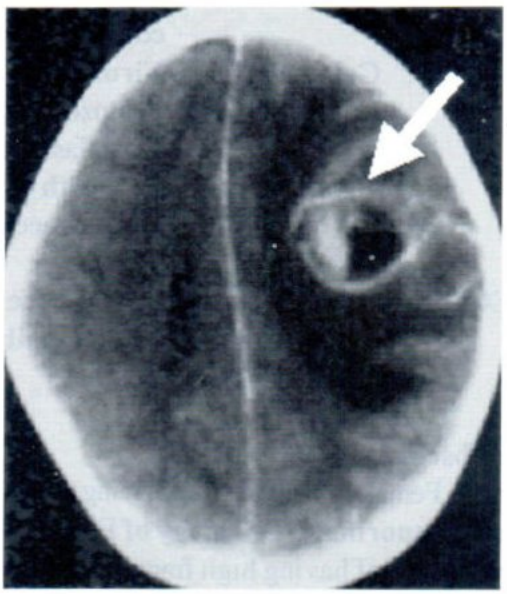

Fig B CE.CT. showed multiple rim ring enhanced wall abscesses at left frontal lobe. The walls of the abscesses are more obvious with contrast enhancement.

CATEGORY II: Cerebritis. **Inflammatory processes involving brain from pre-exsisting pulmonary TB.**

Clinical: Male, age 18 years with underlying pulm. TB. under treatment by anti. TB. drugs but stop treatment without permission from his doctor, for a year. Four days before admission, he had fever, headache, somnolence with worsen signs and symptoms of CNS. involvement. CT. of the brain was done with and without contrast.

Both **Fig A.** NC.CT. and **Fig B.** CE.CT. showed irregular border low density areas in both sides of the cerebral hemispheres. The bigger was in the right temporal lobe. No definite abcess walls were visualized. He improved after anti-tuberculous drugs treatment, both parenteral and intrathecally.

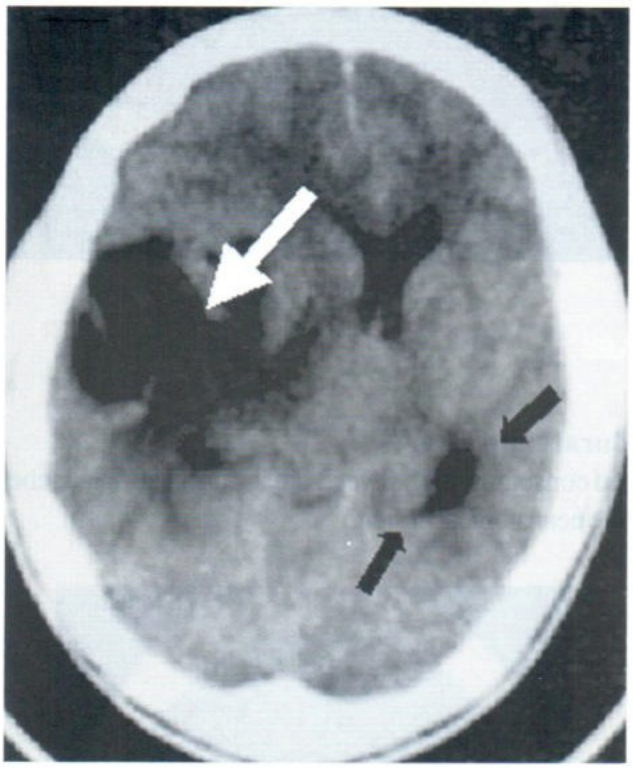

Fig A NC.CT.

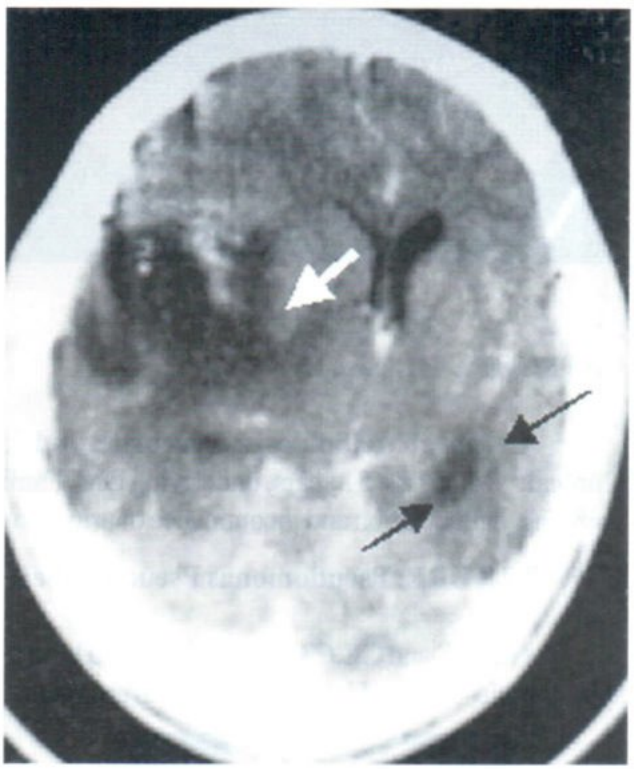

Fig B CE.CT.

CATEGORY III: **Inflammatory processes involving CNS. by specific infection, Melioidosis.**

Brain Abscesses: Melioidosis **case I**
Clinical: Male, age 18 years, high fever with chill on and off for 1 month, headache, projectile vomiting, weakness of left arm and leg. CSF. Culture: Pseudomonas Pseudomallei.

A. Non-contrast media CT.

B. Contrast enhancement CT.

Rim Ring Enhanced wall abscesses at both cerebral hemispheres showing by contrast media. (Pseudomonas Pseudomallei, Pyogenic bacteria)

CATEGORY III: case I

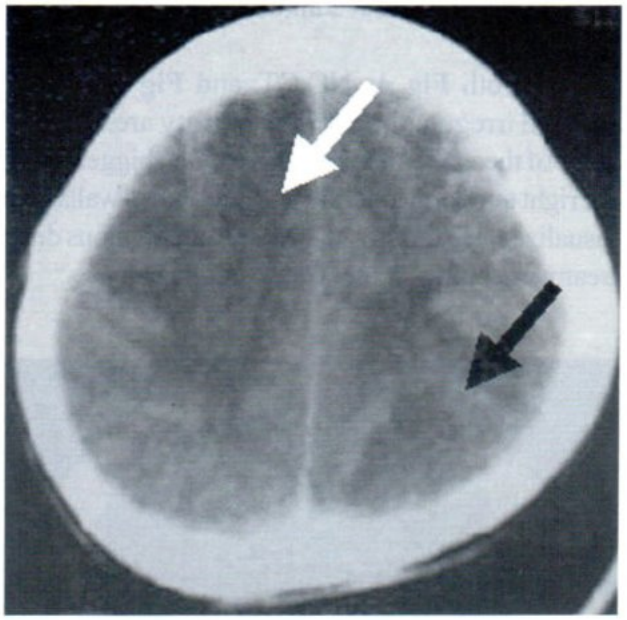

Fig A NC.CT.

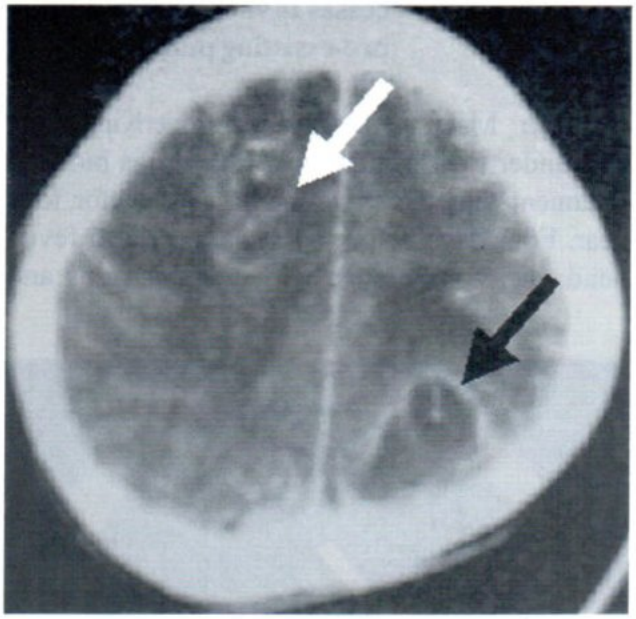

Fig A CE.CT.

CATEGORY III: case II:

Cerebral Mellioidosis: Cerebritis and Subdural empyema.

Clinical: Male, age 51 years, underlying DM. Diminished conscious, high fever 3 days, confused, headache, vomiting, hallucination and incontinence of urine, no definite neurological deficit.

CSF. CULTURE: Pseudomonas Pseudomallei

NC.CT. and **CE.CT.** (Fig.1, 2) showed lesions at Lt. Parieto-occipital lobe with subdural empyema.

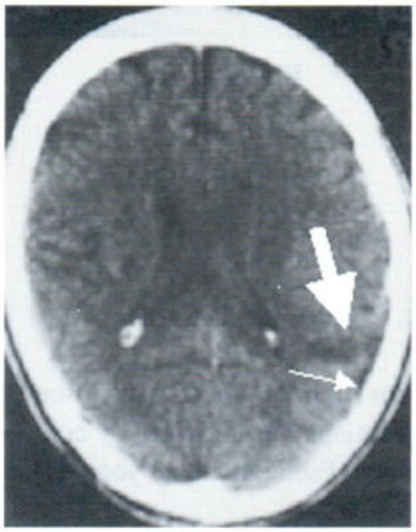

Fig.1 NC.CT.

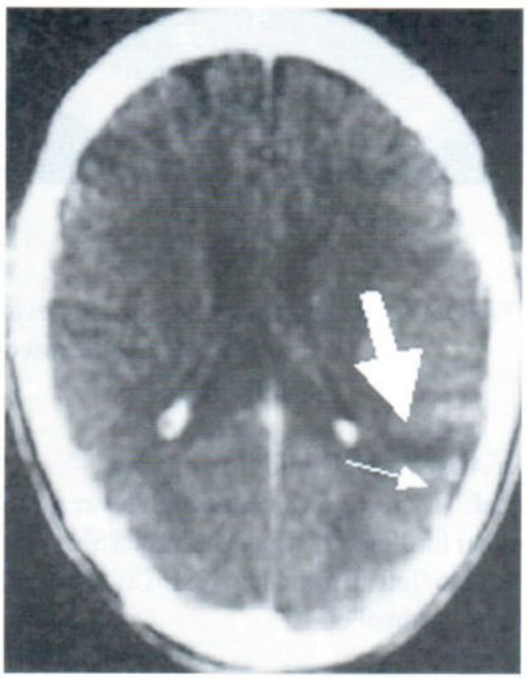

Fig. 2 CE.CT.

Fig. 3,4,5 MRI.

Fig. 3 MRI: T_1W_1

Fig. 4 MRI: T_1W_1 with contrast media, Gad. DTPA.

Fig. 5 MRI: T_2W_1 with contrast media, Gad, DTPA.

Subdural empyema was clearly demonstrated.

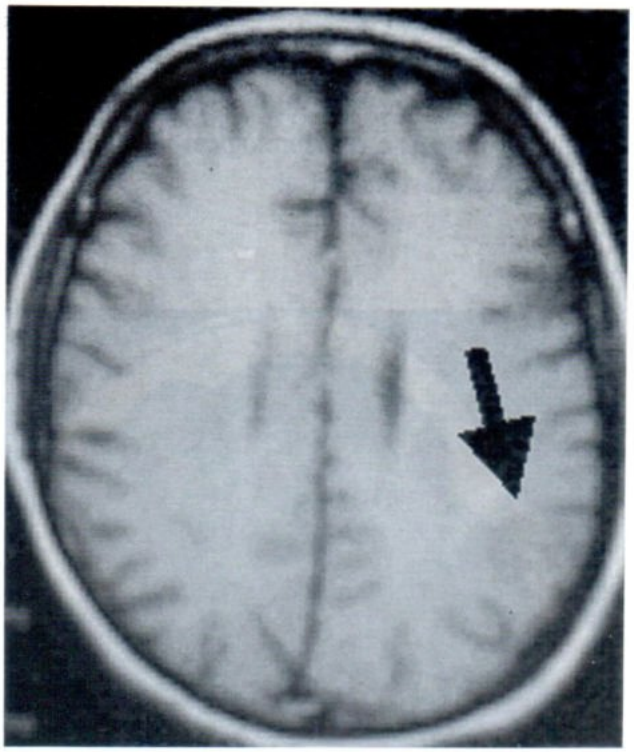

Fig. 3 MRI. T_1W_1

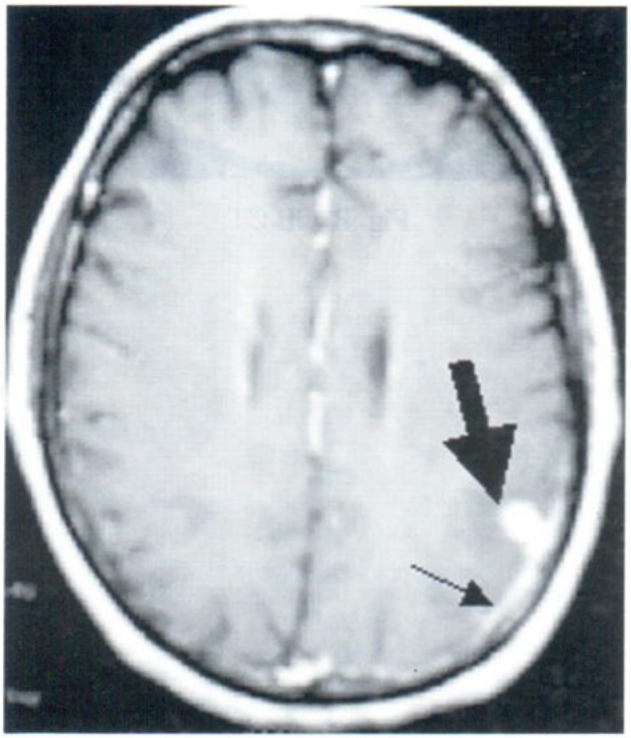

Fig. 4 T_1W_1 with Gad. DTPA.

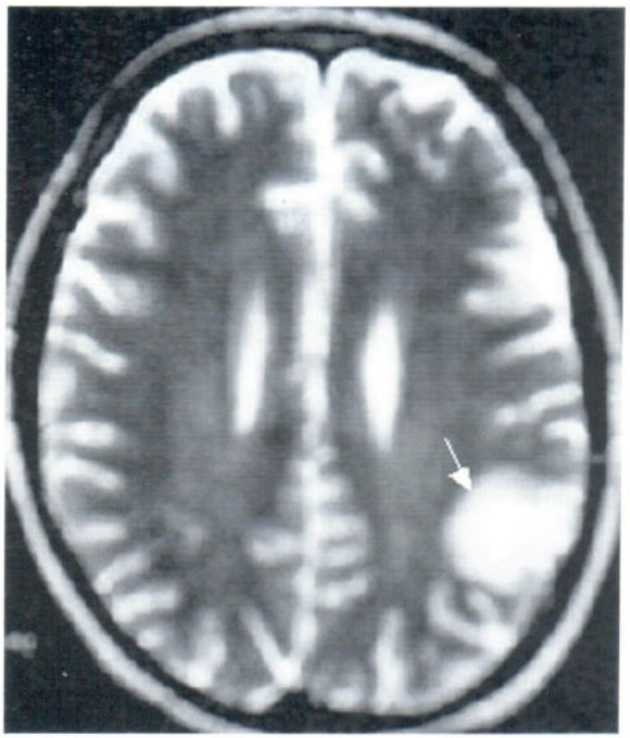

Fig. 5 T_2W_1 with contrast Gad. DTPA.

CATEGORY IV: Specific Infection, Tuberculosis.

Case I: TB. Meningitis

Clinical: Male, age 29 years, Underlying Pulmonary TB., severe headache, no neurological deficit. Lumbar puncture: Acid fast bacilli+ve

Fig.A NC.CT.

Fig.B CE.CT. Marked Enhancement at basal cistern.

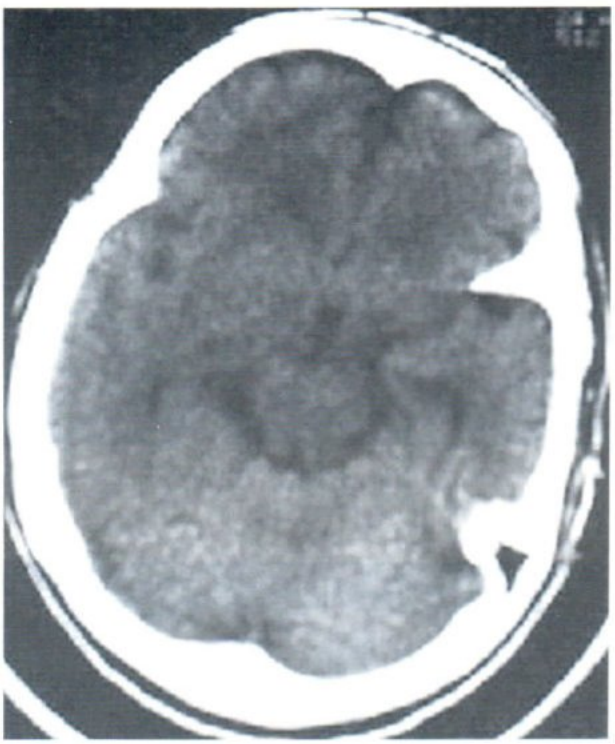

Fig. A NC.CT.

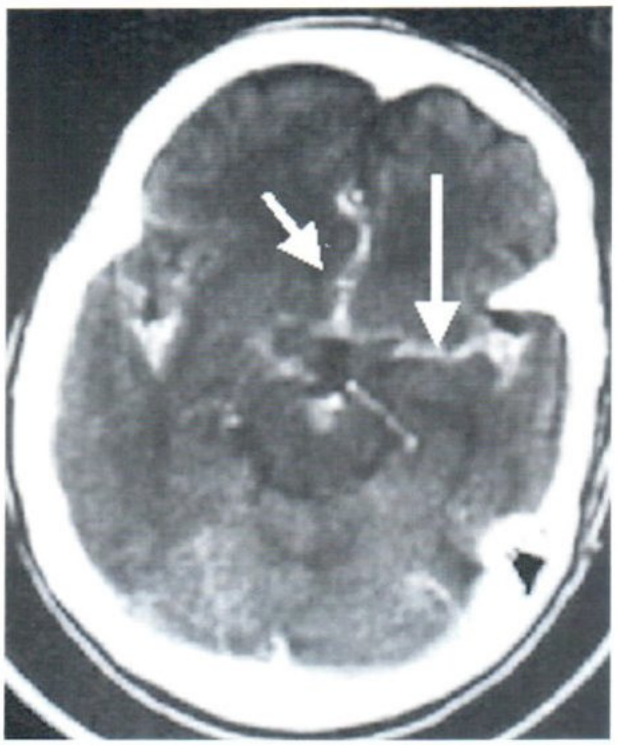

Fig. B CE.CT.

CATEGORY IV: Specific Infection, Tuberculosis

Case II: TB. meningitis

Clinical: Female, age 19 years, chief complaints, headache, vomiting frequently for 2 weeks. Tuberculosis at basal cistern.

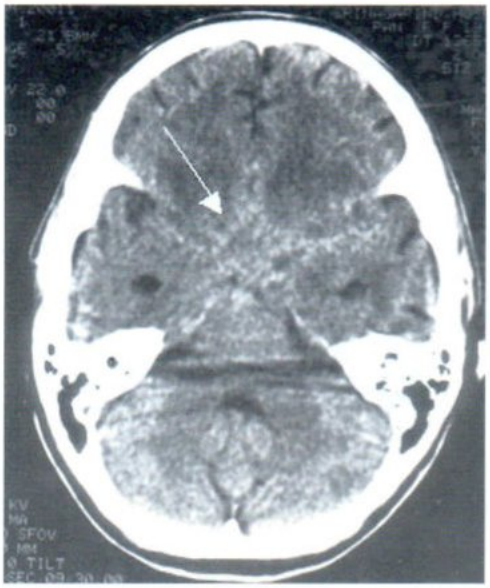

Fig. A Tuberculous lesions at basal cistern in not detectable (NC.CT.)

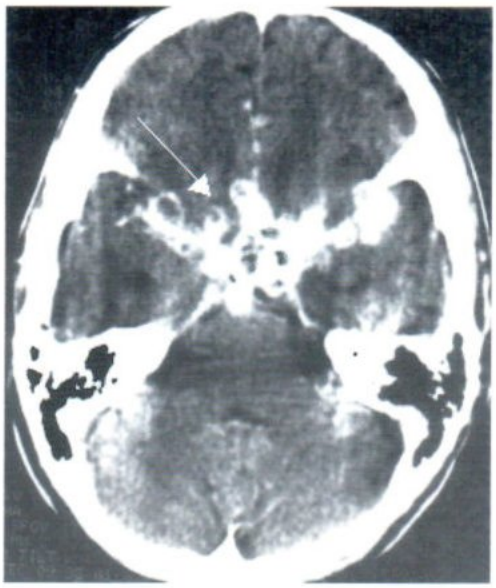

Fig. B Shows nodular enhancement at Basal cistern (CE.CT.)

CATEGORY IV: Specific Infection, Tuberculosis

Case III: TB. Meningitis: Enhancing Plaque at Rt. Basal cistern. Black arrow.

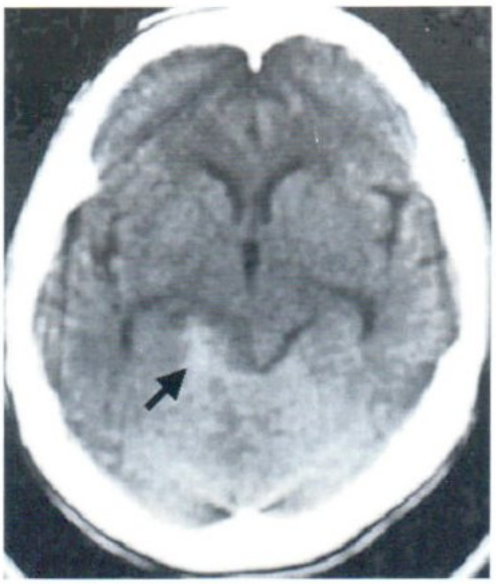

Fig. A NC.CT.

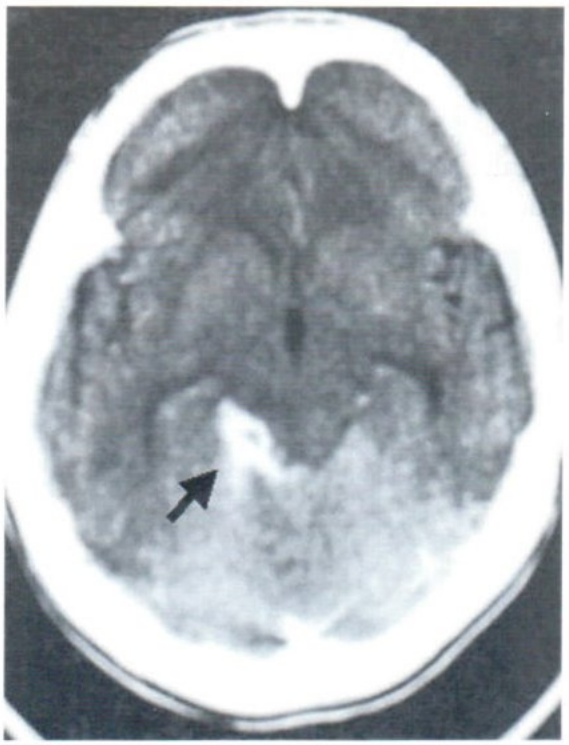

Fig. B CE.CT.

CATEGORY IV: CNS. TB.: Tuberculoma.

Clinical: Male, 23 years, Underlying Pulmonary TB. Severe Headache, Bilateral Papilledema, stiff neck; Lumbar puncture. Tubercle bacilli+ve

Case IV: Tuberculoma Rt., occipital lobe The Tuberculoma at Rt. Occipital lobe having enhancement of the lesion obviously.

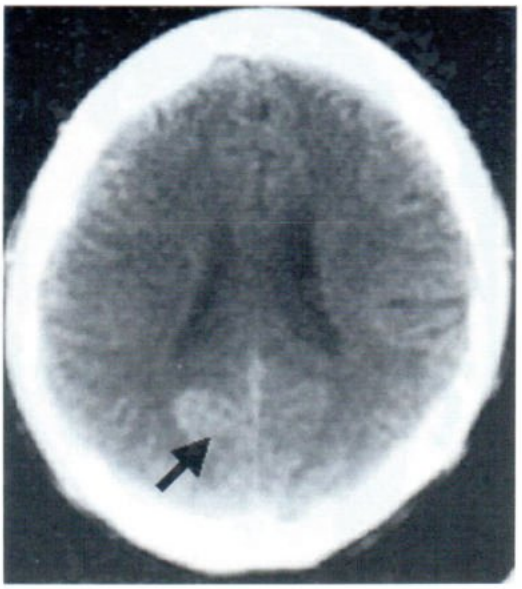

Fig. A NC.CT.

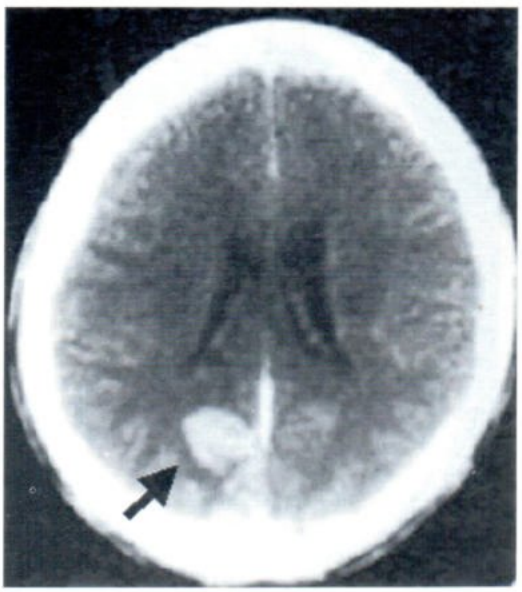

Fig. B CE.CT. showing Tuberculoma Rt. Occipital-lobe with enhancement of the lesion.

CATEGORY V:

Case I CNS.Cysticercosis: Calcified parenchyma
Clinical: Male, age 18 years, CT. shows calcified Cysticercosis in both cerebral hemispheres.

Note: **Cysticercus Cellulose is** the larva of tapeworm which **human is the intermediate host.**

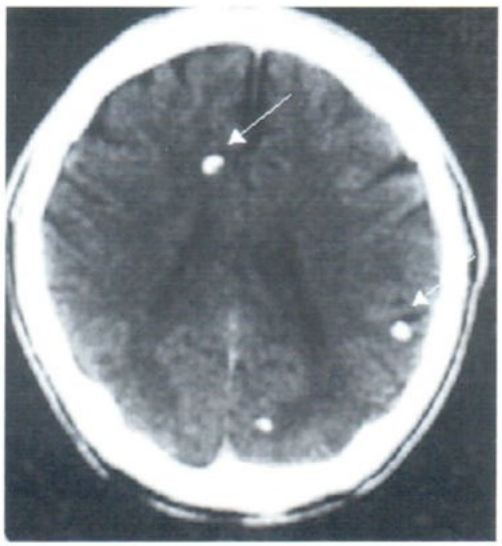

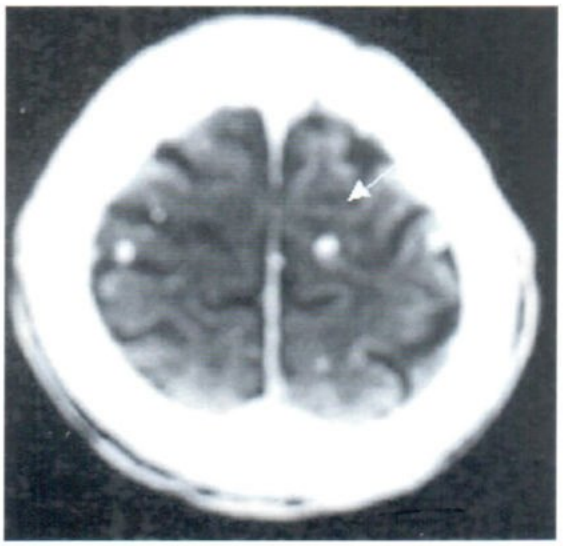

CATEGORY V:

Case II

Clinical: Male, age 38 years, severe headache, convulsion

Fig.A NC.CT.,

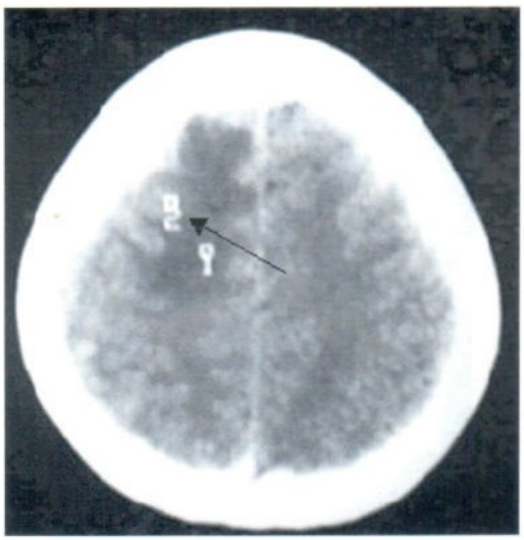

Fig.A NC.CT.

Fig.B CE.CT. Enhancing nodule of Cysticercosis in right frontal lobe with marked perifocal edema.

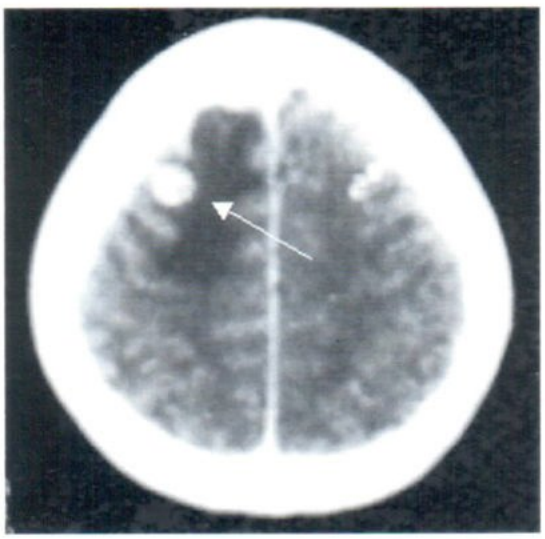

Fig.B CE.CT.

CATEGORY V:

Case III: CNS. Cysticercosis: Intraventricular

Clinical: Male, age 52 years, known case of Intraventricular Cysticercosis post ventriculo-peritoneal shunt.

Sagittal MRI. $T_1 W_1$ after contrast media injection show cyst and point of obstruction after ventriculo-peritoneal shunt.

Upper black arrow shows cysts, lower black arrow shows point of obstruction after having ventriculo-peritoneal shunt.

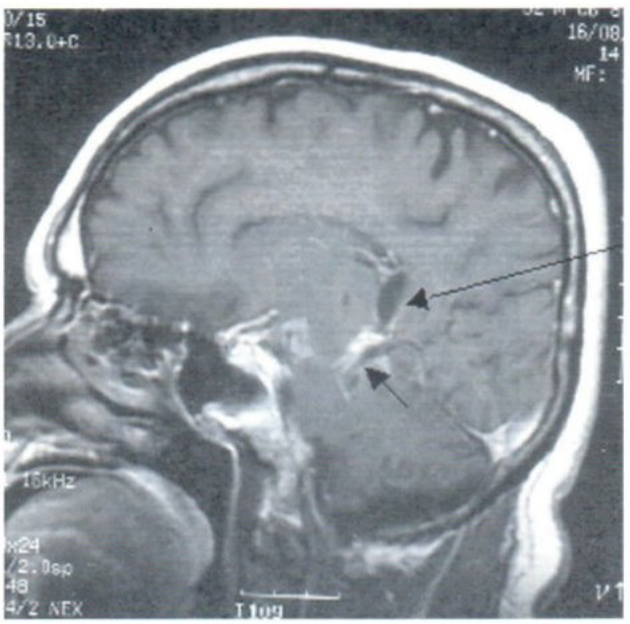

CATEGORY V:

Case IV: CNS. Cysticercosis: Intraventricular.
Clinical: Male, age 38 years, headache, convulsion,
Operation: 4th Ventricular Cysticercosis.

Fig.A. NC.CT.

Fig.B CE.CT., enhancing nodule of cysticercosis in 4th ventricle

Note: Fourth ventricle is irregular shape cavity in Rhombencephalon, between medulla oblongata, pons, where isthmus is in front and cerebellum is behind. It is connected to central canal of spinal cord below and cerebral aqueduct above. It is connected to the subarachnoidal space through the lateral and median apertures.

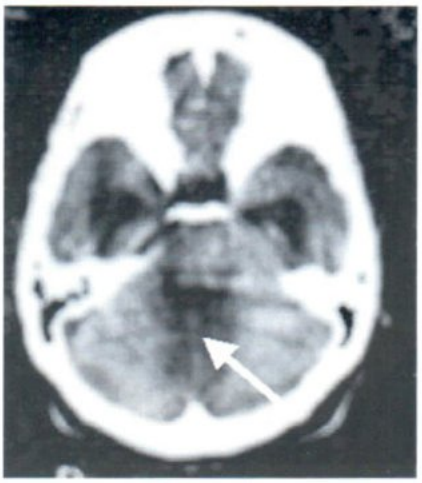

Fig. A

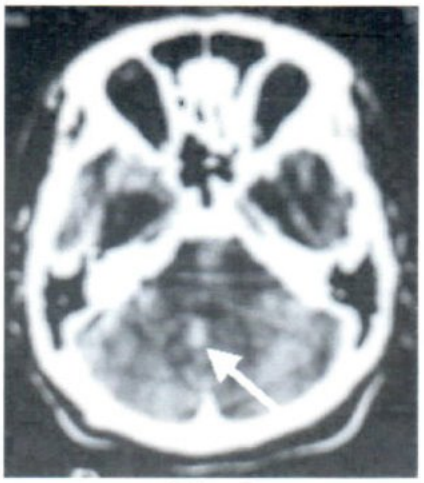

Fig. B

CATEGORY V:

Case V: CNS. Cysticercosis: Leptomeninges
Clinical: Male, age 46 years, severe headache, convulsion.

Fig.A T_1W_1

Fig.B T_1W_1 MRI with Gad. DTPA. Enhancement.

Enhancement of basal cistern, cisterna interpedun- cularis. Leptomeninges consisted of piamater and arachnoid.

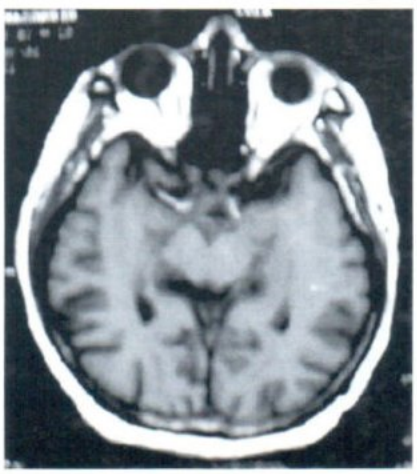

Fig.A T_1W_1 MRI

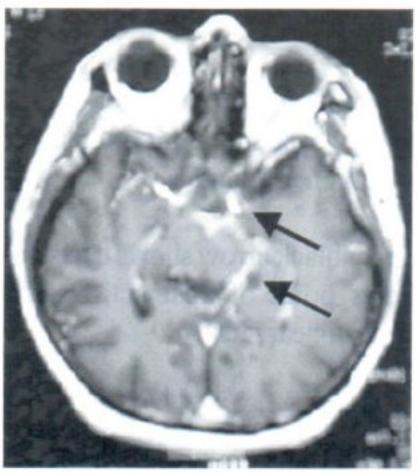

Fig.B T_1W_1 with Gad. DTPA

CATEGORY V:

Case VI: CNS. Cysticercosis: Racemose Pattern (clump of shrubs)

Clinical: Male, age 54 years, Severe headache, convulsion.

Operative findings: Cysticercosis at Rt. Parieto-occipital lobe with calcifications.

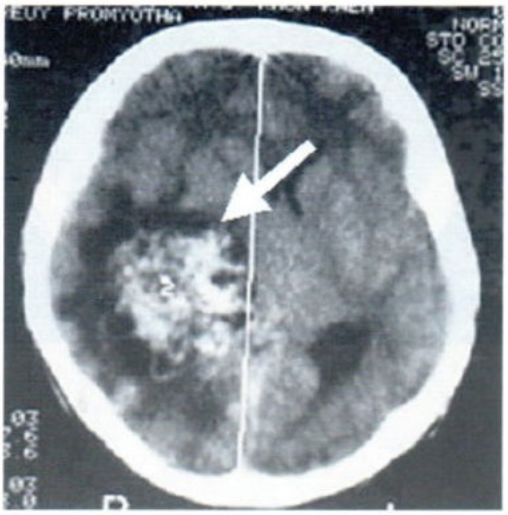

Fig.A Calcified racemose cysticercosis at Rt. parieto-occipital lobe.

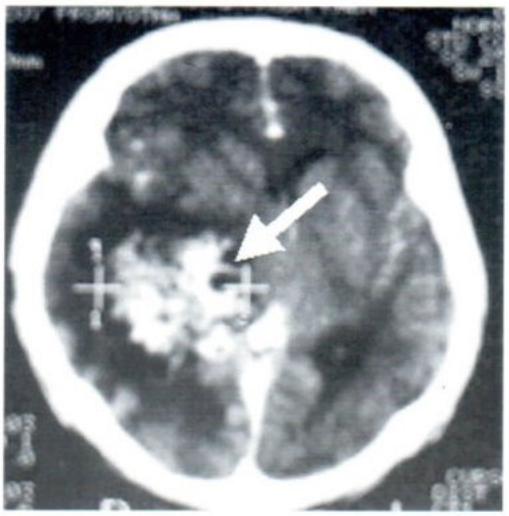

Fig. B Contrast enhancing racemose cysticercosis.

CATEGORY VI: Virus infection

Rabies infection:

Case 1: CT. of the patient with rabies encephalitis **(A.)** before and **(B.)** after injection of contrast media.

Clinical: Male, age 4 years, was bitten by a stray dog. After a few weeks he had symptoms compatible with rabies.

Fig. A NC.CT.

Fig. B CE.CT. The areas of encephalitis are blackening with contrast enhancement.

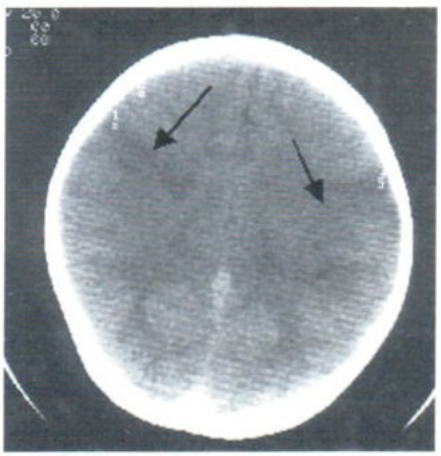

Fig. A NC.CT.

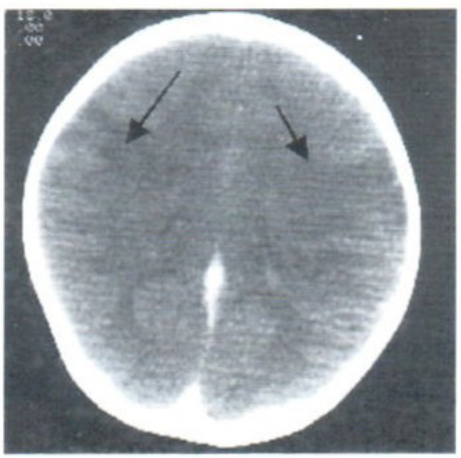

Fig. B CE.CT.

CATEGORY VI:

Virus infection: Case II

Clinical: Male, age 26 years. Heterosexual HIV+ ve, fever, he can not walk for 10 days. Clinical diagnosis. Brain atrophy was diagnosed. CT. scan shows general brain atrophy with enlargement of cerebral sulci the basal cisterns are enlarged.

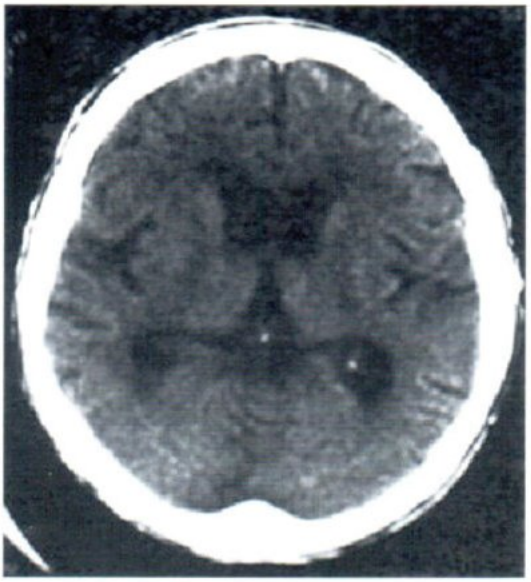

Fig. A Case II

CATEGORY VII: Protozoa secondary to HIV infection.

Case I: Toxoplasmosis, Toxoplasma Capsulatum, HIV+ve

Clinical: Male, age 29 years, severe headache for 1 week. Eye ground showed bilateral papilledema.

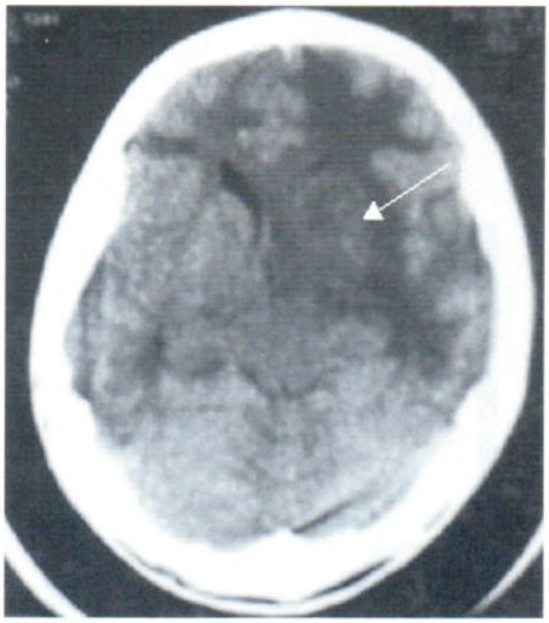

Fig. A NC.CT.

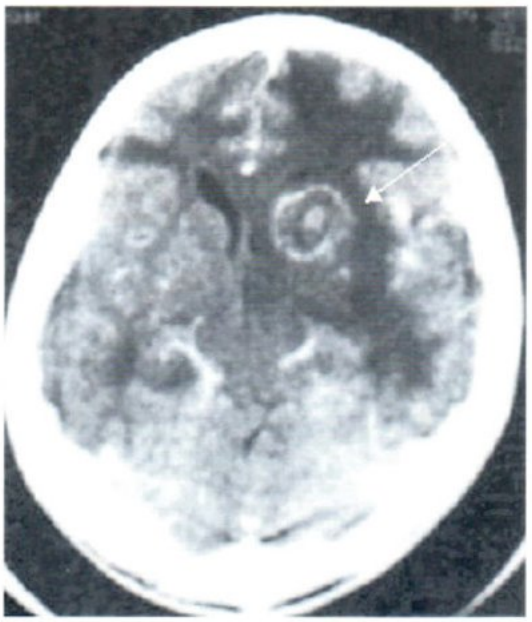

Fig. B CE.CT. show enhancing masses target lesions in the Basal Ganglia are seen.

CATEGORY VII: Protozoa, secondary to HIV infection Case II

Clinical: Male, age 32 years, severe headache for 2 weeks, bilateral papilledema., **HIV with Toxoplasma capsulatum.**

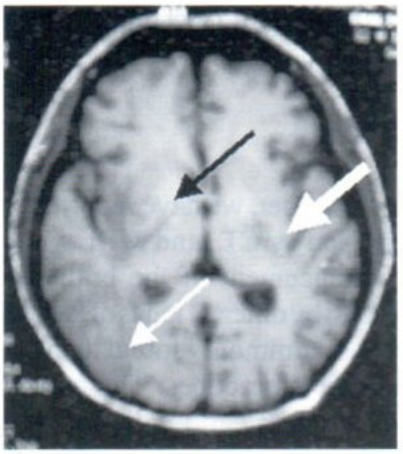

Fig. A T_1W_1 without contrast. No obvious lesions are seen.

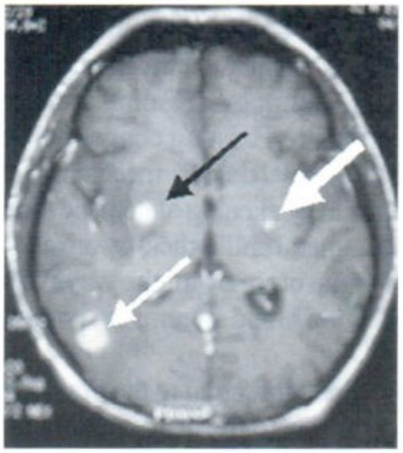

Fig. B T_1W_1 with Gad-DTPA enhancement many enhancing lesions in both cerebral hemi spheres are seen.

CATEGORY VIII: Fungi, secondary to HIV infection.

Case I: HIV with Cryptococcus neoforman.
Clinical: Male, age 26 years severe headache, stiff neck for 6 days.

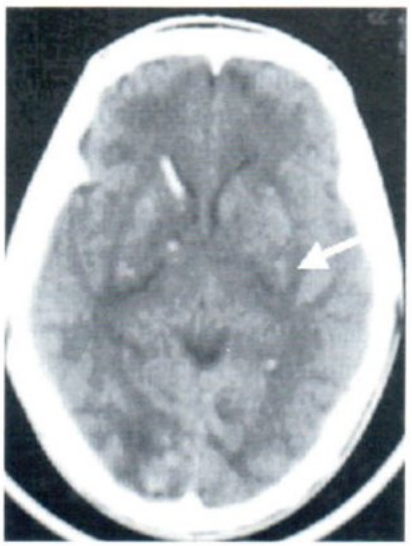

Fig. A NC.CT. small Cryptococcomas in basal ganglia, both sides.

Fig. A Small Cryptococcomas in basal ganglia, both sides are found.

Fig. B CE.CT. enhancing cryptococcomas in basal ganglia both sides.

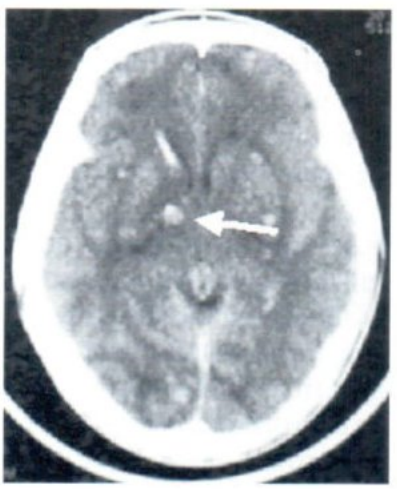

Fig. B CE.CT. enhancing Cryptococcomas in basal ganglia both sides.

DISCUSSION

Common Infections of the brain are usually spreading from neighbouring structures such as respiratory tract infections, e.g. nose, nasopharynx and the other structures around the skull. Apart from that, it may be infected by blood stream spreading from the pre-existing congenital anormally such as congenital heart diseases, Tetralogy of Fallot, or other valvular diseases. These Pre-Existing congenital defect may weakening the normal defense mechanism of the body which resulted in weakening of both the local, general, cellular and humeral antibodies, by primary infection and spread to the brain by all the ways of spreading such as, local, via blood stream, via lymphatic, etc.

The direct infection to the brain is obviously from direct trauma to the head causing damages to the skull, dura mater and Pia, arachnoid. The infected agents may be mixed pyogenic bacterial and specific infection, e.g. tuberculous, spreading from pre-existing pulmonary TB.. The melioidosis, caused by specific infection by bacteria pseudomonas pseudo mallei which has a sporadic spread in the north eastern part of Thailand. Melioidosis may cause cerebritis and subdural empyema which is blood born infection. Cysticercosis caused by cysticercus cellulose, larva of the tape worm. Cysticercosis cerebralis is often found in the north eastern and the northern parts of Thailand because the people in these two provinces are fond of eating raw fermented pork. The tape worms of this species are the intestinal parasites in pigs, human are the intermediate host. People eating raw pork will be infested by the larva of this worm and one or a certain numbers of larva may migrate to the brain and can be calcified in cerebral hemisphere in one or both sides.

Viruses such as Rabies may attack the brain and nearly all the victims are infected by dog bitten. Those who had not been vaccinated by rabies vaccine are mostly fatal. The protozoa are not usually infect the brain as well as the fungus. In this report, we reported one case of protozoa infection secondary to HIV infection, toxoplasmosis, infected by toxoplasma capsulatum. The other case infected by fungus, the cryptococcus neoforman, secondary to HIV infection has been reported. All cases reported here had been reported with pictures of CT with or with out contrast enhancement. T_1W_1, T_2W_1 or T_1W_1 and T_1W_1 with or without Gad-DTPA enhancement. All diagnoses of CT. and MRI. film are confirmed by pathologic sections, autopsy, micro-biological cultures, and, or microscopic slides.

CONCLUSION

In this paper, we have reported the findings of films studied by CT., and MRI. with or without contrast enhancement of the brain and nervous system infected by different kinds of Pathogenic agents from the most commonly found to the most rarely found in clinical practices. The number of cases presented in each categories depend on the number of cases found in each categories. Some are primary infection and some are secondary infection after the immunological mechanism of the victims had been destroyed or weakening by other factors or agents, such as debilitating or chronic progressive diseases, such as old ages, TB. and HIV infection.

REFERENCES

1. Barkovich AJ. Pediatric neuroimaging. New York: Raven press,1995.
2. Chamberlain MC. Pediatric aids: A longitudinal comparative MRI and CT brain imaging study. J Child Neurol 1993; 8:175-181.
3. Faerber E. Cranial Computed Tomography in infants and children. Philadelphia, PA: Lippincot 1986
4. Flodmark O. Neuroradiology of selected disorders of meninges, Calvarium and venous sinuses AJNR 1992; 13: 483-492.
5. Jordan Je, Enzmann Dr, Encephalitis. Neuroimaging clinic. North. AM. 1991; 1: 1-29.
6. Laissy JP, Sawyer P, Parlier C, et. al. Persistent enhancement after treatment for cerebral toxoplasmosis in patients, with AIDS: predictive value for subsequent recurrent. AJNR 1994; 15: 1773-1778.

CONGENITAL ANOMALY OF HEAD AND NERVOUS SYSTEM COMMONLY FOUND IN THAILAND

Vallop LOAPAIBUL[1] M.D.,
Kawee TUNGSUBUTRA[2] M.D., F.R.C.R. (ENGLAND)

ABSTRACT

Congenital ANORMALY of head and nervous system can be diagnosed accurately by CT and/or MRI. The early recognition of the deformed or the deprivation part or parts of the anatomical structures of the normal bones and/or soft tissue structures, early reconstruction of the IMPAIRMENT may help the innocent child to grow up and grow up to be a useful citizen and relief the burden of the family and the country. The conditions commonly found in Thailand and can be amendable are diagnosed by CT and/or MRI will be listed as followed.

1. **Fronto-Ethmoidal meningocoele. 2 cases.**
2. **Agenesis of Corpus Callosum**
3. **DANDY WALKER MALFORMATION (Cyst)**
4. **Schizencephaly: BRAIN CLEFT,OPEN LIP**
5. **Schizencephaly: BRAIN CLEFT, CLOSE LIP.**
6. **Lissencephaly. 6.1 Case 1**
   6.2 Case 2
7. **Holoprosencephaly**
8. **STURGE–WEBER Syndrome (S.W.S.), Neurocutaneous diseases.**

INTRODUCTION

CONGENITAL anormally is a condition which is UNPREVENTABLE and UNPREDICTABLE. Early recognition and Accurate Diagnosis by CT and /or MRI, the impairment and absent parts can be repaired or reconstructed by modern surgery and artificial organ or the donated organ bank in future will be very beneficial.

CONGENITAL ANOMALY;

1. FRONTO-ETHMOIDAL MENINGO -ENCEPHALOCOELE. Case I

Clinical: A boy, age 2 years, There is an abnormal mass between both eyes and between the middle part of nose bridge. The most prominent part is under the left eye obstructing the lower field of vision of medial part of both eyes. (black arrow) No nervous deficit.

Parents want their child to have plastic reconstruction. Fig. A. Non-contrast CT. showing bone defect at the white arrow.

[1] Department of Radiology, Faculty of Medicine, Khon Kaen University, Khon Kaen, THAILAND.

FRONTO-ETHMOIDAL MENINGO-ENCEPHALOCOELE. Case I

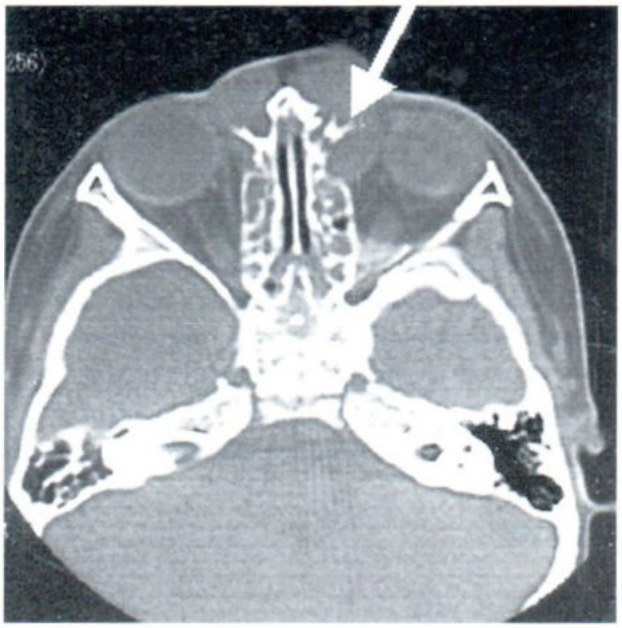

Fig. A NC.CT.

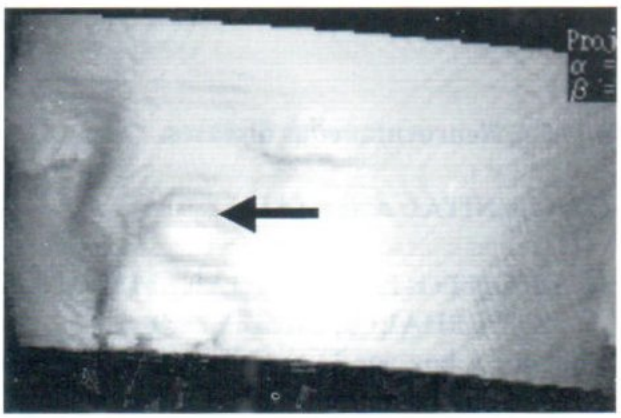

Fig. B 3D. Reconstruction of the CT., black arrow shows Fronto-Ethmoidal Meningocoele.

2. FRONTO-ETHMOIDAL MENINGOCOELE, Case II:

Clinical: A boy, age 8 months, having a bulging mass between the eyes and nose bridge. The bone defect showing as a bulging mass clinically known as "Meningocoele"

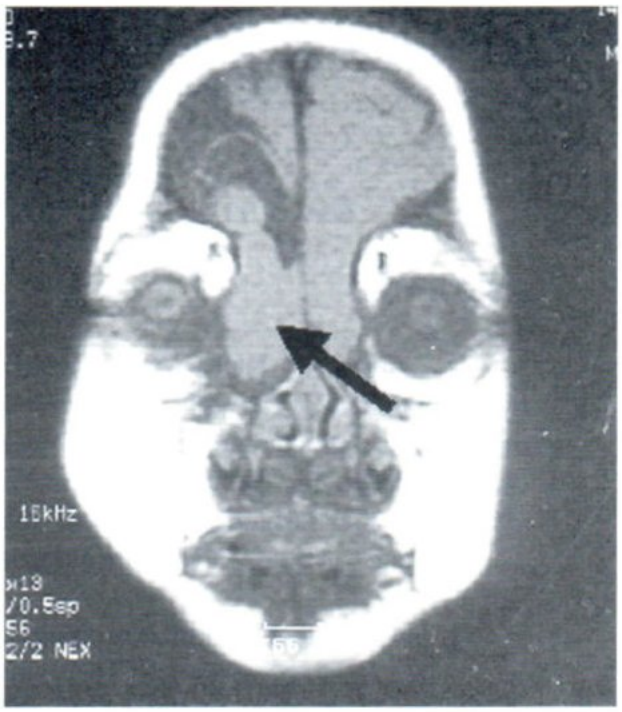

Fig. A MRI, CORONAL, T_1W_1

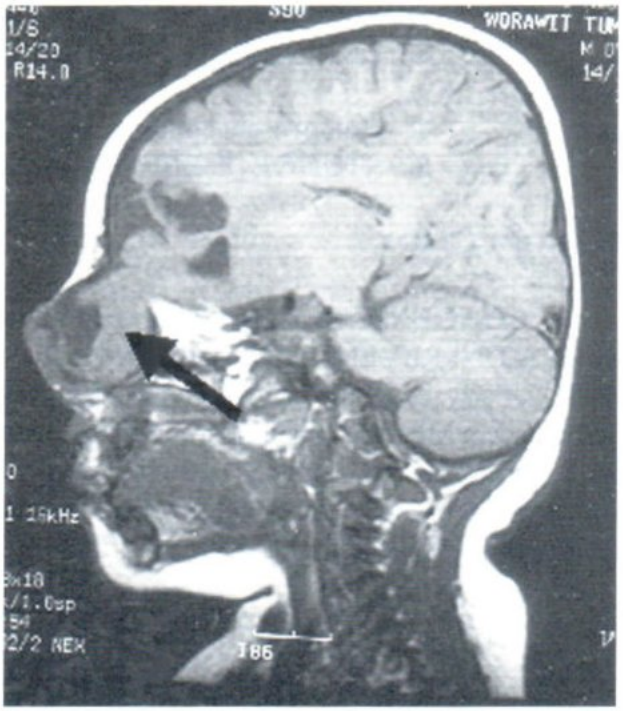

Fig. B MRI, SAGITTAL, T_1W_1

A and B, showing herniation of brain and meninges through the bone defect at the Fronto -Ethmoidal region. (black arrows)

3. AGENESIS OF CORPUS CALLOSAL.

Clinical: Male child, 1 year, head circumference 46 cm., retarded brain and body development. Out standing bigger head than normal child of the same age group.

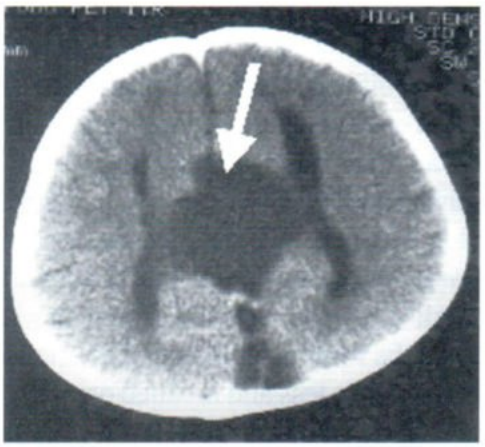

Fig. A NC.CT. shows absence of Corpus Callosum. Having central dorsal Interhemispheric cyst between lateral ventricles.

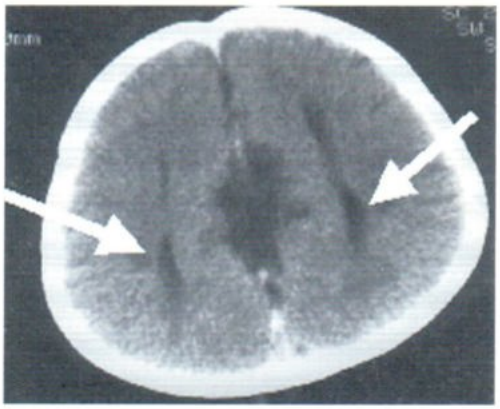

Fig. B NC.CT at different level of the head. CT. at upper level above the cyst, showing the lateral ventricles of both sides running parallelly between the left and right sides of the cyst seen in fig. A.

Corpus Callosum is the transverse nerve fibers which join the rt. and lt. hemispheres together. It is composed of mostly white matter situating at the deeper parts of longitudinal tissue consisted of 4 parts from anterior to posterior, Rostrum, Genu, Trunk and Splenium having a special name as Commissura Magna Cerebri.

4. DANDY WALKER MALFORMATION. (Cyst)

Clinical: Female, 1 month baby, born by Caesarian section: Having larger head than normal baby, vomiting occasionally, no convulsion, retarded development. CT. showed a large cyst at the posterior fossa with connection to the 4th ventricle. (black arrows).

Dandy Walker cyst is a congenital anomaly consisting of aplasia or hypoplasia of cerebellar vermis and cystic transformation of 4th ventricle. Congenital hydrocephalus, Dandy Walker cyst is caused by obstruction of foramen of Luschka and foramen of Magendie, which are the connections between the lateral ventricle and 4th ventricle (APERTURA MEDIANA VENTRICULI QUARTI.)

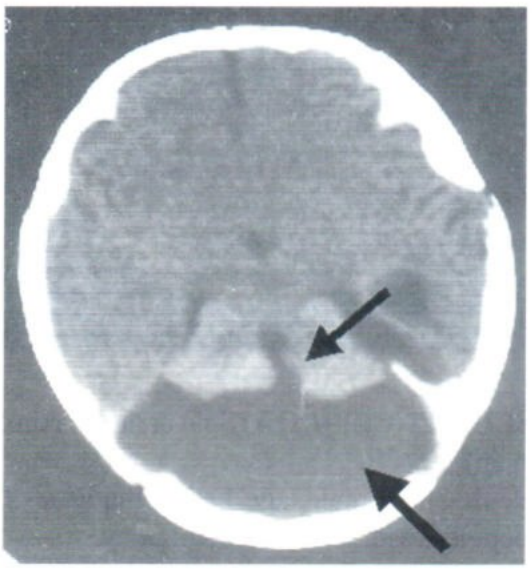

Fig.4 Showed, "DANDY WALKER MALFORMATION", lower black arrow showed large cyst at the posterior fossa. Upper small black arrow showed connection with 4th ventricle.

5. HYDRANENCEPHALY.

Clinical: Child, male, age 3 months, no activities and bodily development. CT. showed cerebral hemispheres are replaced by water or CSF. The brain tissues seen in the picture are parts of cerebellum which is in the posterior fossa. Hydranencephaly is the combination of 2 words; HYDRO+ANENCEPHALY, i.e. Absence of cerebral hemispheres which are replaced by water. The baby is incompatible with life.

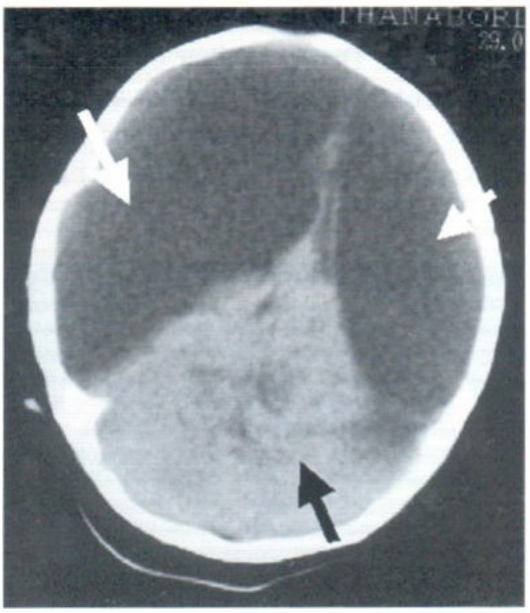

6. SCHIZENCEPHALY; Split brain or brain cleft (open lip)

Clinical: Child, male, age 1 year, big head, slow development with spastic cerebral palsy.

CT. showed empty spaces without brain tissues making the brain cortex, arachnoidal spaces and ventricular lumen have free connection. These findings are called open lips schizencephaly.

Schizencephaly is a condition which there is gray matter lined cleft, starting from ventricular ependyma to PIA mater which may consisted of;

1. There are cysts or cavities in the brain cortex connecting with arechnoidal spaces by pores or clefts.
2. There are cavities in the brain which may be found in fetus in utero or young infants and may or may not connecting with arachnoidal space. These cavities may occur from the result of destructive lesions or may occur congenitally. Schizencephaly may be found in 2 different types. The open lip is compatible with when one open his lips, looking into his mouth through a mirror, one may see a large cavity with a Uvula in the middle. The close lip is looking like one close his lips and only he can see a small cleft between the upper and lower lips. In this case, there is a small cleft connected between the cerebral cortex and the ventricular lumen. If the cleft is wide, the brain tissue is less and is called open lip. On the contrary, if the cleft is narrow, it is a close lip type. Close lip, schizencephaly, there is a small cleft connecting between brain cortex, arachnoidal space and ventricular lumen.

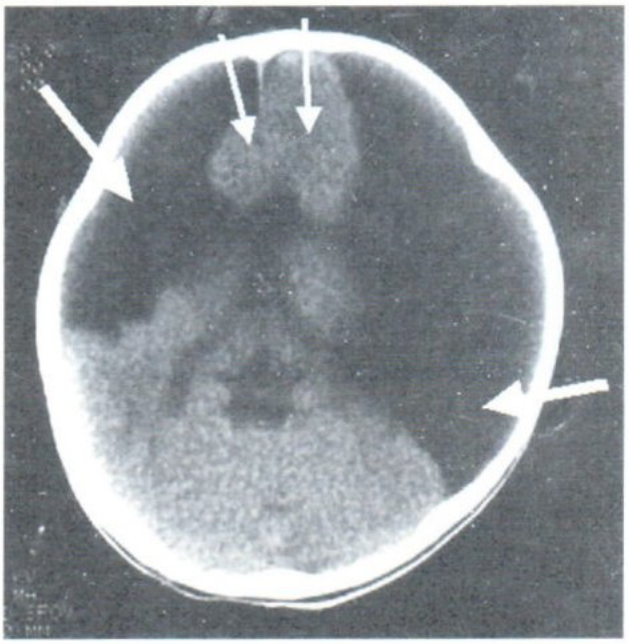

Fig. 6 Open lip Schizencephaly: split brain or brain cleft (open lip)
[A Uvula in the oral cavity]

7. SCHIZENCEPHALY; Brain cleft (close lip)
Clinical: Infant, male, age I year and 7 months. Lt. arm and leg weakness for 1 year. CT. show narrow brain cleft connecting from cerebral cortex to ventricles.

Black arrow showing small cleft connecting between cerebral cortex and ventricle. Schizencephaly: Brain cleft (Close lip)

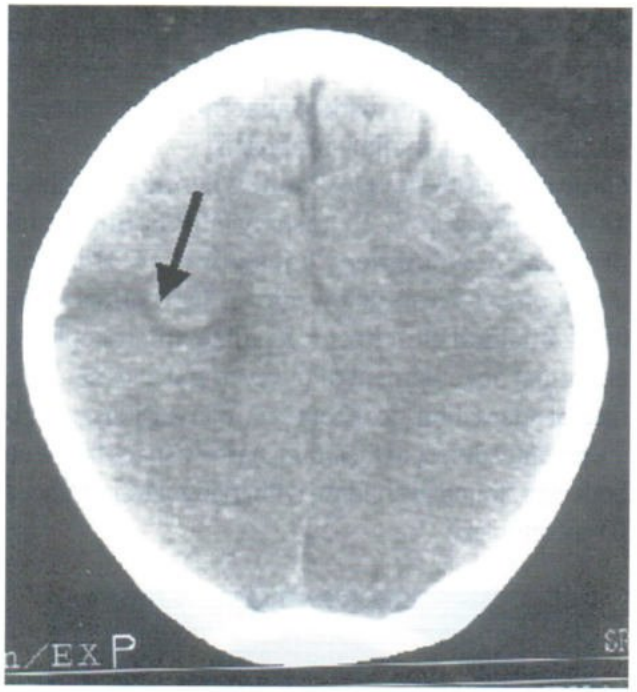

8. LISSENCEPHALY (Smooth brain)
Case I:
Clinical: Female, age 16 years, delay development, both physically and mentally. CT, showed smooth brain, having small number of sulci and gyri. The sulci and gyri are broader than normal brain, looking smooth in outline. The cerebral cortex is thick, cerebral sulci is small in number, each one is broad. Gyri are flat. Lissencephaly having smooth brain, having small number of sulci and gyri. The sulci and gyri are broader than normal brain, looking smooth in outline. The cerebral cortex is thick, cerebral sulci are small in number, each one is broad. Gyri are flat. Lissencephaly having smooth brain, gyrus is shallow or no gyrus, in the worse cases, they are agyria (completely smooth) or pachygyria (incomplete). The convolution number are few. Smooth cerebral hemisphere or small numbers of convolution can be found in some species of mammals such as "bats" or in some rodents.

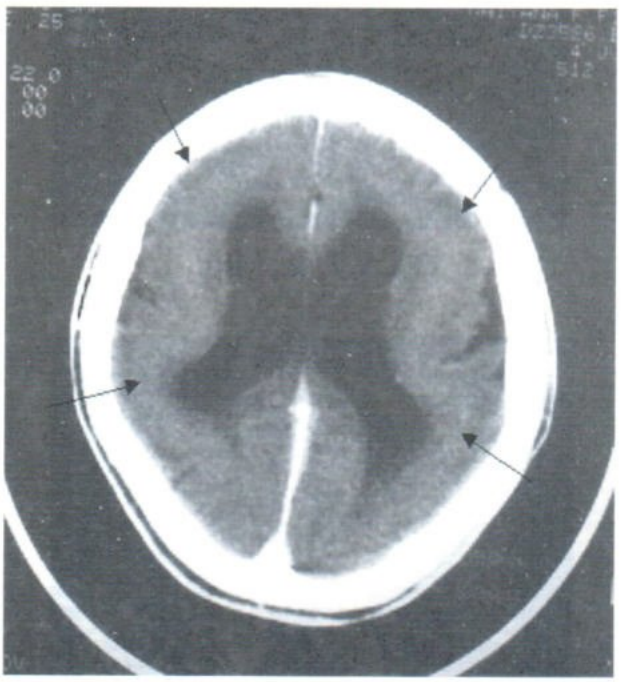

Fig. 8 CT, of lissencephaly showing smooth brain. few numbers of sulci and gyri. The complete absence of gyrus is called "Agyria." The incomplete absence with shallow gyri are called "Pachygyria"

9. LISSENCEPHALY (smooth brain)

Case II:

Clinical: Male child age 5 months, slow development since birth.

Fig. A. is T_1W_1, MRI., **Fig. B.** is T_2W_1, MRI.

Cerebral cortex thick, syvian fissures shallow, the furrows are natural development to increase the area of brain tissues to impove the intelligence of human being. Gyrus is the tortuous elevations or convolution of brain surface.

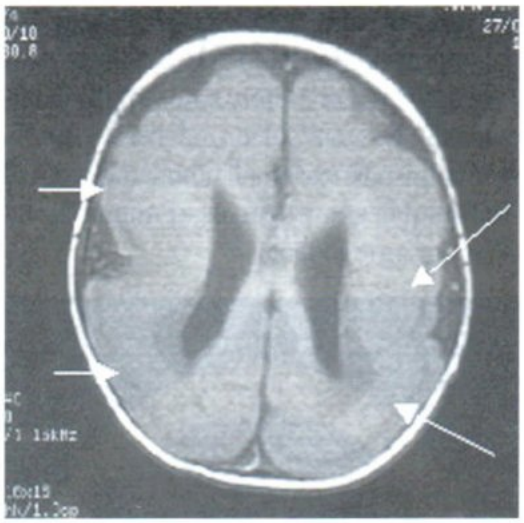

Fig. A T_1W_1, MRI.

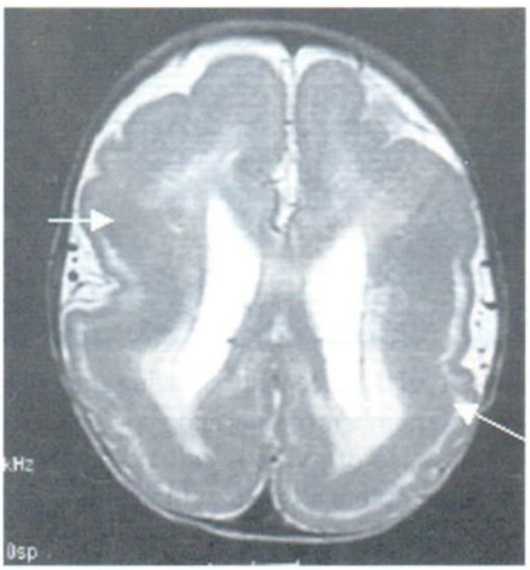

Fig. B T_2W_1, MRI.

10. HOLOPROSENCEPHALY

Clinical: Female, age 6 months retarded development since birth.

CT. shows semilobar holoprosencephaly:

Absence of **septum pellucidum.**

Septum pellucidum is double layers of thin membrane, triangular shape separated the anterior horn of lateral ventricles into left and right sides at the median plane.

Holoprosencephaly: Failure of normal development of prosencephalus together with deficit in midline facial development, There may be only one eye present in the face in case with marked abnormal development. such as cyclops, midline proboscis.

Causes of Mal-Development: Having extrachromosome in group 13-15, trisomy DI. **The abnormal physical development consisting of:** Bilateral development of ears at lower level than normal in the head, bilateral cleft lip, cleft palate, microcephaly, abnormal development of the eyes and eyes sockets, mental retardation, deaf both ears, convulsions, ventricular septal defect in the brain, narrow space between both eyes, found in children with triangular shape head (Hypotelorism)

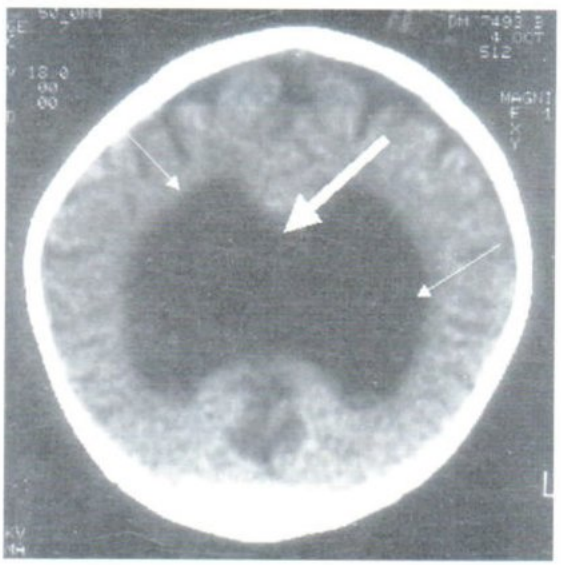

Fig. 10 CT. shows abscence of septum pellucidum.

11. STURGE–WEBER SYNDROME (SWS); CONGENITAL NEUROCUTANEOUS DISEASE.

Clinical: Male, age 14 years.: Convulsion,on and off, controlled by anti-convulsive drugs. The convulsive attacks increase in frequency as the boy grow older.

Fig.A. NC.CT., **Fig.B.** CE.CT. Both figures show gyral enhancement at right cerebral cortex indicating atrophy of right cerebral hemisphere and thickening of calvarium right side.

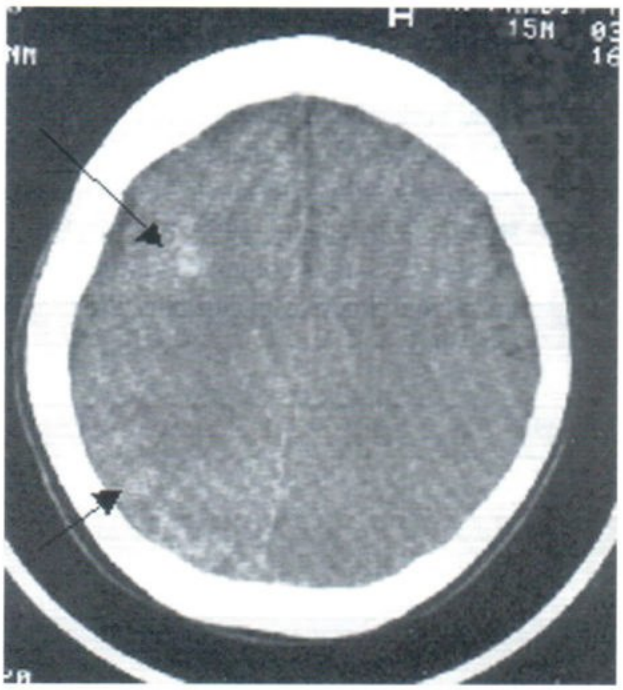

Fig. A NC.CT. shows cortical calcifications.

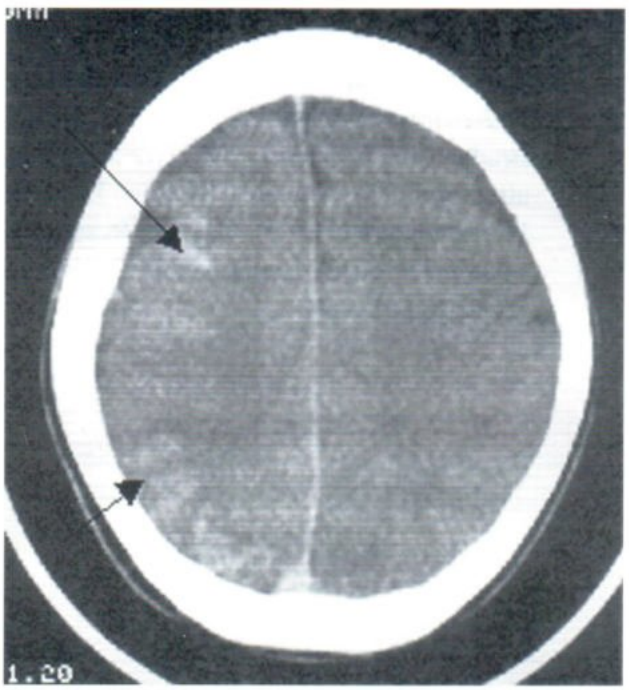

Fig. B CE.CT. shows enhancement of cortical calcifications.

Sturge-Weber syndrome is a congenital abnormality characterized by:

1. Capillaries haemangioma at the face presented at birth with varying areas. It present as a red skin on the face at one or both sides of the face.
2. Presence of angioma at the leptomeninges and choroid, late glaucoma, intra-cranial calcifications,
3. Mental retardation
4. Contralateral hemiplegia and epilepsy due to cerebral hemorrhages from intra-cranial angioma.
5. A port-wine stain half of the face in the area supplies by the first branch of trigeminal nerve due to the abnormalities of cerebral vessels, resulting in contra lateral hemiplegia.

DISCUSSION

The development of CT. and MRI., parallel with the improvement of opaque media using with CT. and MRI making the diagnosis of the lesions in the brain more convenience , accurate and quick. The most important diagnosis are the number of the lesions, the position of the lesion or lesions and the nature of the lesion. The treatment can be pre-planned and choose the right and best method of treatment available.

CONCLUSION

CT. and MRI. with or without contrast media

should be used for prompt and accurate diagnosis of the diseases of central nervous system. The treatment of the lesions in the CNS. should be a team approach. The team should consist of, radiodiagnostician, radiotherapist, surgeon, physician and pathologist.

REFERENCES

1. Zimmerman RA, Bilaniuk LT, Gusuard DA. Pediatric cerebral anomalies. In: Stark DD,
2. Bradley WG Jr, Quencu RM, Hydrocephalus, atrophy, and intracranial CSF flow. In: Stark DD, Bradley WG Jr. eds. Magnetic Resonance Imaging 2nd ed. St. Louis: Mosby-Yearbook 1992; 28:913.967.
3. Gomori JM, Grossman RI. Goldberg HI. Occult cerebral vascular malformations: high field MR imaging. Radiology 1986; 158: 707-713.
4. Teresi LM, Davis SJ. Cerebrovascular maformations. In: Stark DD, Bradley WG Jr eds. Magnetic resonance imaging 2nd ed. St. Louis: Mosby Yearbook; 1991: Chpt 29.
5. Barkovich AJ. Pediatric neuroimmaging. New York: Raven press, 1995.
6. Chamberlain MC. Pediatric aids: a longitudinal comparative MRI and CT brain imaging study. J. Child Neul. 1993; 8: 175-181.
7. Faerber E. Cranial computed tomography in infants and children. Philadelphia, PA: Lippincot 1986.

BRAIN TUMOURS SYSTEMIC CLASSIFICATION AND DIAGONSIS BY CT. AND MRI.

Vallop LOAPAIBUL[1] M.D.,
Kawee TUNGSUBUTRA[2] M.D., F.R.C.R. (England)

ABSTRACT

Brain Tumours can be classified systemically according to the normal anatomical structures from outer layer into the internal structural contents to the brain tissues starting from meninges, the most superficial, to the innermost structure of the brain, i.e. the ventricles. They can be classified as primary tumours and metastatic tumours.

Primary Brain Tumours.

1. Meningiomas, Crista Galli, Frontal, Temporal, Sphenoidal, Peri-sella tumours.

2. Brain Tissues, Consisted of nerve cells and connective tissue cells, specially called Glia cells.

   2.1 Nerve cells, no tumours originated from nerve cells are found at present neither benign nor malignant.

   2.2 Glia Cells 2.2.1. Astrocytoma, cell with one axon and multiple dendrites.
   2.2.2. Oligodendroglioma, cell with one axon and only few dendrites.
   (Olig = Few)

   Malignant Astrocytoma and oligodendroglioma are classified into 4 grades, i.e. grade I, II, III, IV. The grading are classified according to 4 criteria according to

   1. Proportion of malignant cells and fibrous tissue cells, either scanty or abundant.
   2. Proportion of the nucleus and cytoplasm, scanty cytoplasm with large nucleus is more malignant.
   3. Regularity of the size of malignant cells, uniformity of the shape and size of cells in one field of microscopic section of the staining slide.
   4. Properties of nucleus. Normal, regularity of shape, size and staining.
      4.1 Karyorhexis, or broken nucleus.
      4.2 Karyolysis, or dissolved nucleus.
      4.3 Pycnosis, the nucleus have deep staining.

   Grade IV malignant Astrocytoma, the most malignant and most frequently found have a special name as "Glioblastoma Multiforme"

[1] Department of Radiology, Faculty of Medicine, Khon Kaen University, Khon Kaen, THAILAND.

3. Tumours of Embryonal Rest which can make seedling through the ventriculo-spinal system via the CSF. There are five malignant tumours which can make seedling through the cerebro-spinal system.
   3.1 Pineal-Pnet (Primitive Neuro-Ectodermal Tumour)
   3.2 Choroid Plexus Tumour
   3.3 Medulloblastoma (Medulloblast, Cerebello-Pontine Angle)
   3.4 Ependymoma (Primitive Ependymal cells which is the cell lining of the ventriculo -spinal system)
   3.5 Leukaemia

4. Blood Vessels.
   - Haemangioendothelioma - tumour of endothetial lining the wall of blood vessels.
   - Haemangiopericytoma - pericyte cells are cells, which re-enforce the strength of blood vessels.

5. Pituitary. A, B, C cells tumouse.
   A = Acidophile-Hormone producing-Acromegaly, Gigantism.
   B = Basophile-Hormone producing-Cushing syndrome.
   C = Chromophobe, (Non-hormone producing) causing pressure symptoms.
   A, B are Microadenoma - A. Acidophile produce somatotrophin, gonadotrophin etc.
   B. Basophile produce ATCH-Cushing syndrome.
   C, Macroadenoma produce pressure effect: 1. On other two. kinds of cells i.e. A and B cells making deprivation of sex hormones
   in female, making the symptoms of amenorrhea,
   in male, decreasing of libido, delayed or decreasing of the secondary sex characteristics e.g. the growing of beard, pubic hair, the difference between male and female voices.

6. Others or miscellaneous, such as: Optic Glioma, Acoustic Neuroma, Craniopharyngioma, Chordoma or tumour of notochord.

7. Metastatic Tumours to Brain: Bronchogenic Ca. Breast Ca, Thyroid Ca, etc.

INTRODUCTION

Brain Tumours are rather complicated because these are so many different kinds of cells in the brain with different funstone and different natural behaviours. In treating brain tumours, one must have to assess for the following questions: where is the lesion, the number of lesions, sinless or multiple, the natures of the lesions. The treatments have to be carefully planned which will depend as the position, the natures of the tumour, the staging, etc.

The management of brain tumour needs a broad field of knowledges and careful planning of treatment. The first step to do is to get the accrual diagnosis, the sooner, the better. The quickest and

most convenient diagnosis can be dried by CT and MRI, or bolt CT and MRI with or without contras media. Examples of cases will be shown systematically according to classification of Brain tumors and Diagnosis by CT and MRI.

CATEGORY I:

Case I. 1. Meningioma: left frontal lobe.
Clinical: Female, age 30 years, having Headache and weakness of extremities for 1 month. The Roentgen studies were done by CT. and MRI. with and without contrast media.

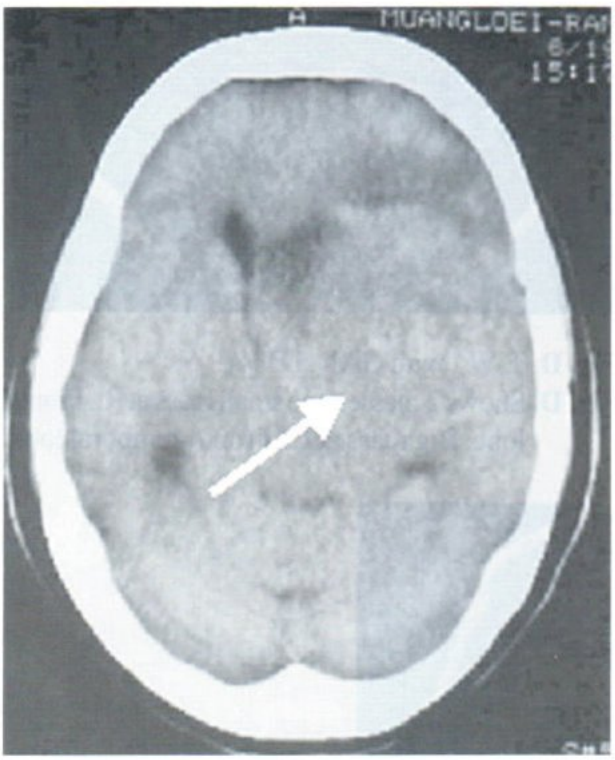

Fig. A Non-contrast. CT, show ill-defined mass at left fronto-temporal region displacing the lateral ventricle, anterior horn to the Rt. Side.

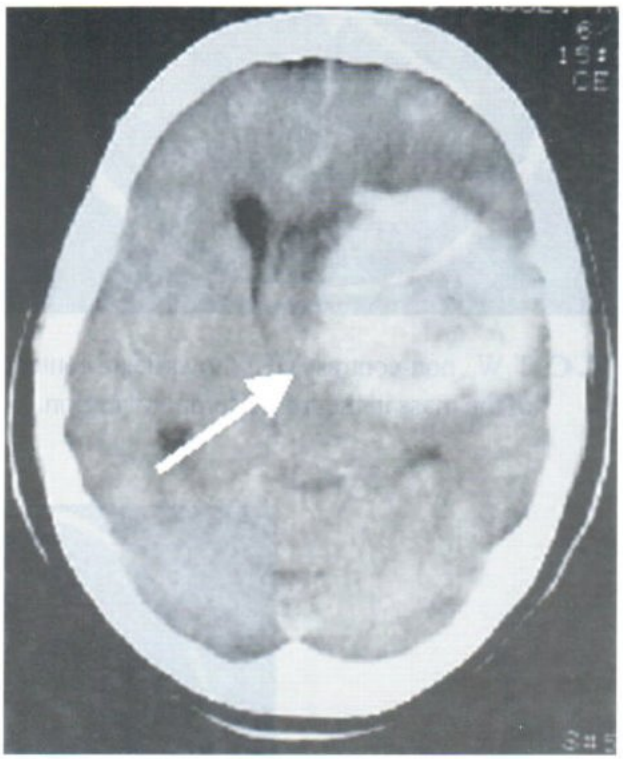

Fig. B Contrast enhancement CT. shows dense enhancing masses at left frontal lobe and one big dense enhancing mass at the fronto-temporal region.

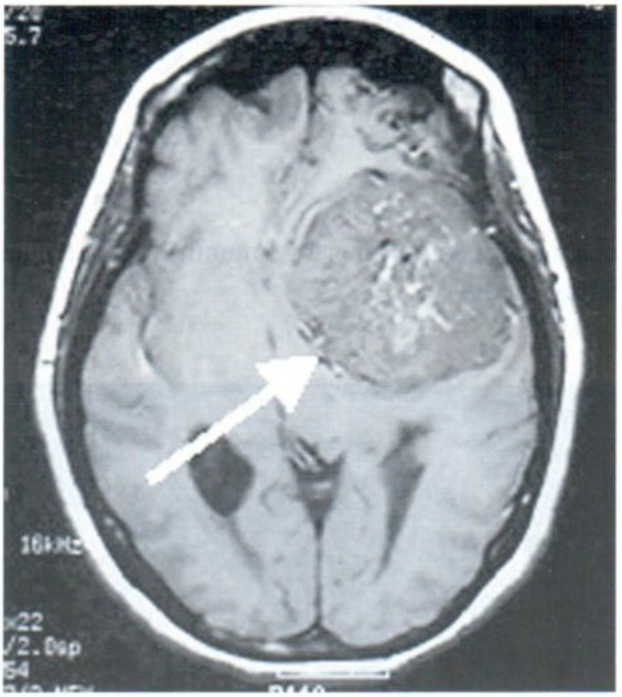

Fig. C T_1W_1, non-contrast MRI shows detail content of the mass in the fronto-temporal region.

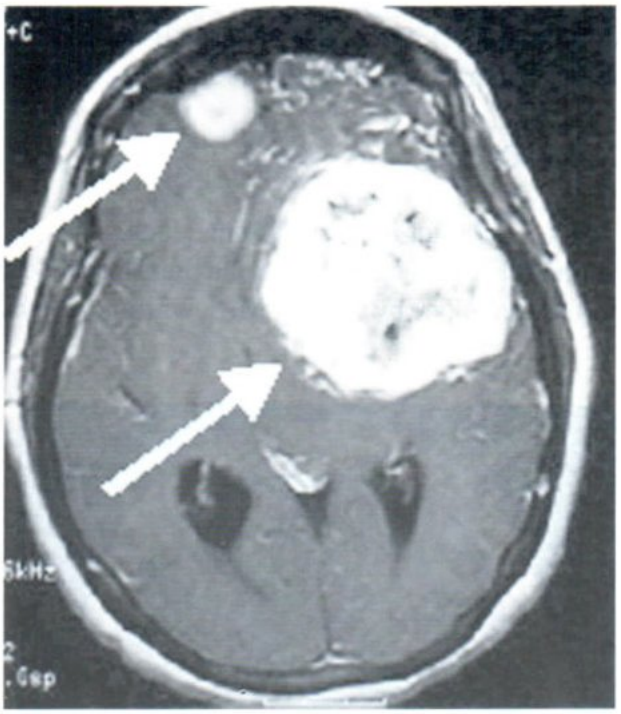

Fig. D T_1W_1, with GAD. DTPA
Fig. D Shows 2 masses one small mass at Rt. Frontal lobe. Big mass at Lt. Fronto-temporal lobe.

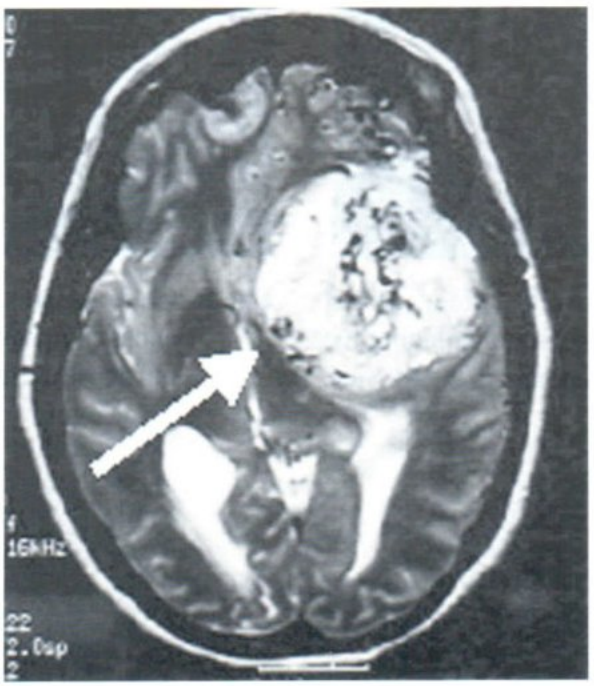

Fig. E T_2W_1, with GAD. DTPA

CATEGORY I:

Case II Meningioma: Petrous ridge Meningioma
Clinical: Female, 54 years, chief complaint hearing defect Rt. side.

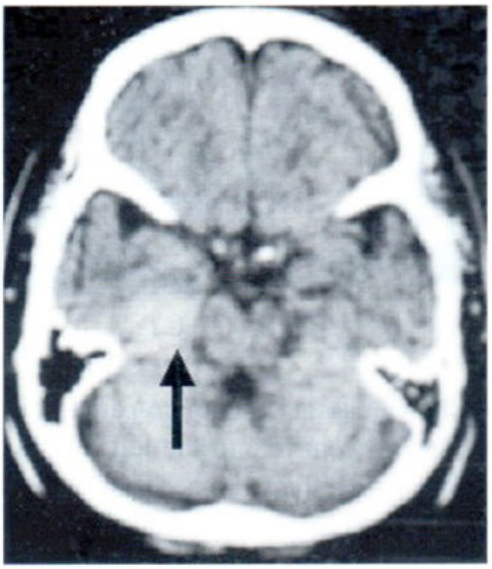

Fig. A Non-contrast CT shows ill defined mass at right petrous ridge.

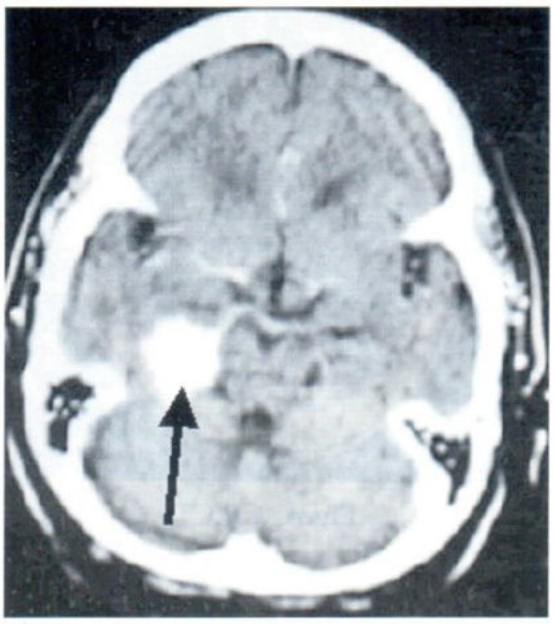

Fig. B Contrast enhancement CT. shows round opaque shadow at the posterior surface of Petrous ridge compatible with Meningioma.

CATEGORY II:

Case I Astrocytoma: grade II
Clinical: Girl: age 10 years. Headache, vomitting 1 week. Left upper and lower extremities weakening.

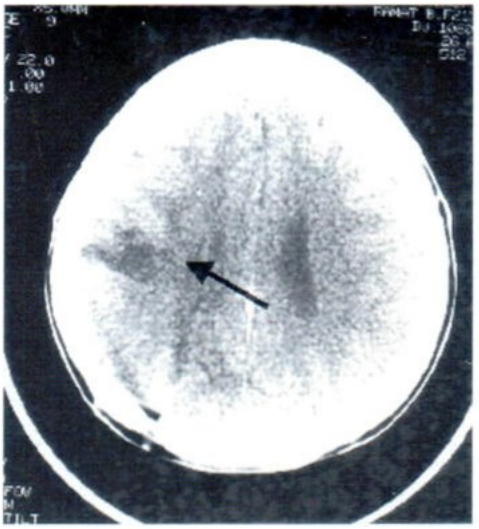

Fig. A NC.CT.

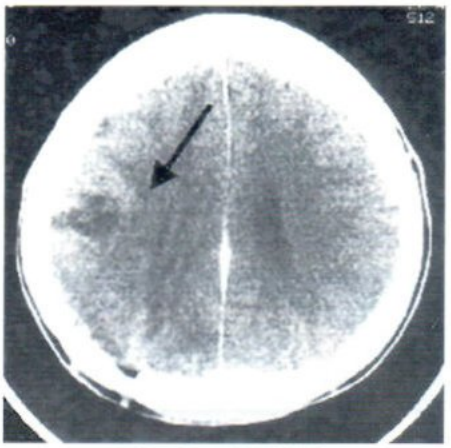

Fig. B CE.CT.

Fig. A and Fig B. NC.CT and CE.CT: An ill-defined non-enhancing mass at Rt. Frontal lobe.
Glia cells tumors are classified as: malignant-Astrocytoma, Grade I, II, III, and IV. Astrocytoma Grade IV have a special name as Glioblastoma Multiforme. Malignant-Oligodendroglioma have also been divided into Grade I to Grade IV according to their cellular differentiation, maturity, and malignant behaviours, the same as Astrocytoma but have no special name in Grade IV.

CATEGORY II:

Case II: Astrocytoma: grade IV (Glioblastoma Multiforme)

Clinical: Female, age 21 years. Headache 2 weeks, left hand and foot weakening.

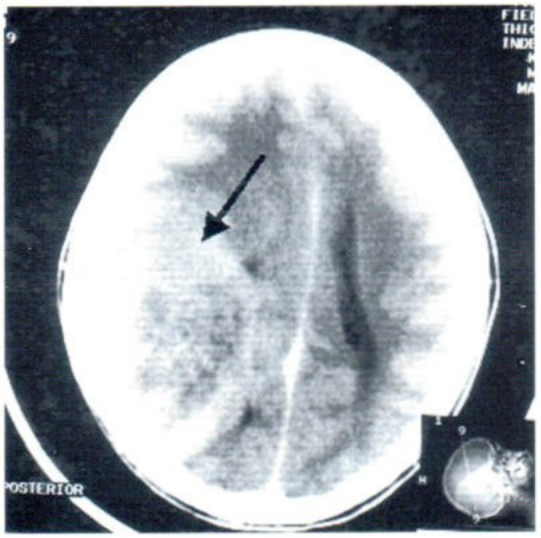

Fig.A NC.CT.

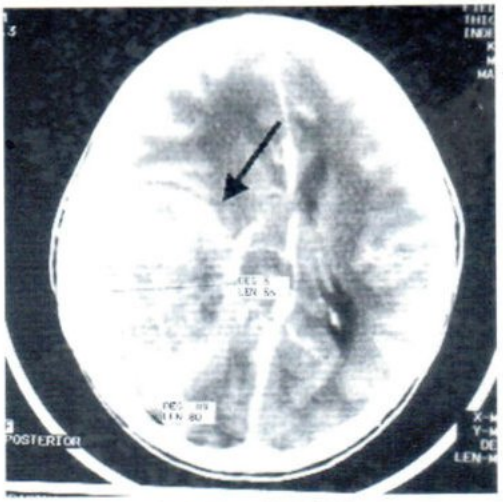

Fig.B CE.CT.

Fig.A. shows mass at Rt. temporo-parietal displacing the Rt. lateral ventricle to the left. **Fig.B.** shows enhancing mass Rt. Temporo-occipital lobe infiltrating larger area than Fig.A. and also invading into the Lt. lateral ventricle at the middle part.

CATEGORY II:

Case III: Glioblastoma Multiforme (GBM)

Clinical: Female, age 60 years, headache, vomiting, weak and drowsy, bed ridden for 1 week. Left upper and lower extremities are weak.

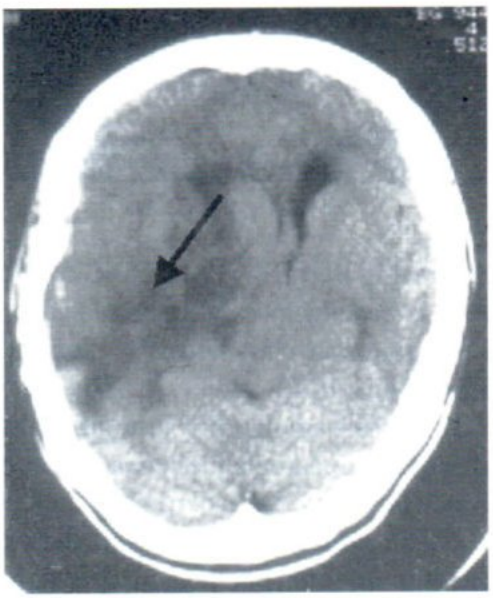

Fig.A NC.CT.

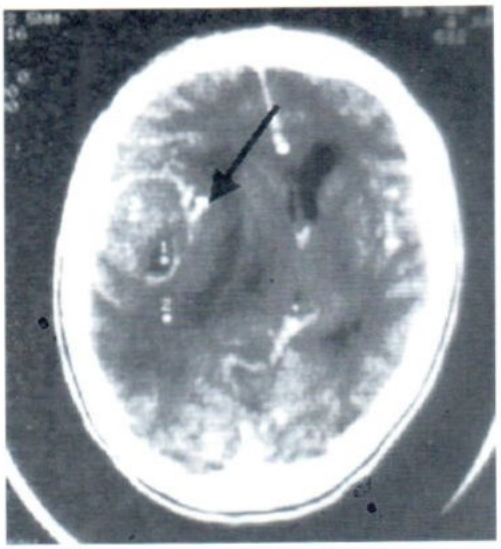

Fig.A CE.CT.

Fig. A. and **Fig. B.** show enhancing mass at Rt. Fronto-temporal lobe infiltrating into the right occipital lobe. The Lt. lateral ventricle is displaced with obliteration of the lower part.

CATEGORY II:

Case IV: Brain stem Glioma

Clinical: Girl, age 4 years. Weakness of both upper and lower extremities NC.CT. shows low density mass in the Pons.

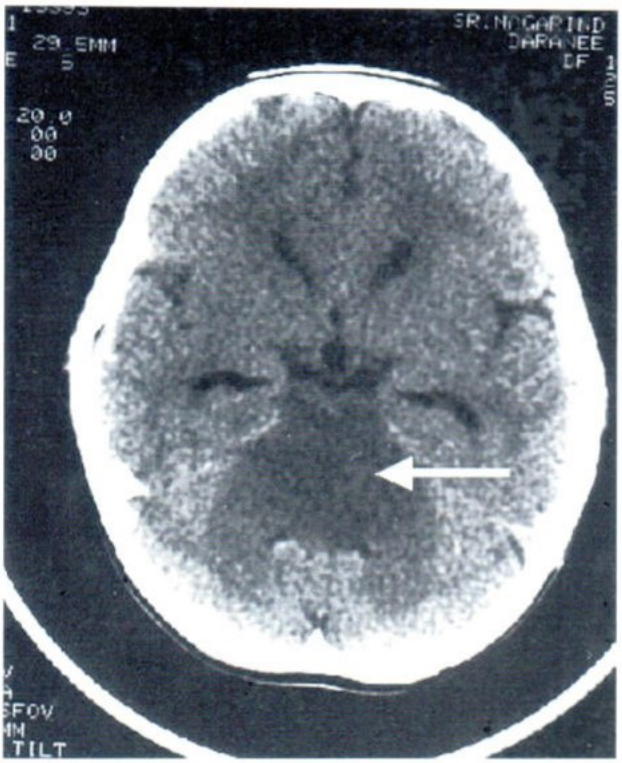

Pituitary Adenoma: There are 3 kinds of cells easily to be remembered A, B, C,

A and B are chromophilic which means having affinity to staining. The adenomas are small and called Microadenoma.

"A" cells are Acidophilic, Staining Red in the histologic section.

"B" cells type are Basophilic, staining Blue.

A. cells produced trophic hormones such as Somatotrophin or growth hormones, and Gonadotrophin, the sex stimulating hormones.

B. cells produce ACTH (Adreno-Cortico Trophic Hormones) causing Cushing Syndromes.

C. cells are called chromophobe, staining pink or neutrophilic. The adenomas are not producing hormones, growing fast and become macroadenomas, causing pressure effects to the neighboring organs and cells. The neighboring organ is optic chiasma causing monolateral or bilateral hemianopsia. The neighboring cells are the A. and B. cells. Pressure on hormone secreting cells caused deprivation of hormones depending on the numbers and types of the secreting cells.

Pressure on "A" cells in male patients will be resulted in decreased libido, the growing of beard will be delayed. In female patients, it will result in amenorrhea or hypomenorrhea, the delayed of menarche, and hypertrichosis.

CATEGORY III: Pituitary Microadenoma

Case I: Female, age 27 years, single, non-married, headache with abnormal nipple discharge without pregnancy.

Theoretical background: Pituitary Microadenoma, Acidophile cell type produced gonadotrophin stimulate ovaries to produce excess of estrogen. Lateral view of skull, normal sella turcica, no ballooning. Hypertension with or without symptoms detectable by taking blood pressure. Discharge or milk running through nipples in single, unmarried or married with no pregnancy, or not after post- partum period.

CT. and MRI with contrast or without contrast show Microadenoma at pituitary. Hormonal assay in the blood showed gonadotrophin and estrogen values increased than normal. Menstruation increased in number of days and quantities of blood in each period.

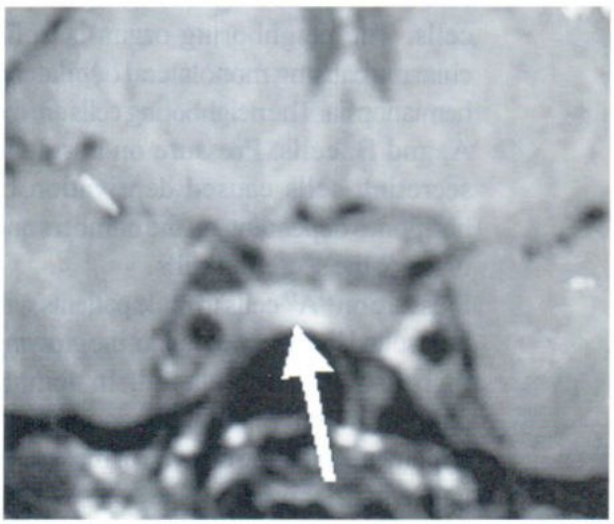

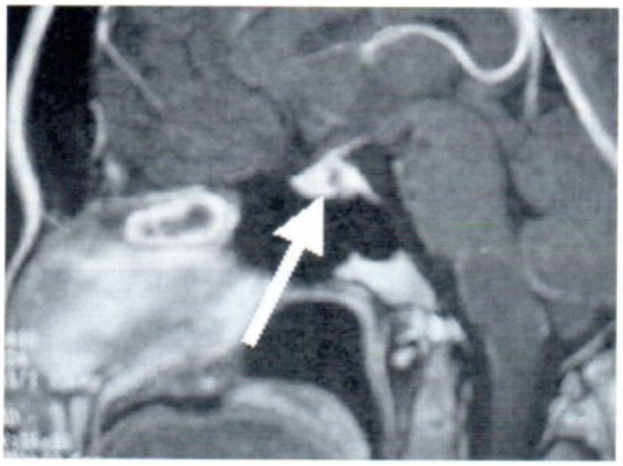

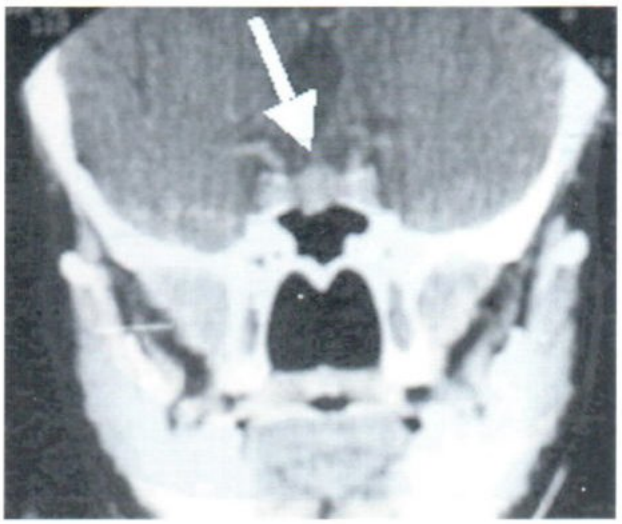

White arrow in each picture shows pituitary gland with microadenoma without ballooning of sella turcica.

CATEGORY III: Pituitary macroadenomas.

Case II: Male, age 43 years, headache, especially temporal region, for 1 month. Fields of vision, narrowing in the temporal fields both sides.

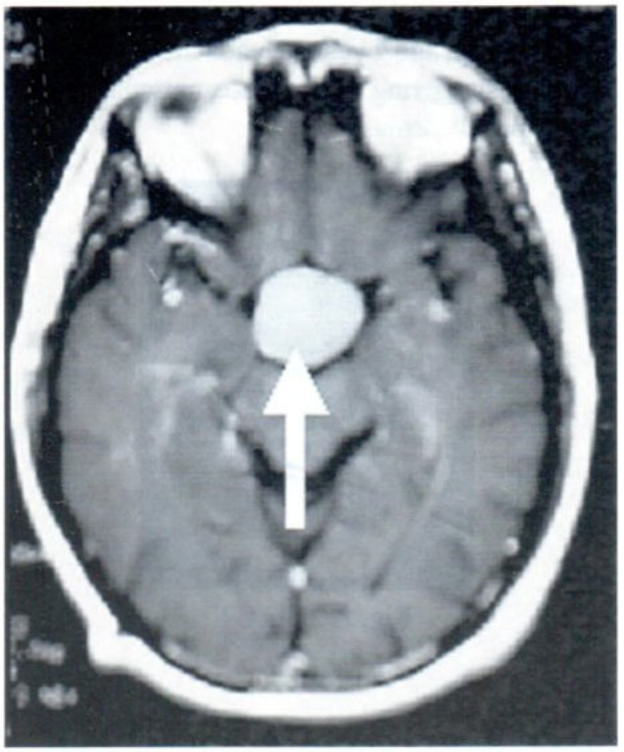

MRI. $T_1 W_1$ with Gad. DTPA enhancement

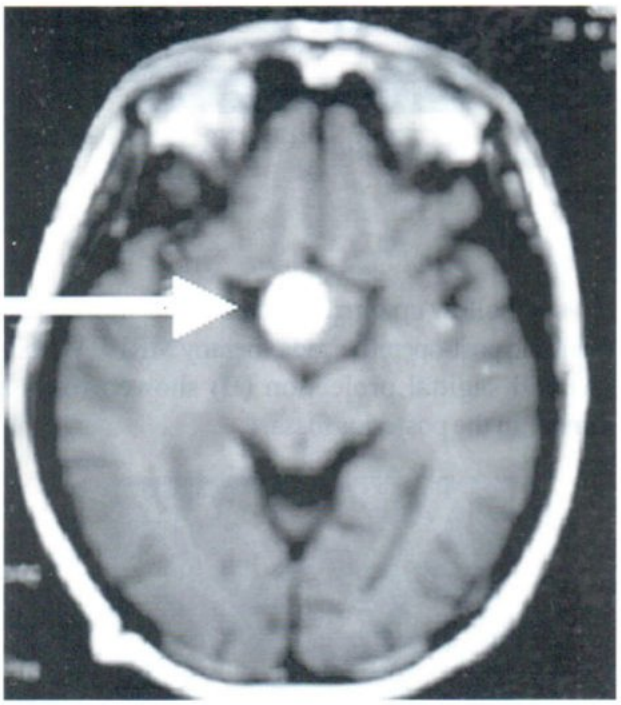

MRI. $T_1 W_1$ Pituitary Macro-Adenoma sella and suprasella parts.

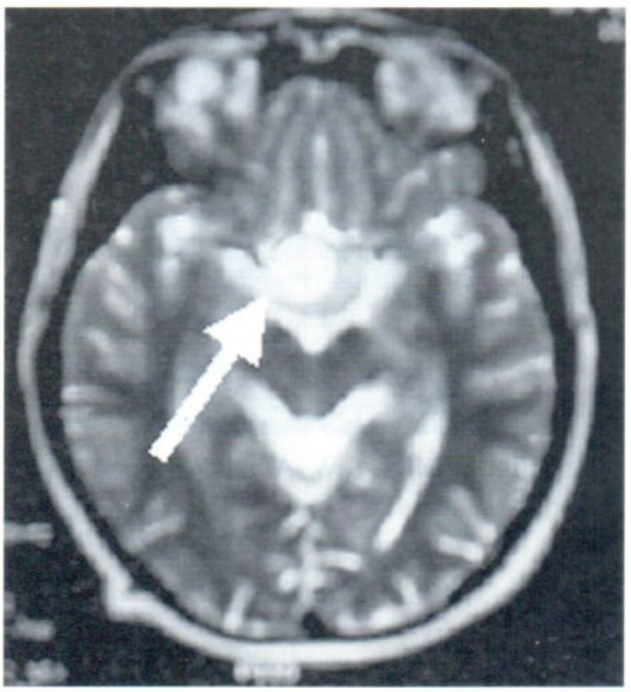

MRI. $T_2 W_1$ Pituitary adenoma sella and suprasella parts contrast enhancement.

CATEGORY: IV.1: Medulloblastoma. **Case I**
Clinical: Boy, age 4 years, Headache for 3 moths, vomitting, staggering, somnolence, muscular spasm, bilateral paplilledema.

A. Non-contrast CT. and **B.** Contrast enhancement CT. show enhancing mass at posterior fossa.

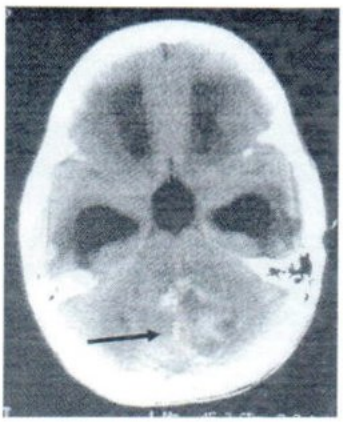

Fig. A NC.CT.

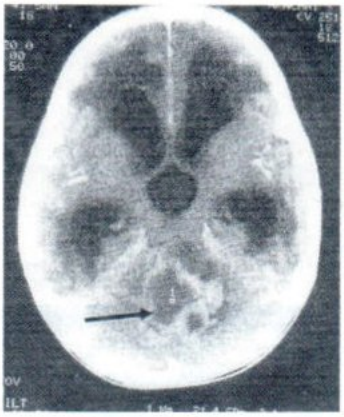

Fig. B CE.CT.

CATEGORY: IV. 2: Medulloblastoma **Case II**
Clinical: Medulloblastoma, age 9 years, headache for 3 months, cerebellar sign positive. Histopathology result: Medulloblastoma.

Follow up film 2 months after surgical treatment and post-operative radiotherapy MRI T_1W_1 axial **(A)** and sagittal projection **(B)** showed residual tumour in the posterior fossa.

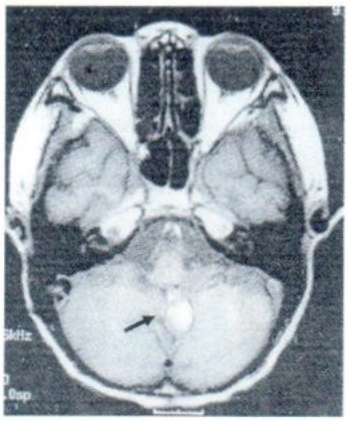

Fig. A MRI. T_1W_1 Axial projection

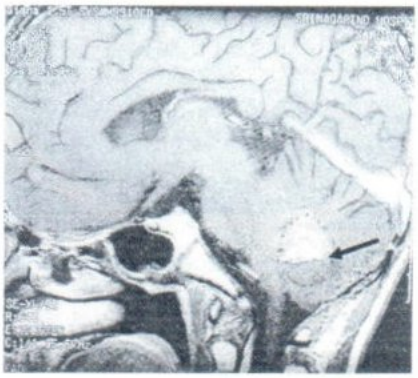

Fig. B MRI. Sagittal projection

CATEGORY V: Acoustic Schwannoma.
Clinical: Male, age 49 years, and loss of hearing Rt. ear.
Fig.A MRI, T_1 W_1 axial projection, **Fig.B** MRI. axial projection with contrast enhancement. Histopathology: Acoustic Schwannoma.

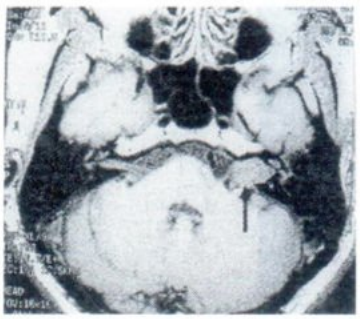

Fig. A Axial MRI. (black arrow)

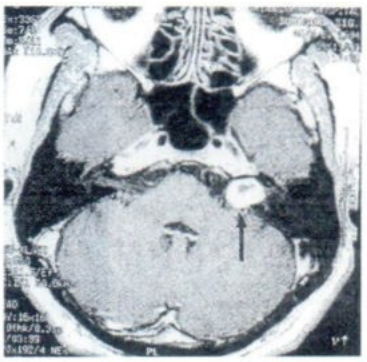

Fig. B Axial MRI. with GDPA enhancement.(black arrow)

CATEGORY VI: Acute Myelocytic Leukemia (AML)
Clinical: Girl, age 3 years, known case of AML. CT. of Brain **(A)** before contrast injection, **(B)** after contrast injection Contrast enhancing masses (black arrows) show extra axial masses in the CSF.

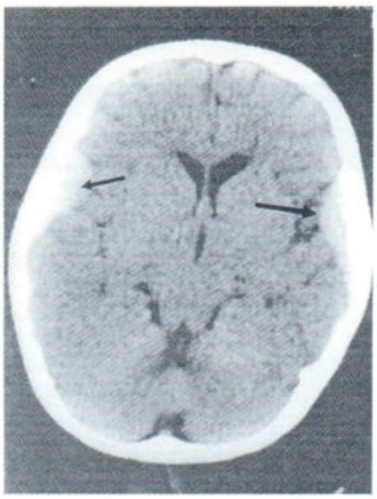

Fig. A NC.CT.

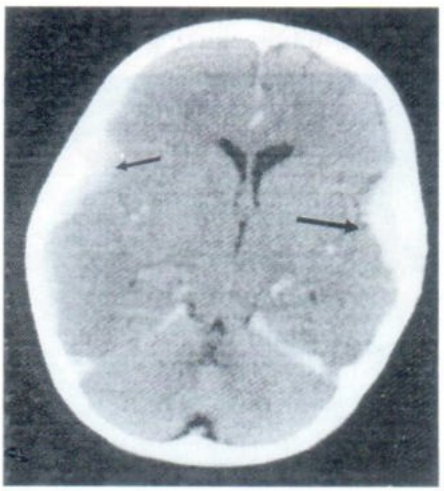

Fig. A CE.CT.

CATEGORY VII: Retinoblastoma

Clinical: Boy, 2 years old, known case of Retinoblastoma. After enucleating of Rt. eye. White arrow at the retina left eye, showing the mass. This is a case of bilateral Retinoblastoma occuring one after the other verifying a genetic cause.

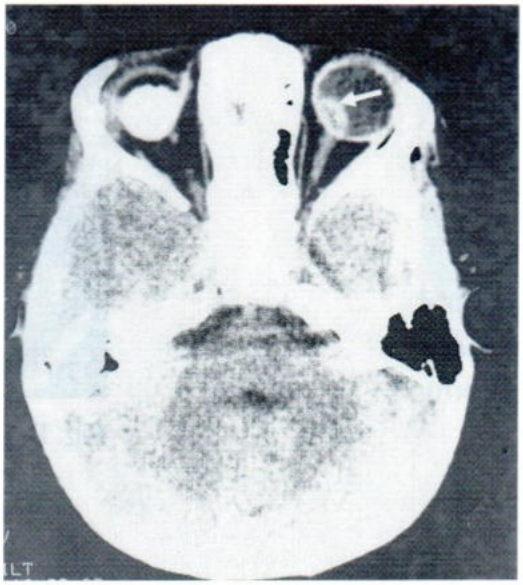

Fig. A White arrow Lt. eye showing Retinoblastoma occuring after enucleation of Rt. eye.

CATEGORY VIII: Brain metastases: CA. Thyroid.

Clinical: Female, age 53 years known case of CA. Thyroid, headache, vomiting.

Fig. A NC.CT. show ill-defined masses in both cerebral hemispheres.

Fig. B CE.CT. Multiple rim ring enhancing masses in both cerebral hemispheres (white arrows)

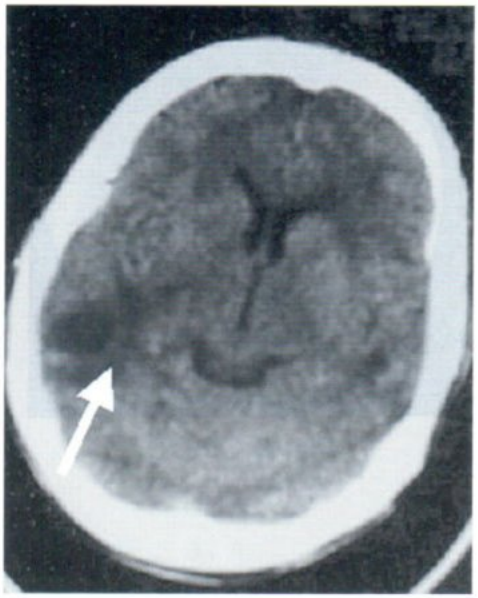

Fig. A NC.CT.

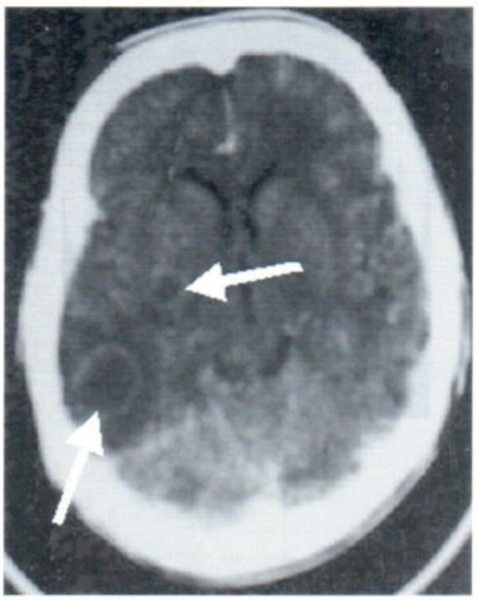

Fig. A CE.CT.

CATEGORY IX: Brain metastasis. Bronchogenic CA. (BCA.)
Clinical: Male, age 73 years, known case of Bronchogenic CA, headache, vomiting, somnolence.
Fig. A NC.CT.
Fig. B CE.CT
Enhancing mass, Haemorrhage in right frontal lobe, compressing and obstructing anterior horn of right ventricle making dilatation of anterior horn right side.

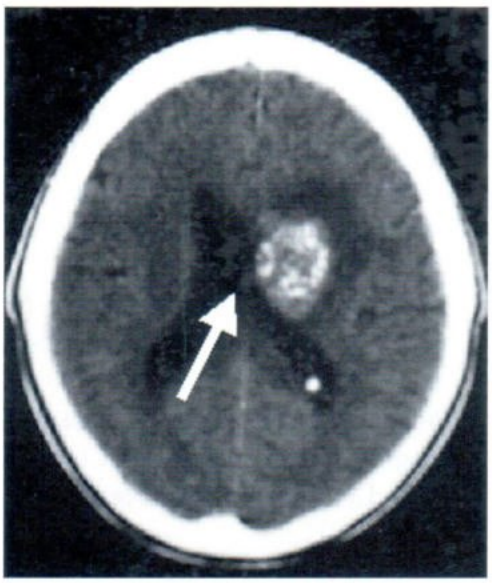

Fig. A NC.CT.

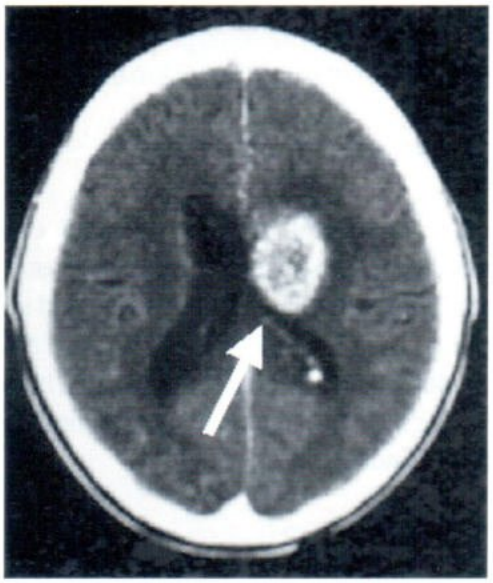

Fig. B CE.CT.

DISCUSSION

There are many kinds of classification of brain tumours in different text books and journals which are rather confusing. In this report we are reporting cases of brain tumours commonly found in Srinakarin Hospital and Medical School, Khon Kaen University, Khon Kaen, Thailand in the past 30 years.

In our Faculty of Medicine, Khon Kaen University Hospital, we have been using the International Classification base on the normal anatomical structures of human structures of Nervous System from the meningies, to the brain tissues, to the ventricles. All the normal contents of the brain tissues can be become a tumour which may be benign or malignant. All kinds of cell composition in the brain including the embryonal cell rest can become tumors and do the seedling along the cranio-spinal and the central nervous system via the CSF. around and inside the CNS. by the central canal of spinal cord and ventricles of brain in the skull. As in other systems of human body, brain tumors are divided into two big groups i.e, primary tumors and metastatic tumors. The primary tumors have the tumor cells originated from the varieties of normal cells of the brain contents, such as the meninges, the glia cells, the embryonal cells rest such as the pineal, the choroid plexus cells, the medulloblast, the ependymal cells, and the white blood cells in the CSF. causing leukaemia. The wall of blood vessels cells may cause tumors called haemangioendothelioma and haemangiopericytoma. The pituitary cells, A, B, C, also cause both hormones producing and hormone non-producing tumors. Making many different trophic symptoms in both male and female victims. The macro-adenoma may also cause pressure symptoms on the

adjacent cells and nerves causing deprivation of hormones if the surrounding cells are the hormones producing cells. If the adjacent structures are cranial nerve, it will cause dysfunction or non-function of the cranial nerve or nerves, detectable clinically by non-functioning of the cranial nerves which had been pressed by the tumors or tumors. Metastatic tumors in the brain may cause symptoms produced by both the primary and the metastatic tumors in the brain.

CONCLUSION

CT. and MRI. with or without contrast enhancement may be used either both or one after the other. This paper had demonstrated and studied the findings of CT. and MRI. of all these patients together with the laboratory blood chemistry, hormonal assay findings in correlation with clinical findings and pathological findings.

REFERENCES

1. Barkovich AJ. Pediatric neuroimmaging. New York: Raven Press, 1995
2. Blews DE, Wang H, Kumar AJ, et al. Intradural spinal metastases in pediatric patients with primary intracranial neoplasm: GD-DTPA enhanced MR versus CT myelography. J Compt Assist Tomogr 1990; 14: 730-735.
3. Castillo M. Contrast enhancement is primary tumors of brain and spinal cord. Neuroimaging Clin. North Am. 1994; 4: 63-80.
4. Chamberlain MC. Pedriatic aids: a longitudinal comparative MRI and CT. brain imaging study. J Child Neurol 1993; 8: 175-181.
5. Faerber E. Cranial computed tomography in infants and children. Philadelphia, PA: Lippincot 1986.
6. Sze G, Shin J, Krol G, et al. Intraparenchymal brain metastases: MR imaging versus contrast -enhanced CT. Radiology 1988; 168: 187-194.
7. Taphoorn MJ, Heimanas JJ, Kaiser MC, et al, Imaging of brain metastases. Comparison of CT and MR imaging. Neuroradiology 1989; 31: 391-395.
8. Wolf M, Ziegengeist S, Michalik M, et al. Classification of brain tumors by CT image Walsh Spectra. Neuroradiology 1990; 32: 464-466.

PITUICYTOMA; BENIGN SPINDLE CELL TUMOR OF POSTERIOR PITUITARY GLAND: A CASE REPORT

Hungspreug, S M.D., Phudhichareonrat, S M.D., AND Leum-udom, A M.D.

ABSTRACT

Pituicytoma is one of the rare benign primary tumors of the posterior pituitary gland, originated from intrinsic special glial cells of the gland. The previous nomenclature of posterior pituitary tumors has been confusing with pituicytoma. "Pituicytoma" should be neurohypophyseal astrocytoma only. Clinical and laboratory presentations as well as neuroimaging are not specific; the correct diagnoses are achieved only after histopathological examinations. This article revealed a clinical presentation, neuroimaging findings and pathological features of a large sellar/suprasellar tumor in a 46-year-old male, having diagnosed of pituicytoma.

INTRODUCTION

Tumors occupying the sellar and suprasellar spaces are common, and their morphologic spectrum is well known. Most frequently encountered are pituitary adenoma, meningioma, craniopharyngiomas, germ cell tumors, gangliogliomas, harmatomas, epidermoids, lipomas and metastasis. The most common tumors found in the posterior pituitary are secondary metastases presumably due to the rich vascular supply.[1] Intrinsic tumors arising in the posterior pituitary gland are very rare. Pituicytoma is one of the rare, poorly characterized benign primary tumors of the posterior pituitary gland, originated from intrinsic special glial cells (modified astrocyte) of the gland. There were only four reported cases of this astrocytic tumors published during 1994 -2001. This case report contains clinical presentation, neuroimaging findings and pathological features of this type of tumor that may masquerade as the pituitary adenoma.

CASE REPORT

A 46-year-old Thai male was referred to the Prasat Neurological Institute, Bangkok for the evaluation of a sellar/suprasellar mass. He complained of 8-month history of progressive decreased vision that more pronounced on the left eye. He was recognized of narrowed visual field, especially on the temporal side. One-weak before admission, he complained of dizziness and blindness. He denied increased urination, diminished secondary sexual hair, weight gain or loss or galactorrhea. His medical history was unremarkable.

Physical examination on admission revealed a well-nourished man with no signs of hypophysial dysfunction. Neurological examination showed severe visual impairment of both eyes; finger count on the right and hand movement on the left. There were an afferent pupillary defect on the right and non-functioning on the left. Fundoscopic examination revealed left optic disc atrophy. The remainder of his neurological examination was normal.

Laboratory studies including electrolytes, blood glucose, urinalysis and a complete blood count were all within the normal limits. The endocrine studies

Department of neuroradiology, neuropathology and neurosurgery, Prasat Neurological Institute, Bangkok, Thailand.

for the pituitary gland were normal except for decreased serum level of morning cortisol to 0.58 mg/dl (normal 4.3 -22.4 mg/dl).

Preoperative computed tomography revealed a well-defined, midline mass in the sellar region with suprasellar extension. The tumor was solid, homogeneous attenuation and slightly denser than brain (fig 1). Homogeneously intense enhancement was noted after administration of contrast media (fig 2, 3). MRI of the brain with gadolinium revealed a large, sellar-suprasellar mass that displaced and compressed the optic chiasm and optic tracts, more on the left. The mass was hypointense on T1W image, had heterogeneously and moderately enhancement with gadolinium, and heterogeneous increased signal intensity on T2W image (fig 4, 5, 6). The tuber cinereum and stalk were not identified as well as non-visualized normal posterior pituitary bright spot. The radiological appearances could not distinguished from those of macroscopic pituitary adenoma.

The patient received 1-day preoperative intravenous hydrocortisone and underwent a right supraorbital craniotomy. The tumor was confined below right optic nerve and compressed and distorted right and left A1-ACA and left optic nerve. The olfactory nerve was also compressed by the tumor. Nearly total tumor removal was performed and the residual tumor was situated above the right optic nerve.

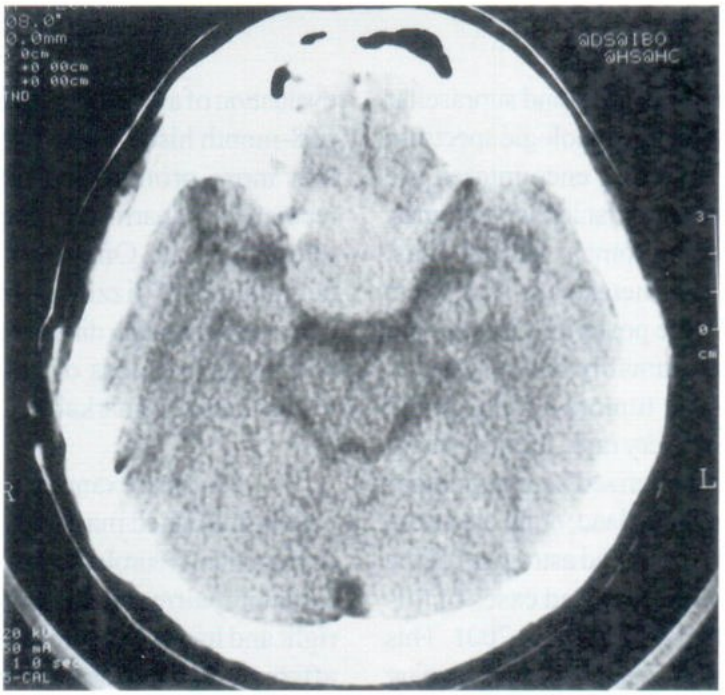

Fig 1 Non-enhanced axial CT scan shows midline homogeneous mild hyperattenuated-solid mass occupying within sellar region with suprasellar extension

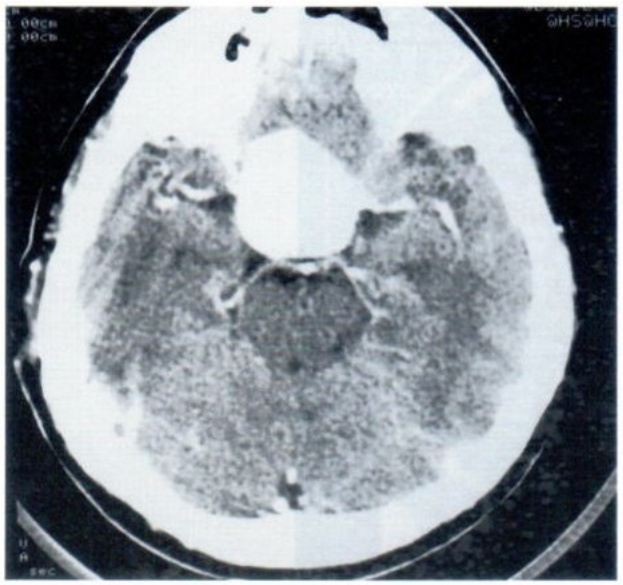

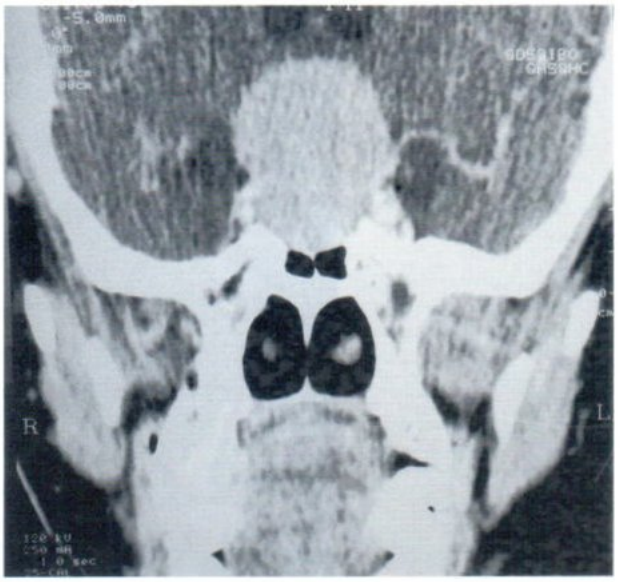

Fig 2 Axial and **Fig 3** coronal contrast enhanced CT reveals a large homogeneous intense enhancement to the mass that is occupying in a ballooning sellar turcica with suprasellar extension, giving a figure -of-eight in appearance.

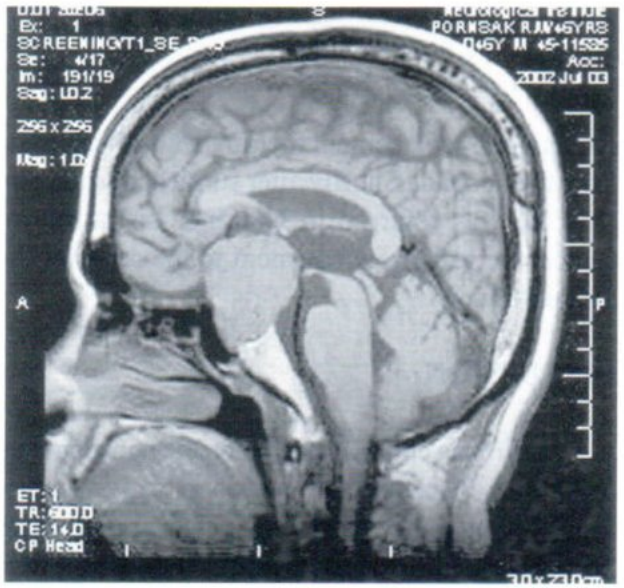

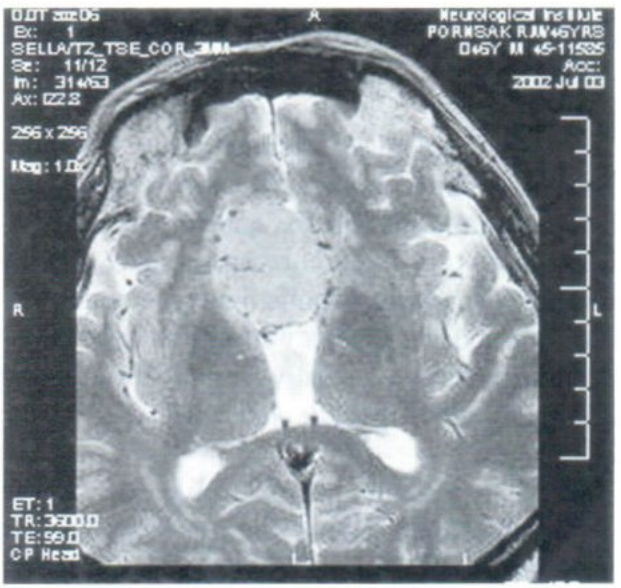

Fig 4 MRI sagittal SE T1 (TR/TE 600/14) in midline slice and **Fig 5** axial FSE T2W (TR/TE 3300/58) show a large sellar-suprasellar mass of relatively hypointense to gray matter on T1W and heterogeneous hyperintensity signal on T2W. The normal posterior pituitary bright spot is absent. The pituitary stalk could not be identified as the tumor size is large. Also noted on T2WI, there are prominent vascular signal void structures around the mass.

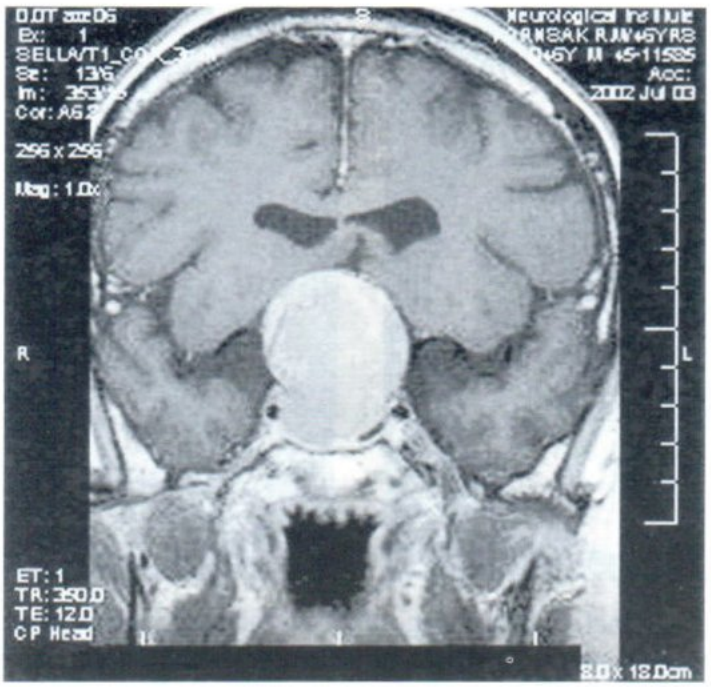

Fig 6 MRI coronal T1W (TR/TE 350/12) scan following intravenous gadolinium injection shows rather heterogeneously and modeately enhancement of the tumor mass.

On histological examination, the submitted tissue consisted of moderately cellular tumor. The tumor cells are medium in size, spindle shape and have round to ovoid, hyperchromatic nucleus with moderate cytoplasm. Mitotic figure, necrotic area, microcyst and granular body are absent. In addition, the tumor cells give a positive result with antibody against glial fibrillary acidic protein (GFAP).

The patient's postoperative course was uneventful. No episode of diabetes insipidus was documented. The hormonal assays in the fourth postoperative day showed slightly elevated serum level of morning cortisol to 2.4 mg/dl, but still lower than normal serum level (normal 4.3 -22.4 mg/dl). Decreased serum levels of LH2 and FSH were reported about 0.03 mIU/ml (normal 1.5 -9.3 mIU/ml) and 0.32 mIU/ml (normal 1.4 -18.1 mIU/ml), respectively. He was doing-well and receiving oral predisolone replacement therapy when discharged from the hospital. Shortly after surgical decompression, he was referred to National Institution of Cancer for radiation treatment to the sella for the residual tumor.

DISCUSSION

From a clinical standpoint, the nonadenomatous lesion in the pituitary region may give a radiological appearance identical to that of a pituitary adenoma and lead to misdiagnosis. Because intrinsic tumors arising in the posterior pituitary gland are very rare, the sellar region tumors are often thought to represent other more frequently occuring tumors such as pituitary adenoma, craniopharyngioma, germ-cell tumor or meningioma as well as other less common lesions such as metastatic carcinoma, schwannoma and chordoma.

The previous nomenclature has been confusing, the term "pituicytoma" have been used for a variety of tumors of the posterior pituitary[2] such as granular cell myoblastoma,[1] granular cell tumor, and choristoma.[3,4,5] The pituicytoma is most commonly found in older female people, with a sex ratio of 2:1 and in general appears after than the age of 30.[3,5] Few cases have clinical symptoms but most symptomatic tumors have been diagnosed as craniopharyngioma or meningioma before surgery.[4]

The clinical manifestations of the tumor of neurohypophysis or pituitary stalk are usually nonspecific such as headache and hypopituitarism. Compression of the optic pathways, causing loss of visual acuity, visual field defects (bilateral temporal field deficits) and optic atrophy, frequently occurs.[6,7] Mark suprasellar expansion may obstruct the third or lateral ventricles, causing signs of hydrocephalus or increased intracranial pressure.[8] Despite the involvement of the neurohypophysis and the pituitary stalk, diabetes inspidus is not a typical feature.[7] Clinical or laboratory signs of partial pituitary insufficiency or hyperprolactinemia, presumbly caused by the stalk effect.[8]

Anatomically, the neurohypophysis includes the posterior lobe of the pituitary (infundibulam process), the stalk or infundibular stem, and the median eminence of the tuber cinereum. The cellular elements that found in the posterior pituitary include pituicytes, microglia, portal blood vessels and terminal aborizations of the hypothalamic neurosecretory neurons. Pituicytes are considered to be modified glial cells.[1] On the current studies, most investigators consider pituicytoma to arise from pituicytes or Schwann cells of the posterior lobe of the hypophysis.[4] Hurler T, et all[1] as well as Rossi ML, et al[2,9] concluded that the term "pituicytoma" should be reserved for neurohypophyseal astrocytoma since the tumor are reviewed by some to originate from intrinsic glial cells of the gland, or the pituicytes.

There are only a few reports that clearly described the neuroimaging features of astrocytomas in the sellar region.[2,9] The tumor may occupy the stalk, posterior lobe or both. Computed tomogram show sharply-demarcate isodense or hypodense tumor with homogenous dense enhancement after administration of contrast medium. MRI also shows solid and partly cystic, discrete masses, which are usually isointense on T1W image, hyperintense on T2W images and which become hyperintense with contrast enhancement. If the tumor is large, the pituitary stalk and pituitary gland are not identified.[9]

Surgical removal by transphenoidal approach, which was associated with considerably less morbidity than was craniotomy, is the therapy for these tumors, as for other sellar lesions. The surgical goal should be limited to decompression of the suprasellar if total excision seems too hazardous.[10] Although curable by total excision, subtotal resection can be associated with recurrence.[11] Postoperative radiation therapy appears to further increase the mean survival time and extent time to tumor recurrence after subtotal resection.[8]

CONCLUSION

Such clinical appearances, laboratory datas and neuroimaging findings of the pituicytoma are not specific and may also be observed in other neoplasms of the sella, and probably because of their rarity, none have been diagnosed preoperatively.[5] Solid contrast-enhancing masses in the sellar region, are often thought to represent other frequency sellar region tumor such as pituitary adenoma. The correct diagnoses of these tumors are usually achieved only after histopathological examinations of tumor tissue. From the study of this case, the diagnosis of pituicytoma should be considered if the tumor is suspected to be originated in the posterior lobe of the pituitary gland.

REFERENCE

1. Hurley TR, D'Angelo CM, Clasen RA, et al. Megnetic resonance imaging and pathological analysis of a pituicytoma: case report.Neurosurgery 1994 Aug; 35(2): 314-317.
2. Rossi ML, Bevan JS, Esiri MM, et al. Pituicytoma (pilocytic astrocytoma). J Neurosurg 1987 Novr; 67: 768-772.
3. Sholkoff SD, Kerber C, Cramm RE, et al. Parasellar choristoma. Am J Roentgenol 1977 Jun; 128:1051-1052.
4. Ji CH, Teng MMH, Chang T. Granular cell tumor of the neurohypophysis. Neuroradiology 1995; 57: 451-452.
5. Lafitte C, Aesch B, Henrey-Lebras F, et al. Granular cell tumor of the pituitary stalk. J Neurosurg 1994 Jun; 80:1103-1107.
6. Roncaroli F, Scheithauer BW, Cenacchi G, et al. Spindle cell oncocytoma of the adenohypophysis: a tumor of folliculostellate cells? Am J Surg Pathol 2002; 26(8): 1048-1055.
7. Losa M, Saeger W, Mortini P, et al. Acromegaly associated with a granular cell tumor of the neurohypophysis: a clinical and histological study. J Neurosurg 2000 Jul; 93:121-126.
8. Schaller B, Kirsch E, Tolnay M, et al. Symptomatic granular cell tumor of the pituitary gland: case report and review of the literature. Neurosurg 1998 Jan; 42(1): 166-170.
9. Uesaka T, Miyazono M, Nishio S, et al. Astrocytoma of the pituitary gland (pituicytoma): case report. Neuroradiology 2002; 44:123-125.
10. Becker DH, Wilson CB. Symptomatic parasellar granular cell tumors. Neurosurgery 1981 Feb; 8(2): 173-180.
11. Brat DJ, Scheithauer BW, Staugaitis SM, et al. Pituicytoma: a distinctive low-grade glioma of the neurohypophysis. Am J Surg Pathol 2000 Mar; 24(3): 362-368. à 11

CHORDOID MENINGIOMA: A case report.

Noppaklao ITTIPHANITPHONG,M.D.[1]

ABSTRACT

"Chordoid meningioma" is an uncommon histopathological variant of meningioma. I report a case of chordoid meningioma occurring in a 53 year-old female patient. Nonenhanced CT scan of the brain showed a low density mass(25HU) with rimlike calcification and surrounding edema in left temporal lobe.The enhancement was thick-irregular ring configuration.This mass presented as intra-axial location.Its lateral margin was close to left sylvian fissure,but no border revealed dural attachment.

Surgical excision was performed and the pathologic result established the definit diagnosis.

INTRODUCTION

Meningiomas are some of the most common intracranial tumors.The 1993 World Health Organization classification of CNS tumors described 14 distinct histopathological variants.[1] One of these variants is the chordoid meningioma,a very rare subtype,that comprises approximately 0.5% or less of all meningiomas.[2]

The term "chordoid meningiomas" was first used by Kepes et al in 1988 to describe meningiomas that were composed of spindle or epithelial cells forming chordoma-like clusters and cords,in a myxoid matrix.Prominent lymphoplasmacellular infiltration was also a feature in these tumors.[3]

A literature survey revealed that the majority of case reports were discussed mainly on the clinical manifestations and histopathology. In this report,I describe a case of chordoid meningioma, highlighting the strange CT features.

CASE REPORT

A 53 year-old female patient presented with a four-year history of psychosis.Seven days before admission,she had many episodes of focal seizures with loss of consciousness.Physical and neurological examination was unremarkable.

In a routine laboratory test,the hemoglobin, mean corpuscular volume and mean corpuscular hemoglobin were 11.0g/dL,85.8fL and 27.7pg, respectively.Normocytic hypochromic anemia was noted.The total protein,albumin and globulin were 8.7g/dL,3.1g/dL and 5.6g/dL, respectively.

Axial computed tomography(CT) of the brain revealed a hypodense lesion(25HU) with rimlike calcification and moderate degree of surrounding edema in left temporal lobe(Figure 1). Intense thick irregular ring enhancement was seen on post contrast study(Figure 2).Lateral margin of the mass was close to left sylvian fissure,but no dural attachment was seen.There was no bone destruction or hyperostosis.

[1] Department of Radiology, Sawanpracharak Hospital, Nakornsawan, THAILAND 60000

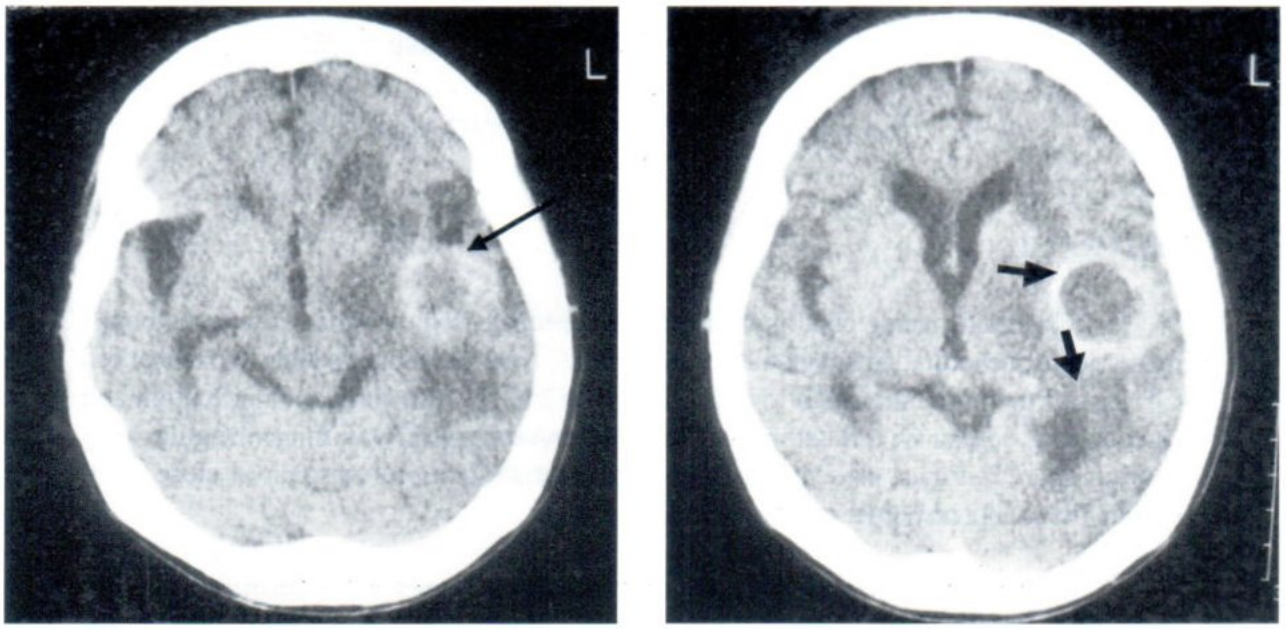

A B

Fig. 1 (A and B) Axial nonenhanced CT scan of the brain showed a low density mass (25HU) at left temporal region. Lateral margin of the mass was close to left sylvian fissure (black arrow), but no dural attachment was seen. Rimlike calcification (arrowhead) and perilesional edema were noted.

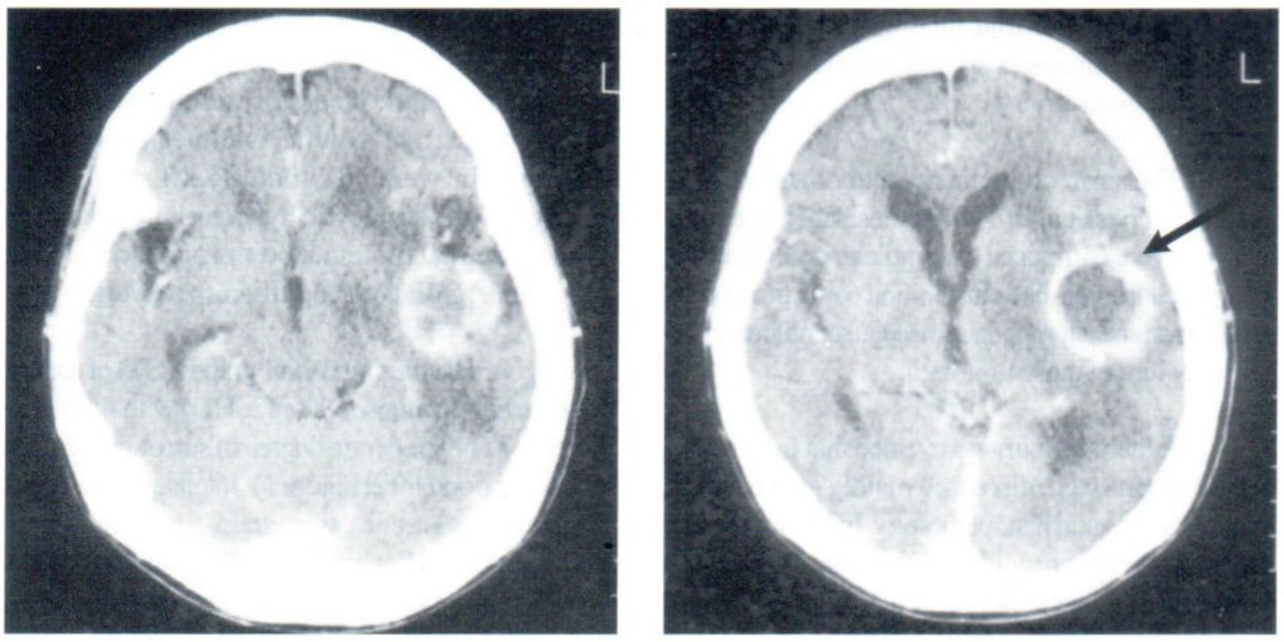

A B

Fig. 2(A and B) Axial contrast-enhanced CT scan of the brain showed intense thick irregular ring enhancement (black arrow) of the left temporal mass.

No precise diagnosis could be made because of its findings were not typical for any type of brain lesion.The differential diagnosis for calcified brain mass was considered among tuberculoma,astrocytoma, oligodendroglioma,ependymoma and meningioma.

The patient underwent a left temporal craniotomy for tumor resection. At surgery,the mass was intra-axial,near to left sylvian fissure and not adherent to dura.It appeared well-defined,centrally cystic (containing straw-color,high-proteinaceous fluid) with whitish hard solid wall that suspected to be calcified.The mass was 3 cm in size.Nearly all part of this mass was removed and sent for histopathological examination.Some part of this mass was left due to arterial attachment.Postoperative diagnosis was between cystic glioma and tuberculoma.

At pathology,the specimen consisted of trabeculae of eosinophilic vacuolated cells in the mucoid matrix.There were prominent lymphocytic-plasmacytic infiltrate within the stroma(Figure 3,4). Immunohistochemically,tumor cells showed a typical membranous staining of meningioma for epithelial membrane antigen in focal areas(positive EMA). None of tumor cells expressed glial fibrillary acidic protein(negative GFAP). All these findings were consistent with those of chordoid meningioma.

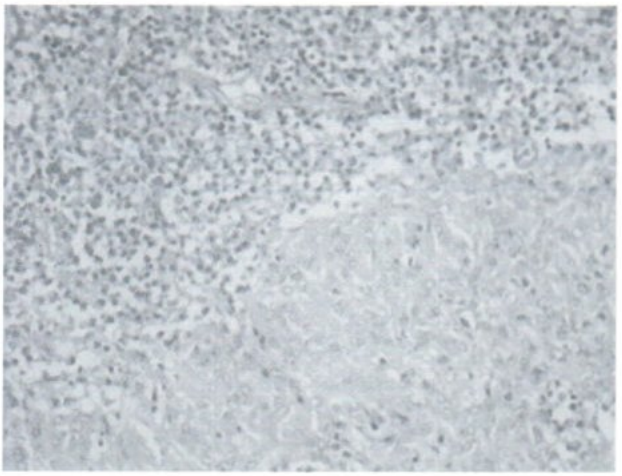

Fig. 3 The stroma (upper left) contains a lymphocytic-plasmacytic infiltrate. The tumor is seen in the lower right consisting of vacuolated cells.

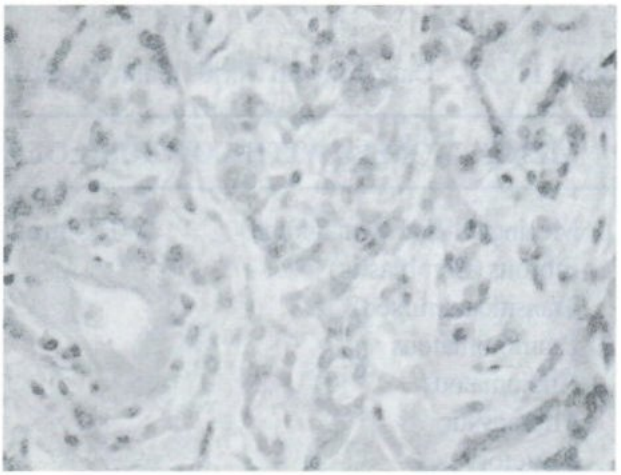

Fig. 4 The tumor is predominantly composed of eosinophilic, vacuolated cells formin trabeculae similar to chordoma.

DISCUSSION

Meningiomas are generally benign tumors comprised of neoplastic meningothelial cells of the arachnoid. They are the most common nonglial primary brain tumor and the most common intracranial extra-axial neoplasm.[4]

Meningiomas are thought to be adult tumors;peak occurrence is between 40 and 60 years of age. Incidence in women outnumbers that in men.[4]

Less than 10% of all meningiomas ever cause symptoms5.A variety of clinical signs and symptoms based on compression of surrounding structures. The patient's symptoms depend entirely on the location of the tumor;although headache,personality change, paresis and seizures are comprise of the classic presentation.[6]

Most meningiomas are extra-axial dural-based lesions.The most common sites of occurrence

included: cerebral convexities ,parasagittal region, sphenoid ridge,parasellar region ,olfactory groove and posterior fossa.[6] Approximately 2% of intracranial meningiomas have no dural attachment.These tumors arise from choroid plexus stromal cells and grow as intraventricular masses.[7]

Plain and contrast-enhanced CT scan detect 85% and 95% of intracranial meningiomas, respectively.[8] NECT scans typically show a sharply circumscribed round or smoothly lobulated mass that abuts a dural surface,usually at an obtuse angle. Approximately 70% to 75% of all meningiomas are homogeneously hyperdense relative to adjacent brain, 25% appear isodense. Hypodense tumors are seen in 1% to 5% of cases and true cystic meningiomas with large intratumoral fluid-filled cysts are also uncommon.[4] Calcification is seen in 20% to 25% and can be diffuse,focal, sandlike,sunburst,globular and even rimlike patterns.[4] Peripheral edema is seen in 60% of cases and may be extensive. CECT scans show intense, relatively uniform enhancement in 90% of all cases. 10% to 15% of meningiomas have an atypical pattern with rimlike tumor enhancement.[9-10]

There are many different histologic subtypes of meningiomas.The WHO classified variable histologic variants based on risk of recurrence and aggressive behavior (Table 1)

Table 1 Data from the world Health Organization classification of Tumors

MENINGIOMAS WITH LOW RISK OF RECURRENCE AND AGGRESSIVE GROWTH	
Meningiothelial meningioma	WHO grade I
Fibrous (fibroblastic)	
Transitional(mixed)	
Psammomatous	
Angiomatous	
Microcystic	
Secretory	
Lymphoplasmacytic-rich	
Metaplastic	
MENINGIOMAS WITH GREATER LIKELIHOOD OF RECURRENCE AND/OR AGGRESSIVE BEHAVIOR	
Atypical	WHO grade II
Clear cell	
Chordoid	
Papillary	WHO grade III
Anaplastic (malignant)	

NECT = Non-enhanced CT., **CECT** = Contrast-enhanced CT.

Kepes et al for the first time, described "Chordoid meningioma"as a distinct meningeal tumor occurring in children and this was associated with systemic manifestations such as refractory microcytic anemia, hypergammaglobulinemia and angiofollicular lymphoid hyperplasia (Castleman disease).[11]

Histopathologically, these tumors were composed of spindle or epithelial cells forming chordoma-like clusters and were scattered in a myxoid matrix. Prominent lymphoplasmacellular infiltration was also a feature in these tumors.[3] In a large series of 42 patients with mean age about 44 years old studied by Couce et al and a 33 year-old case reported by Je-young Yeon et al observed that none of their cases had any systemic manifestations as reported by Kepes et al.They expressed the possibility that the systemic manifestations associated with this tumor are limited to chordoid meningiomas occurring in the childhood.[2,12]

De Tella Jr. et al reported CT findings of a case of chordoid meningioma who showed a large high density mass at right temporal region with dense contrast enhancement and minimal peritumoral edema.[13] Varma et al reported two cases of chordoid meningioma. The first case appeared isodense lesion with heterogeneous enhancement and mild perilesional edema in right frontal parasagittal region. The second case showed a well-defined heterogeneous hypodense mass in right frontal parasagittal region, a broad base towards the anterior third of the falx cerebri with heterogeneous enhancement and moderate perilesional edema causing mass effect and subfalcine herniation.[14]

Similar findings of the CT images of our case and the previously reported cases is evident of perilesional edema, but the mass density, location and pattern of enhancement are different.

In our case,because it appeared intra-axial location,with large intratumoral cyst,rimlike calcification and ring enhancement,which are not classic pattern of meningiomas,leading to differential diagnosis among intra-axial lesions such as astrocytoma, oligodendroglioma, ependymoma and tuberculoma. Even surgical findings did not indicate meningioma. Pathological and immunohistochemical diagnosis was necessary.

Generally,meningioma is considered for a mass adherent to falx or dura, however,we found that meningioma cannot be entirely excluded for an intra-axial mass as well.

Chordoid meningioma is classified as WHO gradeII, by its aggressive behavior and high recurrence rate, particularly after subtotal resection. Periodic follow-up and imaging studies after surgery are indicated.[6]

CONCLUSION

I report unusual or misleading CT features that may not be suggestive of meningioma such as intra-axial location, large intratumoral cyst,rimlike calcification and ring enhancement that proved by histopathology to be a very rare subtype,chordoid meningioma. Because meningiomas are common,the radiologist must be aware of their less frequent and uncharacteristic imaging features in order to suggest the correct diagnosis in cases that are atypical.

ACKNOWLEDGEMENT

I would like to thank Assistant Professor Wantana Prapakorn and Assistant Professor Kanokporn Oranratanachai; Department of Radiology, Chiengmai University for their advices and comments in this paper, Associate Professor Pongsak Mahanupab; Department of Pathology, Chiengmai University for the histopathology report,and Dr.Sompong Yoongtong;Department of Surgery, Sawanpracharak Hospital for surgical information of this case.

REFERENCE

1. Kleihues, Paul MD et al. The WHO classification of tumors of the nervous system.Journal of Neuropathology and Experimental Neurology 2002;3:215-225.
2. Couce ME, Aker FV, Scheithauer BW. Chordoid meningioma: A clinicopathologic study of 42 cases. Am J Surg Pathol 2000; 24:899-905.
3. Burger PC and Scheithauer BW. Tumors of the central nervous system. Washington: Armed Forces Institute of Pathology 1994:259-285.
4. Buetow MP,Burton PC, Smirniotopoulos JG. Typical, atypical and misleading features in meningioma. Radiographics 1991;11:1087-1100.
5. Kallio M, Sankila R, Hakulinen T, Jaaskelainen J. Factors affecting operative and excess long term mortality in 935 patients with intracranial meningiomas. Neurosurg 1992; 31:2-12.
6. Chamberlain MC.Intracerebral meningiomas. Current Science 2004;6:297-305.
7. De la Sayette V, Rivaton F, Chapon F et al. Meningioma of the third ventricle.Neuroradiol 1991;33:354-356.
8. New P, Aronow S, Hesselink J. National Cancer Institutes study: evaluation of computed tomography: the diagnosis of intracranial neoplasms IV meningiomas. Radiol 1980; 136: 665-675.
9. Zagzag D, Gomori JN, Rappaport ZH, Shalet MN.Cystic meningioma presenting as a ring lesion. AJNR 1986;7:911-912.
10. Kulali A,Ilcayto R,Fiskeci C.Cystic meningiomas.Acta Neurochir (Wien) 1991;111:108-113.
11. Kepes JJ,Chen WY,Connors MH,Vogel FS. Chordoid meningeal tumors in young individuals with peritumoral lymphoplasmacellular infiltrates causing systemic manifestations of the Castleman syndrome. A report of seven cases.Cancer 1988;62:391-406.
12. Je-Young Yeon, Jung-Il Lee, Jong-Hyun Kim,Yeon-Lim Suh.Chordoid meningioma: A case report.J Korean Med Sci 2003;18:768-771.
13. De Tella OI Jr, Herculano MA, Prandini MN, Stavile JN, Bonatelli Ade P. Chordoid meningioma:report of two cases. Arq. Neuropsiquiatr.2003; 61 (1) : 91 - 94.
14. Varma DR,Rao BR,Parameswaran S,Gupta AK, Joseph S,Radhakrishnan VV.Chordoid meningioma : A report of two cases. Neurology India 2003;51:52

CASE SERIES: COMPENSATED HYPOTHYROIDISM PRESENTED AS SIMPLE GOITRE

Dr. M.A. Taher

ABSTRACT

A lady of age 23 years from Babukhan, Rangpur came to our centre for estimation of thyroid hormones (tri-iodothyronine, T_3 & thyroxine, T_4) and thyrotropin (thyroid stimulating hormone, TSH) on 4 Oct. 2001. She had high TSH, but normal T_3 & T_4 which is known as compensated hypothyroidism. She had a small goitre and was given thyroxine tablets 50 to 100 micrograms (mcg) per day, but her TSH level was found to be very high on 19 Feb. 2002, most probably due to irregular thyroxine intake (Table 1). She had a fine needle aspiration cytology (FNAC) from her neck mass on 30 April 2002 which revealed benign nature of her goitre. She stopped thyroxine in January 2003 and her goitre aggravated as confirmed by thyroid scintigraphy using technetium (Tc-99m) under computerized gamma camera on 26 July 2003 (Fig.1). She was advised to start thyroxine again.

TABLE 1 : Hormones levels

Date	T3 nmol/L	T4 nmol/l	TSH mIU/L
4 Oct. 01	1.8	76	11
19 Feb. 02	2.8	65	100

Normal ranges : T3 = 0.8 - 3.16 nmol/L
T4 = 64.5 - 152 "
TSH = 0.3 - 6 mIU/L

Fig.1 Scintigraphy showing enlarged thyroid.

Director ,Center for Nuclear Medicine & Ultasound,Post Box # 16 Rangpur 5400,Bangladesh.

DISCUSSION

When iodine deficiency tends to become increasingly severe, it is evidenced first by a drop in T_4 along with a stationary serum T_3 level or even a compensatory rise, owing to the stimulation by TSH. Although the effects of this situation on certain target organs are still insufficiently documented, the individual does not seem to be clinically affected, and retains euthyroidal status. This is known as compensated hypothyroidism.[1] Thyroxine is used in diffuse non-toxic goitre, initially 50-100 mcg daily, preferably before breakfast, adjusted in steps of 50 mcg every 3-4 weeks until normal metabolism is maintained (usually 100-200 mcg/day) ; where there is cardiac disease, initially 25 mcg/day or 50 mcg on alternate days, adjusted in steps of 25 mcg every four weeks.[2] The combination of normal free thyroxine index (FTI) with modest elevation in TSH is considered diagnostic of subclinical hypothyroidism and consistent with a failing thyroid gland. Serum T_3 may be normal in subclinical or mild hypothyroidism. Titrating and fixing the long -term replacement dose of thyroxine is best done on clinical grounds. TSH may also be used to titrate dosage ; a persistently elevated TSH indicates lack of adequate thyroxine replacement except in rare patients with longstanding primary hypothyroidism or TSH-secreting pituitary tumors who may still secrete TSH despite becoming euthyroid. TSH determinations may also be falsely elevated in rare patients exposed to rabbits who develop antibodies to the rabbit immunoglobulin used in the radioimmunoassay,[3] but our patient had high TSH due to inadequate replacement of thyroxine.

REFERENCES

1. Thilly CH, Bourdoux P, Contempre B, Swennen B, Strategies for combating endemic goitre and iodine deficiency disorders (IDD).1988 No.175/176 Children in the tropics. International Children 's Centre, Paris pp. 5-68.
2. British National Formulary No. 32 Sept. 1996, p. 297. British Medical Association and Royal Pharmaceutical Society of Great Britain, London.
3. Safrit HF. Thyroid disorders. In Fitzgerald PA (ed.) : Handbook of clinical endocrinology. 1986 Jones Med. Pub. Greenbrae, CA pp. 122-169.

CASE SERIES : LIVER ABSCESSES MIMICKING NEOPLASMS AND RUPTURED INTO ANTERIOR ABDOMINAL WALL AND PLEURAL CAVITY

DR. M.A.TAHER

ABSTRACT

We like to report two cases of liver abscesses in two men of 27 and 38 years of age, the younger one presented as a cauliflower-like fungating ulcer extending from the right hypochondrium to the right iliac fossa, the later one presented with brown cough and fever. Both the patients were followed up to clinical cure. One of them had serial ultrasonography and radionuclide scans also.

CASE 1

A man of 27 years came to the surgery department of Dhaka Medical College Hospital with a provisional diagnosis of neoplasm involving anterior abdominal wall. He had a big cauliflower-like fungating ulcer from right hypochondrium to right iliac fossa. Prof. Mirza Mazharul Islam FRCS diagnosed it as a liver abscess and prescribed iodoquin and metronidazole tablets and daily dressing. The patient improved gradually over the next five weeks and was discharged in good condition.

CASE 2

A man of 38 years came with complaints of right upper abdominal pain, fever and 'brown' cough Ultrasonography (USG) showed a semicytic area of 11x7 cm in upper right hepatic lobe adjacent to right dome of diaphragm and 2.5 cm high right pleural effusion. We made a diagnosis of liver abscess ruptured into pleural cavity. But the patient showed another sonographic report from a private clinic of Dinajpur which diagnosed it as a case of hepatoma. To avoid confusion, we performed a radio-colloid liver

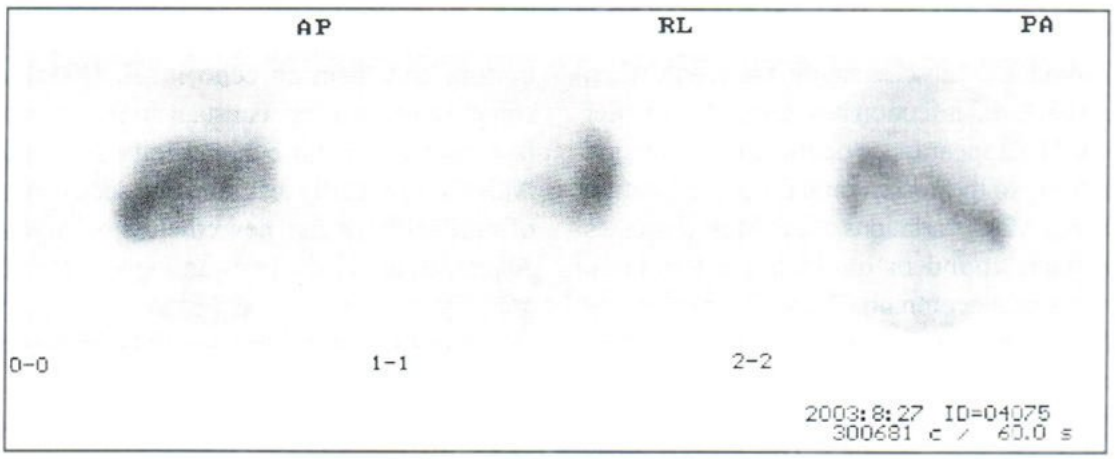

Fig.1 Liver abscess in right lobe.

Director, Center for Nuclear Medicine and Ultasound, Post Box No.- 16 Rangpur 5400,Bangladesh.

scintigraphy (99m Tc stannous fluoride 5 mCi i.v.) with gamma camera and a well-defined photon -deficient area was seen in upper right hepatic lobe,and all other areas of liver have taken up radio-colloid uniformly (Fig.1). The patient was improved after percutaneous drainage of pus,medications with cephalexin and metronidazole injections followed by tablets, as confirmed by clinical follow-up, USG and hepatobiliary scan (Bridatec).(Fig. 2)

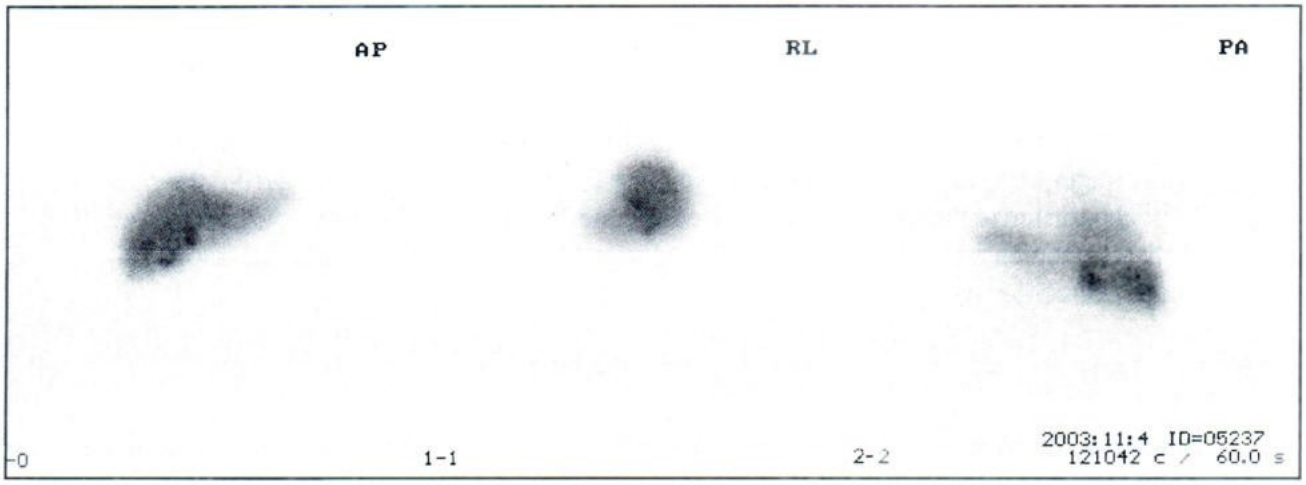

Fig 2 Normal hepatobiliary scan after nine weeks

DISCUSSION

Isotope liver scan show, over 80% of amoebic abscess as a filling defect in the liver.[1] Abnormal findings on a chest X-ray are common but non-specific. Elevation of the right dome of diaphragm, atelectasis and a modest pleural effusion are common. The right hemithorax may become totally opaque following rupture of an abscess into the pleural cavity. Gas within the abscess cavity is seen only when secondary bacterial infection has developed or after aspiration. The appearances on ultrasound depend on the maturity of the abscess and the precise nature of its contents. Many variations occur. Most abscesses are irregularly round or ovoid but a lobulated appearance is not uncommon. The wall is moderately well-defined and irregular but it becomes smoother as the abscess is mature. No wall may be seen at all or there may be an echo-poor rim, or halo, possibly due to surrounding edema. Most amoebic liver abscesses are echolucent though in some the contents are isoechoic because the infected liver has not yet undergone autolysis. A hyperechoic abscess is the least common and could be mistaken for a primary or secondary tumour. Both isoechoic and hyperechoic abscesses progress to a hypoechoic mass within 1-2 weeks and all abscesses eventually become anechoic as their contents become thinner in consistency.[2] In mature abscesses, necrotic material may sink to the bottom and form an echo level. Distal acoustic enhancement is a very constant and important feature irrespective of the echogenicity of the abscess. Although generally less than that seen behind a cyst of similar size, it can, nevertheless,be quite striking. Aspiration is usually unrewarding as the trophozoites are only present in the wall of the abscess and not in its contents even when typical 'anchovy paste' is recovered. No definite ultrasound feature exist to distinguish pyogenic from amebic abscesses, although certain findings have been described that may help to predict this etiology.[3] Common causes of liver abscess are amebiasis, portal bacteremia due to

appendicitis or diverticulitis, biliary tract diseases, trauma and generalized septicemia.[4] Sometimes gas is also detected in a liver abscess.[5]

REFERENCES

1. Berger LA. Cystic and infective disease of the liver. In Wilkins RA & Nunnerley HB. (editors) : Imaging of the liver, pancreas and spleen. Blackwell, Oxford, 1990 : 147-171.
2. Boultbee JE, Simjee AE, Rooknoodeen F, Engelbrecht HE. Experiences with grey-scale ultrasonography in hepatic amebiasis. Clin Radiol 1979 ; 30 : 683-689.
3. Oleszczulk - Raszke K, Cremin BJ, Fisher RM, Moore SW, Millar AJ. ultrasonic features of pyogenic and amebic hepatic abscesses. Pediatric Radiol 1989 ; 19 : 230-233.
4. Rambo WM, Black HC. Intrahepatic abscess. Am Surg 1969 ; 35 : 144-148.
5. Halvorsen RA, Foster WL, Wilkinson RH, Silverman PM, Thompson WM. Hepatic abscess: sensitivity of imaging tests and clinical findings. Gastrointestinal Radiol 1988; 13 : 135-141.

ACUTE ABDOMEN DUE TO DEAD WORM IN GALL BLADDER

Dr. M. A. Taher

Occasionally acute epigastric pain occurs due to roundworms in gallbladder. Recently we found such a case and would like to report it considering its rarity.

CASE REPORT

A woman of age 20 years came with the complaints of severe upper abdominal pain, vomiting and restlessness. Vomitus contained four dead roundworms. Ultrasonography revealed distended gallbladder with a coiled bright structure which represented a dead ascaris (Fig.1).

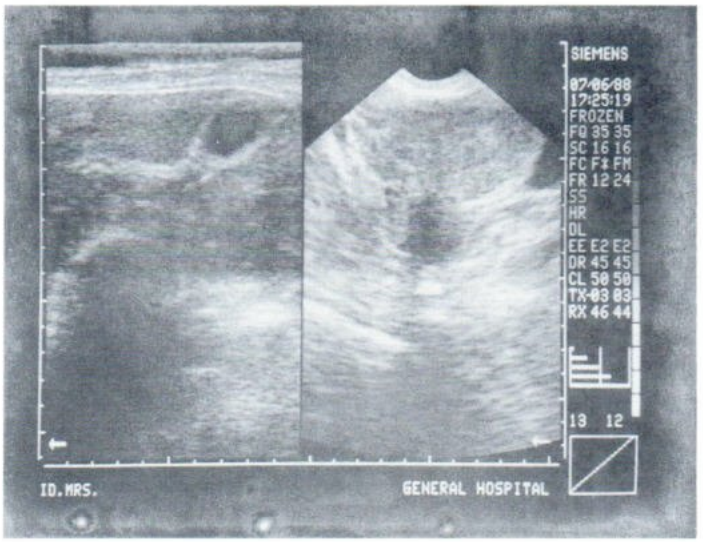

Fig. 1 Dead worm in gallbladder

DISCUSSION

Ascaris lumbricoides was first discovered by Ligneous in1758. The detailed life-cycle of the ascaris, however, was not known until 1916. One quarter of the world's population is infected with ascariasis.[1] Clinical manifestations may result from the migration of larvae through the lungs and from the presence of adult worms in the small intestine, hepatobiliary system and pancreatic ducts. The adult worms may measure upto 45 cm in length.

Sonography is a rapid non-invasive way of imaging which shows the ascariasis in the biliary tree as a bull's eye on transverse section, as a long echogenic shadow in longitudinal section or as coils or amorphous fragments,[2-11] intraluminal mass with 3 or 4 linear echogenic interfaces and sometimes round "target" sign.[12]

Director, Nuclear Medicine Centre, Box No.-16, Rangpur, Bangladesh.

REFERENCES

1. Montorfano M. Ultrasound and ascariasis. Ultrasound Quarterly 1999; 15: 206-209.
2. Cremin BJ. Ultrasonic diagnosis of biliary ascariasis: "A bull's eye in the triple O". Br J Radiol 1982; 55: 683-684.
3. Cerri GG, Leite GJ, Simoes JB et al. Ultrasonographic evaluation of the ascaris in the biliary tract. Radiology 1983; 146: 753-754.
4. Schulman A, Loxton AJ, Heydenrych JJ et al. Sonographic diagnosis of biliary ascariasis AJR 1982; 139: 485- 489.
5. Khuroo MS, Zargar SA, Mahajan R, Bhat RL, Jarid G. Sonographic appearances in biliary ascariasis. Gastroenterology 1987; 93 (2): 267-272.
6. Schulman A, Roman J, Dalrymple R et al. Sonography of biliary worms (ascariasis). 1982; JCU 10: 77.
7. Mehta P, Sharma AK, Saluja S, Prabhu NK. Biliary ascariasis: ultrasound diagnosis. 1995; JCU 23: 500-501.
8. Peck RJ. Ultrasonography of intestinal ascariasis. J Clin Ultrasound 1990; 18: 741-743.
9. Khan An, Ali M. Sonography of hepatobiliary ascariasis with new observations. Eur J Ultrasound 1996; 3: S 30.
10. Khan HA. Non-invasive diagnosis of biliary ascariasis, Bangladesh J. Ultrasound 1991; 1: 11-12.
11. Taher MA. Biliary ascariasis. ASEAN J Radiol 2001; VII (1): 27-28.
12. Mahmood T, Mansoor N, Quraishy S, Ilyas M, Hussain S. Ultrasonographic appearance of Ascaris lumbricoides in the small bowel. J Ultrasound Med 2001; 20: 269-274.

ROLE OF ULTRASONOGRAPHY IN DIAGNOSIS OF INFANTILE HYPERTROPHIC PYLORIC STENOSIS-A PRELIMINARY WORK IN THE NORTHERN PART OF BANGLADESH

Dr. Md.Murshed Ali,[1] Dr. Md.Jafrul Hannan,[2]
Dr. Kazi Habibur Rahman,[3] Dr. Md.Rezaul Karim[4]

INTRODUCTION

Infantile Hypertrophic pyloric stenosis (IHPS) is commonly encountered in pediatric practice. The typical infant with this lesion presents with nonbilious projectile vomiting and dehydration if the diagnosis is delayed. IHPS accounts for one third of nonbilious vomiting occurrences in infants and is the most common reason for laparotomy before 1 year of age.[1]

IHPS is seen in 2-3/1000 infants in North American and accounts for 30% of all patients presenting with nonbilious vomiting before 1 year of age.[1] The onset of vomiting may occur as early as the first week of life and can be as delayed as late as age 5 months. A striking male preponderance is seen, with a male-to-female ratio of 4-6: 1.[2]

IHPS is more common in whites and is seen less commonly in African, American infants or infants of Asian descent.[3]

Despite its status as a common disease, the cause of IHPS is unclear; however, a definite genetic component exists, since an increased incidence is observed in families in which a sibling or parent has had the disease. The pylorus appears as an enlarged pale muscle mass in IHPS and usually measures 2 to 2.5 cm in length and 1 to 1.5 cm in diameter. Histologically the mucosa and adventitia are normal. There is marked muscle hypertrophy involving the circular layers, which produces partial or complete luminal occlusion. The ethiology of IHPS are genetic, racial and male predominance.[4] The risk increased for the first-bone infant with positive family history and certain ABO blood group.[1,3,4]

Ultrasonography probably has contributed to the changing face of the disease in the past 2 decades, since it results in earlier diagnosis and treatment. Ultrasonography (US) is important and has become the most common imaging technique for the diagnosis of IHPS.[5] In our country, all the Center for Nuclear Medicine and Ultrasonography (CNMU), have the facility of routine ultrasonography for the diagnosis of IHPS. This study was carried out in the Center for Nuclear Medicine and Ultrasound, Rangpur which is located in the northern part of Bangladesh.

[1] Medical Officer, Center for Ultrasound and Nuclear Medicine Rangpur, Bangladesh.
[2,3,4] Asstt. Prof. of Department of Pediatric Surgery Rangpur Medical College and Hospital, Rangpur, Bangladesh.

MATERIALS AND METHODS

This study was carried out in the CNMU, Rangpur during the period of July 2003 to June 2004. A total of 66 patients were referred to our center with the complaint of severe vomiting developed about 3-6 weeks after birth. The vomiting occurred immediately after every feeding and was projectile. Our of 66 infants 28 were male and 38 were female, aged between 4 to 7 weeks and the clinical diagnosis was IHPS.

Therefore, US is recommended because its sensitivity and specificity are close to 100% for this disease. If clinical suspicion for IHPS is moderate to high, US also is recommended.

Sonographic examination was done using Toshiba JUST VISON-400 5 MHz curvilinear and 8 MHz linear probe in supine position. In the epigastrium both longitudinal and transverse views were obtained. The water filled stomach was a landmark. In some cases stomach was outlined very easily containing food. Two sonographic criteria were used e.g. pyloric diameter D and the pyloric muscle thickness T and length of pylorus L.

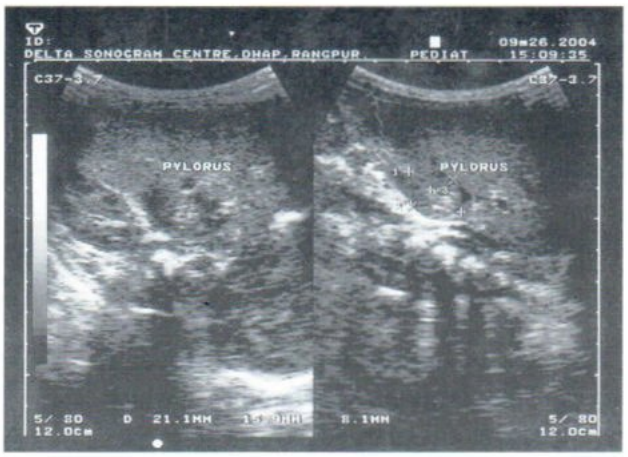

Fig.1

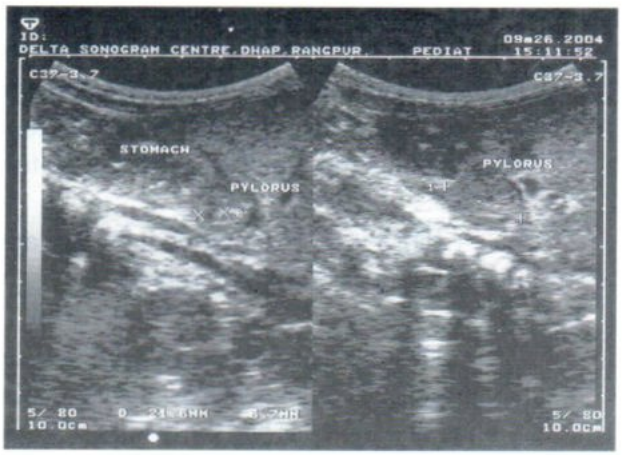

Fig.2

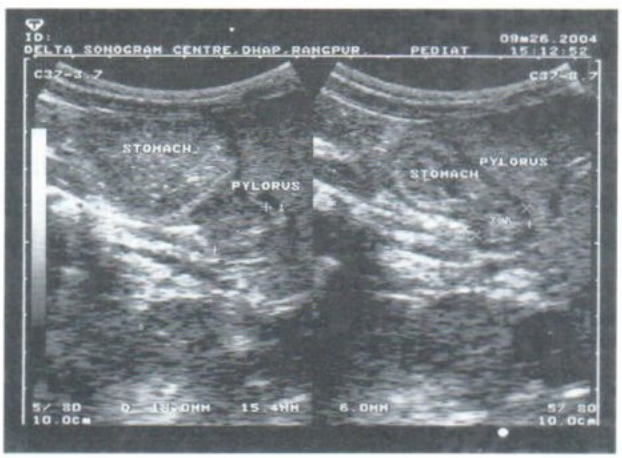

Fig.3

RESULTS

In 63 out of 66 referred cases, had a pyloric diameter D, range between 12.5 to 14.9 mm, the pyloric muscle thickness, T range between 4.0 mm to 6.7 mm, and the pyloric length L were 18 mm to 23. Two cases had D, T and L less than the expected sonographic parameter and they were excluded. In one case we did not visualized pylorus due to excessive upper abdominal gas but which was diagnosed as IHPS by radiology.

In all 63 cases, diagnosis were confirmed by laparotopy and treated by pyloromyotomy (Ramstad).

DISCUSSION

Infantile Hypertrophic Pyloric Stenosis (IHPS) is a well-known pediatric problem. The circular muscle layer becomes thickened, which narrows the pyloric channel and elongates the pylorus. With this process, the mucosa becomes redundant and may appear hypertrophic. With elongation and thickening of the muscle, the pylorus deviates upward toward the gallbladder. The gallbladder serves as a marker, since in IHPS, the pylorus can be seen adjacent to the gallbladder and anteromedial to the left kidney. The thickened pylorus narrows the pyloric channel, resulting in gastric outlet obstruction, gastric distension, and retrograde peristalsis in the stomach.[6]

Sonography has become an important diagnostic adjunct in the western world in the evaluation of vomiting infants who are suspected to have IHPS.[5]

The usual presentation of IHPS is with severe vomiting which starts between 3-6 wks (rare <10 days and >11 weeks). The baby will be normal otherwise. Vomiting after every feeds is copius and nonbilious and some times blood stained due to gastritis or esophagitis. The key feature is readiness and ability to feed again immediately after vomiting. The patient may have dehydration, malnutrition, weight loss and stunted growth.[6]

Early diagnosis and proper treatment is very important for the normal life of the baby. If untreated patient may die due to dehydration and metabolic alkalosis. About 75% definitive diagnosis can be made clinically. Physical examination of upper abdomen is very important. Careful and skilled palpation of the abdomen may reveal tumor like mass of the enlarged pylorus, which is traditionally called pyloric tumor. It feels like an olive or a small pebble.[7]

The preferred diagnostic test is a contentious topic, with a wealth of articles over the last decade discussing cost-effectiveness and the changing face of this disease. The first and most important step in patient workup of suspected IHPS is physical examination. If the pyloric olive is felt, the patient may proceed directly to the operating room without imaging. Many surgeons are uncomfortable with this, since a false-positive physical examination leads to a negative laparotomy. Therefore, US is recommended because its sensitivity and specificity are close to 100% for this disease. If clinical suspicion for HPS is moderate to high, US also is recommended.[8]

Currently, deaths resulting from HPS are rare. Morbidity is linked directly to the duration and frequency of vomiting. Protracted vomiting causes decreased intake and increased loss of essential nutrients and electrolytes, which results in dehydration and metabolic alkalosis. This is in part a result of the accessibility and accuracy of US in the diagnosis of IHPS. When clinical procedure fails than imaging procedure is requedted. The real time Ultrasonography is the first lirte of imaging technique than barium meal study and air contrast medium test.[2,3,4]

The most commonly used sonographic

T = Thickness, L = Length

criteria for diagnosis of positive IHPS is a pyloric muscle thickness of 4 mm or more and a pyloric channel length 16 mm or more. The other criteria is pyloric diameter D greater than or equal to 12 mm and pyloric muscle thickness T greater than or equal to 3 mm showed the positive and negative predictive values 1.00 and 0.80, respectively.[5]

In this study we used three sonographic parameters such as pyloric Diameter (D), Pyloric Muscle Thickness (T) and length of the pylorus(L). The 63 referred cases had significantly larger D, T and L (D=2.5 mm to 14.9 mm and T=4.0 mm to 6.6 mm L=18mm to 23mm). All the patients under went operative intervention and the peroperative findings were correlated with the pre-operative sonographic diagnosis. Sixty three patients were correctly diagnosed for IHPS. Our study shows the sensitivity 95% specificity 100% and accuracy 96%.

CONCLUSION

US has high sensitivity, specificity, snd accuracy in the diagnosis of HPSS. Errors in diagnosis do occur and relate to the operator inexperience, distended formula and gasfilled stomach, overdistended antrum may be mistaken for the pylorus.

This study suggests that proper sonographic criteria are helpful in establishing the diagnosis of IHPS.So ultrasound can be introduced as a first approch in our country for the diagnosis of the IHPS because ultrasound has no radiation hazards, better patient and parent acceptance, no contrast medium and above all reliable diagnosis.

REFERENCES

1. Schecher et al. in The epidemiology of infantile hypertrophic pyloric stenosis. Paediatr Perinat Epidemiol. 1997 Oct;11(4):407-27.
2. Schwartz MZ. Hypertrophic Pyloric Stenosis. In Ravitch Pediatric Surgery, O.Neill JA, Rowe MI, Gross JL et al. Fifth Edition, 1998. Mosby, Missouri: 1111-17.
3. Rasmussen L, Green A, Hansen LP. The epidemiology of infantile hypertrophic pyloric stenosis in a Danish Population, Int J Epidemol 1989;18:431.
4. Mitchell LE, Risch N. The genetic of infantile hypertrophic pyloric stenosis, Am J Dis Child 1992;147:1203.
5. Yip WC, Wong ML, Tay JS, Prabhakaran K, Wong HB. Infantile hypertrophic pyloric stenosis: evaluation of sonographic criteria. J Singapore Pediatr Soc 1989;31(3-4):111-5.
6. Huftons JM, Beasley SW, Wood Ward AA. Jones Clinical Pediatric Surgery Diagnosis and Management, Fifth Edition, 1999:129-134.
7. Tack ED et al. Pyloric stenosis in sick premature infant: clinical and radiologic findings. Am J Dis Child 1988;142:68.
8. Huftons JM, Beasley SW, Wood Ward AA. Jones Clinical Pediatric Surgery Diagnosis and Management, Fifth Edition, 1999: 129-134.
9. Keller H, Waldermann D, Greiner P: Comparison of preoperative sonography with intraoperative findings in congenital hypertrophic pyloric stenosis, J Pediatr Surg 22:950, 1987.

ISOTOPE RENOGRAM IN ECTOPIC KIDNEY

Dr. M.A. Taher

ABSTRACT

Ultrasonography (USG) may provide some clue to the diagnosis of an ectopic kidney. However, functional confirmation is bast to be done by isotopic renogram, as depicted by a rare case reported below.

CASE REPORT

A young man of age 17 years complained of pain in left loin. Ultrasonography (USG) done elsewhere reported 'normal kidneys', but intravenous urography (IVU) revealed ectopic (pelvic) left kidney with mild hydronephrosis. Isotope renogram with technetium 99m DTPA (diethylenetriamine pentaacetic acid) showed normal right kidney and small ectopic left kidney just at the pelvic brim on the right side with mild obstruction (Fig. 1)

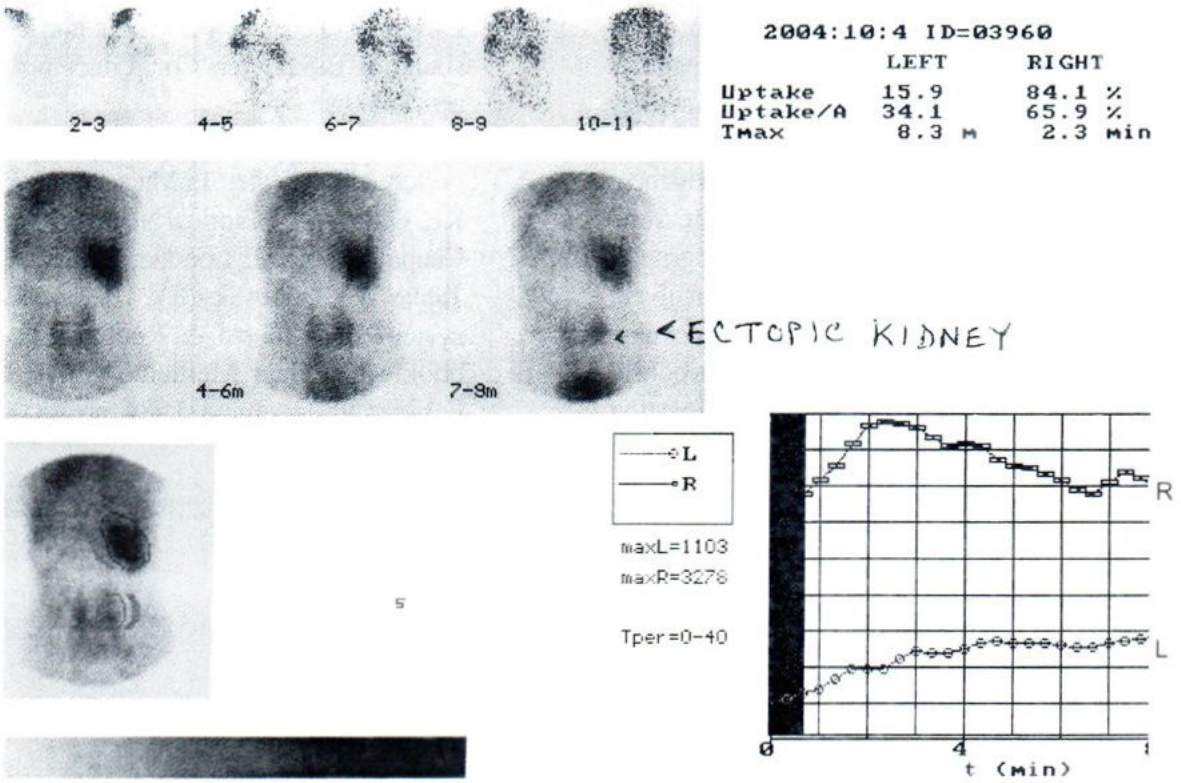

Fig.1 DTPA RENOGRAM

Director, Center for Nuclear Medicine and Ultrasound, Rangpur, Bangladesh.

DISCUSSION

Ectopic kidney may be presented due to failure of the complete ascending migration of the kidney from its primitive location at the 1st or 2nd sacral body level or excessive cranial migration beyond its normal location. Crossed renal ectopia is a condition in which the affected kidney is located entirely or primarily on the opposite side of the abdomen.[1] The ectopic kidney lies below the normal contralateral kidney, and the two organs are almost always fused. Approximately 50 cases of intrathoracic kidney have been reported. Usually a mass is seen on chest X-ray and USG or CT demonstrates it to be a kidney.[2] A colonic flexure or loop of small bowel may occupy the empty renal fossa mimicking a mass or kidney (pseudokidney sign).[3] Apart from being displaced, most pelvic kidneys are normal. Occasionally, however, a pelvic kidney is grossly abnormal in appearance because it is affected by dysplasia, duplication, anomalies, vesicoureteral reflux and/ or hydronephrosis. Diagnostic error may be avoided if the ipsilateral renal fossa is examined routinely in patients with pelvic pathology.[4] Radionuclide renal scan is valuable for the proper assessment of many congenital anomalies affecting the renal tract. The assessment of horseshoe kidney or ectopic kidney can be done much more easily than with intravenous urography (IVU), because once the radioisotope has been given, a whole-body search can be undertaken if necessary, whereas a small pelvic kidney, especially if it is poorly functioning, cannot always be seen against the background of the pelvic bones.[5] The spinal column may significantly attenuate low-energy gamma rays, so that anterior view of the kidneys may be wise to be taken.[6]

REFERENCES

1. Kurjs DR, Lsurin S. Pediatric radiology. In Pettersson H (ed.) A Global Text Book of Radiology. The NICER Institute, Oslo 1995 pp.533-609.
2. Summer TE, Volberg FM, Smolen PM. Intrathoracic kidney--diagnosis by ultrasound. Pediatr Radiol 1982; 12:78-80.
3. McCarthy S,Rosenfield AT.Ultrasonography in crossed renal ectopia. J Ultrasound Med 1984;3:107-112.
4. Zwiebel WJ. Normal variants and developmental anomalies of the urinary tract. In: Zwiebel WJ,Sohaey R.Introduction to Ultrasound, W.B.Saunders Co. Philadelphis 1998 pp. 176-185
5. Britton KE, Maisey MN, Hilson AJW.Renal radionuclide studies. In Maisey MN, Britton KE, Gilday DL : Clinical Nuclear Medicine, Chapman and Hall, London,1983,pp.93-133.
6. Tauxe WN,Dubovsky EV. The genitouinary system. In Harbert J, da Rocha AFG. Textbook of Nuclear Medicine vol. II Lea & Febiger, Philadelphia, 1984. pp. 481-521.

ROLE OF PREOPERATIVE ULTRASONOGRAPHY IN IDENTIFYING POTENTIAL PROBLEMS IN LAPAROSCOPIC CHOLECYSTECTOMY.

Dr. Md.Murshed Ali.[1] MBBS;M-Phil (NM),[2]
Dr. Md.Jabed Akher. MBBS;FCPS(Surgery).

INTRODUCTION

Since its introduction in 1987, laparoscopic cholecystectomy has rapidly established itself as a viable alternative to conventional open cholecystectomy. In many countries, it is now the method of choice in dealing with cholelithiasis. This procedure was initially recommended as a treatment for patients with billiary colic, but with increasing experience, it is being offered to patients with cholecystitis or pancreatitis, as well as patients with a previous history of abdominal or pelvic surgery.[1] The present literature indicates that laparoscopic cholecystectomy can be carried out successfully in at least 90% of cases of symptomatic cholelithiasis,[1-6] with success rates of 95% being achieved in some studies.[1-2-6]

Laparoscopic cholecystectomy (LC) is now the gold standard treatment of symptomatic gallstones and is the commonest operation performed laparoscopically worldwide. The indications for its use in the treatment of gallstone are the same as open operation although the cholecystectomy rate has increased by an average of 20%, including in Scotland, since the introduction of LC.[3-9] The exact reasons for this are not known but the rise is somehow linked to perceptions on the part of patients, general practitioners and surgeons that the magnitude of the intervention is reduced by the laparoscopic approach. To a large extent, this is true but the potential for overall morbidity associated with the surgical treatment of gallstone disease is increased by the higher cholecystectomy rate which also impacts on the overall health care costs. In contrast, large retrospective series of LCs from several countries indicate that the overall mortality of cholecystectomy has decreased since the advent of the laparoscopic approach.[4-10]

Clearly, preoperative ultrasound evaluation has a limited role to play in the detection of adhesions, but it would be expected to play a role in the detection of acute and chronic inflammation of the gall bladder and possible in the detection of aberrant anatomy. The object of this study was to assess the role of preoperative ultrasound evaluation of the gall bladder in predicting difficult or failed laparoscopic cholecystectomy.

SUBJECTS AND METHODS

A preoperative ultrasonography was performed in the Center for Nuclear Medicine and Ultrasound, Rangpur during the period of january/2004 to june/2004. A total of 60 patients (47 women

[1] Medical Officer, Center for Ultrasound and Nuclear Medicine Rangpur, Bangladesh.
[2] Asstt.Prof. of Department of Surgery, Rangpur Medical College and Hospital, Rangpur, Bangladesh.

and 13 men, age range: 31 years to 59 years, were diagnosed to be Cholelithiasis, ultrasonography and Laparoscopic surgery were done. The indications for surgery included billiary colic (52 patients), resolving or recently resolved episodes of cholangitis (6 patients) and recently resolved episodes of gallstone pancreatitis (2 patients).

Each patient underwent preoperative ultrasound examination (Toshiba JUST VISION-400). A note was made of the presence or absence of calculi, number of calculi, size of largest calculus, the degree of gall bladder contraction or distension, thickness of the gall bladder wall, the presence or absence of gall bladder tenderness, pericholecystic fluid collections, sloughed membranes, striated appearance to the gall bladder wall, and commom bile duct diameter. Patients with billiary colic underwent ultrasonographic examination during their initial surgical consultation.

On admission for surgery, a careful clinical history was taken, and patients were excluded if there was a change in symptomatology during the time interval between the ultrasound examination and surgery. Patients with resolving acute cholecystitis / pancreatitis/cholangitis were scanned in the days immediately prior to surgery.

On ultrasound examinations, gallstone bigger than 14 mm were considered likely to cause problems in removal. A gall bladder wall thickness of more than 3 mm was considered to be abnormal. Tenderness over the gall bladder was considered to be the evidence of acute inflammation.

Gall bladder contraction was defined as a transverse diameter less than 2 cm. A small contracted gall bladder was considered likely to represent chronic inflammatory changes. A common hepatic duct measurement of 8 mm or greater was considered to be abnormal. Laparoscopic cholecystectomies were performed by two surgeons in a standard fashion using four ports.

Postoperatively, a comparison was made of the ultrasound findings and the operative notes. The following informations were recorded: (1) uneventful, difficult, or failed laparoscopic surgery, (2) the cause of the intraoperative defficulties, and (3) reasons for conversion to open cholecystectomy.

RESULTS

Fourty five laparoscopic cholecystectomies were performed without difficulty. Seven laparoscopic cholecystectomies were successfully completed, but only after some intraoperative difficulties were experienced. Eight cases were converted to open cholecystectomy.

In 45 patients who had a successful laparoscopic cholecystectomy, the preoperative ultrasound examination indicated at least one calculus bigger than 14 mm. Only 1 of these cases presented minor problems; in that case, the stone required extention of paraumbilical hoe prior to removal. The remaining 44 patients presented no problems.The number and size of gallstones as estimated by ultrasonography did not contribute any useful information, and the following results do not include calculus size or number as a component of the ultrasound assessment.

Fifty two patients had laparoscopic cholecystectomy for billiary colic. Table 1 outlines the results in this group. There were 4 failed laparoscopic cholecystectomies; 2 of these were secondary to introgenic complications. In 1 patient, who was very obese, there was difficulty maintaining an adequate pneumoperitoneum and keeping the colon clear of the operative field. Two patients has thick-walled, contracted gall bladders that could not be removed laparoscopically. In both cases, these findings were seen in the preoperative ultrasound examination (Figure 1).

Of the 8 patients with technically difficult surgery, 3 had adhesions from previous surgery, 1 patient was very obese and also proved to have a

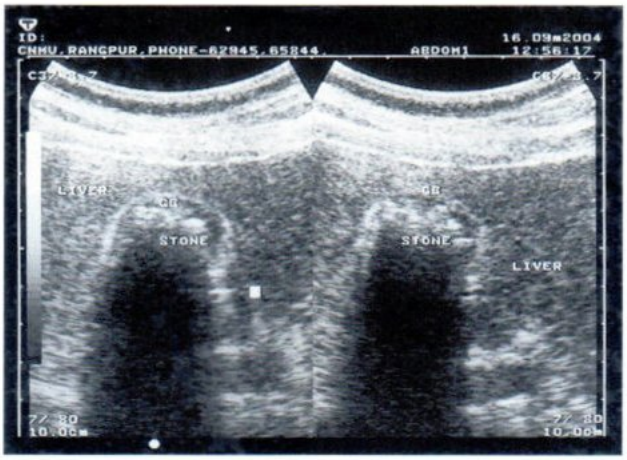

Fig 1

Table 1 Result of Laparoscopic Cholecystectomy in patient with Biliary Colic.

	Number of cases	Non GB related problem	Problematic GB Resection
Unsuccessful	04	02	02(2*)
Difficult	08	03	05(3*)
Uneventful	40(6)	--	--

* Preoperative ultrasonography diagnosed as potential problematic.

difficult arterial dissection, one patient had a very large calculus that required extention of para- umbilical hole prior to removal, and 5 patients had chronically inflamed gall bladders. The preoperative ultrasound examination in 3 of these last 5 cases showed thick -walled gall bladders, which were not tender on examination (Figure 2).

Forty patients had uneventful surgery, including 8 patients who had thick-walled gall bladder with or without gall bladder contraction in a preoperative ultrasound examination (Figure 3).

Six patients had laparoscopic surgery for resolving acute cholecystitis. Table 2 outlines the results in this group. Of the 2 unsuccessful cases, 1 had adhesions from previous surgery and another one had unexpectable inflamed gall bladders. All 2 patients had acutely inflamed gall bladders in the preoperative ultrasound examination, and 3 also had gall bladder wall thickening. A single case proved uneventful despite of the thick-walled appearance of the gall bladder in the preoperative ultrasound examination.

Two patients had resolved cholangitis. One had uneventful surgery and one was converted to open cholecystectomy. The reason for conversion was a combination of mechanical problems and difficult anatomic dissection. In both cases, the preoperative ultrasound examination was normal.

In the 2 patients with resolved pancreatitis, 1 had uneventful surgery and 1 was converted to open cholecystectomy because of severe inflammatory changes in the gall bladder. The preoperative ultra-

sound examination in both cases was entirely normal.

In 8 of the 40 uneventful laparoscopic cholecystectomies in the total study group, there was preoperative evidence of a thick-walled gall bladder with or without gall bladder contraction, yet these posed no problem at surgery. There were no ultrasound features that identified the unsuccessful, difficult, or uneventful laparoscopic cholecystectomies.

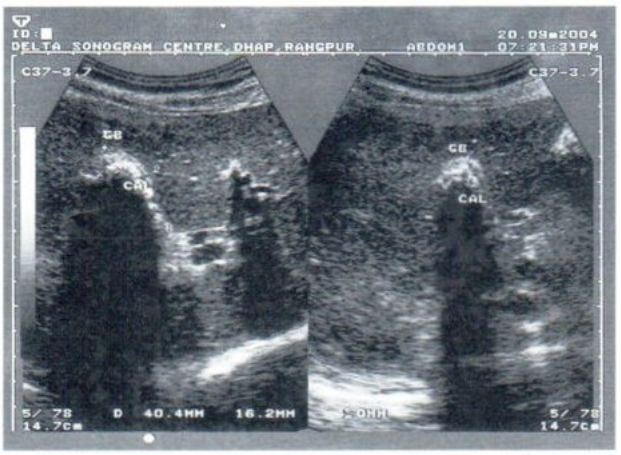

Fig 2

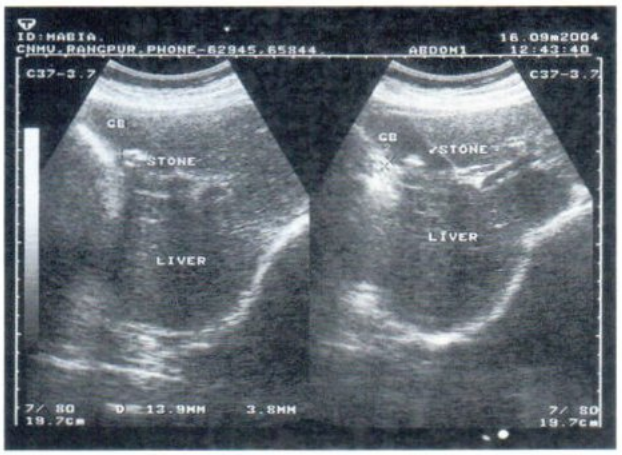

Fig 3

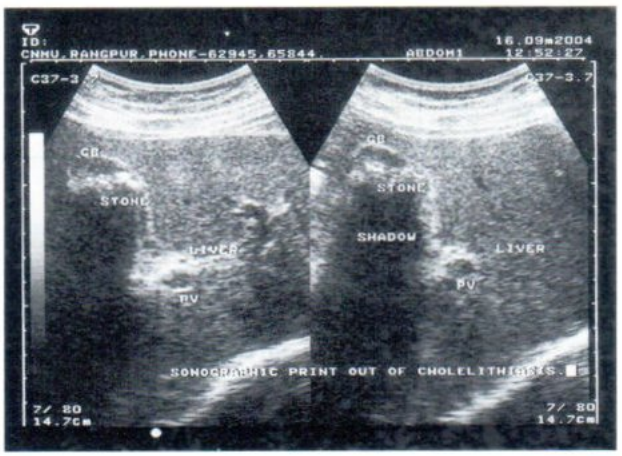

Fig 4

Table 2 Result of Laparocopic Cholecystectomy in patient with Recently Resolved Acute Cholecystitis.

	Number of cases	Non GB related Problem	Problematic GB Resection
Unsuccessful	4	1(1)*	3(3)
Difficult	1	--	1(0)
Uneventful	1(1)	--	--

* Preoperative ultrasonography diagnosed as potential problematic.

DISCUSSION

Most female had heard of laparoscopy, also known as Band-Aid or Bellybutton surgery. Gynaecologist have long used this technique to tie the fallopian tubes and to dissect the female reproductive organs. Now the use of laparoscopy has been expanded to include removing a diseased gall bladder.[4]

The main benefit of this procedure is the easy recovery for the patient. There is no incisional pain as occur with standard abdominal surgery. The patient is up and walking about, the same day. In fact, upto 90% of the patients go home the same day. The remainder are usually discharged the next day. And within several days, normal activities can be resumed. So the recovery time is much quicker. Also, there is no scar on the abdomen.[2]

In a recent review of the Canadian experience with 2201 laparoscopic cholecystectomies, there were 95 conversions to open cholecystectomy, giving an overall rate of conversion of 4.3%.[1] In those centers that had performed fewer than 100 laparoscopic cholecystectomies, the conversion rates were higher. In the most experience center, which had performed 679 procedures, the conversion rate was only 2.8%, and laparoscopic cholecystectomy was offered to all patients with symptomatic cholelithiasis. This overall conversion rate was similar to that found by Meyers[6] when he reviewed 1518 laparoscopic cholecystectomies.

In the study by Litwin et al,[1] acute and chronic inflammation of the gall bladder, aberrant anatomy, the need for ductal exploration, and one case of polycystic disease accounted for 34 of the 95 conversions. The remaining 61conversions resulted from adhesions, intraoperative complications, mechanical problems, and 1 case of small bowel obstruction.

These result suggest that preoperative ultrasound evaluation could reduce the overall conversion rate to approximately 3%.

In our study there were 8 conversions to open cholecystectomy (4 billiary colic, 2 acute cholecystitis, 2 pancreatitis) because of inflammatory changes in the gall bladder. The preoperative ultrasound examination detected either increased gall bladder wall thickness with or without gall bladder contraction.

In the 6 patients in whom gall bladder resection proved to be difficult, preoperative ultrasound, examinations demonstrated abnormalities other than cholelithiasis in 2 cases. However, in 8 of 45 uneventful cases, similar gall bladder findings were present. There was no objective difference in the abnormal ultrasound findings in uneventful, difficult, and failed cases.

None of the 6 patients with resolving acute cholelithiasis had evidence of gengrenous cholecytitis on either ultrasound assessment or examination of phological specimens. It seems probable that ultrasonic findings of pericholecystic fluid collections, sloughed membranes, or a striated appearance to the gall bladder wall would be associated with a difficult or failed laparoscopic cholecystectomy.

Intraoperative difficulties arose in only in case as a result of a large gallstone. The stone measured 2 cm and required extention of para-umbilical hole prior to removal. In another 32 patients, the preoperative ultrasound examination documented stones in excess of 14 mm, yet no operative difficulties arose. It is likely that in these patients we were measuring several small stones adjacent to each other and not a single calculus, or when a single calculus did measure in excess of 14 mm, its other dimensions allowed it to be easily removed.

This study was performed at the commencement of the laparoscopic cholecystectomy program at our hospital. One surgeon involved was relatively experienced, and, theoretically, preoperaive ultra-

sound examination should have been useful at this stage. It is anticipated that with increasing surgical experience many of the problems encountered in the difficult and failed cases will prove less troublesome in the future. This expected reduction in conversion rate will reduce further the value of detailed preoperative ultrasound assessment.

We anticipate that the majority of the patient will be offered to laparoscopic cholecystectomy, irrespective of the ultrasound appearance of a thickened gall bladder wall, contraction, or tenderness. The result of surgery will depend on the experience of the surgeon and will not be predictable by the preoperative ultrasound evaluation. Our findings are similar to those of Mcloughlin et al.[8]

CONCLUSION

Gall bladder removal by laparoscopic surgery is an exciting development because of it offers so much to the patient. The surgeons carefully evaluate each case and discuss it with the patients. While problems can occurs with the procedures they are unuseful. In most instances, patients experience excellent result and resume their normal activities very quickly. For successful removal of gall bladder by Laparoscopic surgery mostly depends on the expertise of the surgeon and appropriate patient selection depending upon the sonographic findings, that is detailed preoperative ultrasound assessment of the gall bladder, confirmation of presence of stone, size, number of stone, thickness of walls, as well as evaluation of others right quadrants organs an important to exclude significant pathology to outside the gall bladder.

REFERENCES

1. Litwin DE, Girotti MJ, Poulin EC, et al: laparoscopic cholecystectomy Trans-Canada experience with 2,201 cases. Can J Surg 35: 291-296,1992.
2. Legorreta AP, Silber JH, Costantino GN, Kobylinski RW, Zatz SL. Increased cholecystectomy rate after the introduction of laparoscopic cholecystectomy. JAMA 1993; 270 (12): 1429-32
3. Vander Velpen G C, Shimi S M, Cuschieri A. Outcome after cholecystectomy for symptomatic gallstone disease and effect of surgical access: laparoscopic v open approach. Gut 1993; 34: 1448-51.
4. Nathanson L K Shimi S, Cuschieri A. Laparoscopic cholecystectomy : the Dundee technique. Br J Surg 1991; 78: 155-9
5. Nathanson L K, Easter D W, Cuschieri A. Ligation of the structures of the cystic pedicle during laparoscopic cholecystectomy. Am J Surg 1991;161 350-4
6. Meyers WC: A prospective analysis of 1,518 laparoscopic cholecystectomies. N Engl J Med 324:1072-1078,1991.
7. Eagle K M, Brudage B H, Chaitman B R et al. Guidelines for perioperative cardiovascular evaluation for noncardiac surgery: report of ACC/AHA Task Force on Practice Guidelines. Circulation 1996; 93: 278-317
8. McLoughlin RF, Gibney RG, Mealy K, et al: Radiological investigation in laparoscopic compared with conventional cholecystectomy an early assessment. Clin Radiol 45:267-270, 1992.
9. Lam C M, Murray F E, Cuschieri A. Increased cholecystectomy rate after the introduction of laparoscopic cholecystectomy in Scotland. Gut 1996; 38: 282-4
10. Zucker KA, Bailey RW, Gadacz TR, et al: laparoscopic guided cholecystectomy. Am J Surg 161:36-42, 1991.

A LARGE SEMINOMA ARISING IN ONE OF BILATERAL UNDESCENDED TESTES: A CASE REPORT

Phuvitoo SUNGTONG, M.D.[1]

ABSTRACT

A large seminoma arising in an undescended testis was diagnosed in a 53-year-old infertile man who had bilateral undescended testes and presented with progressive enlargement of abdominal mass. Plain KUB revealed evidence of a large soft tissue mass without calcification in left-sided and mid lower abdomen. CT scan showed a large left-sided retroperitoneal mass, extending from the level of left renal hilum to the left inguinal canal. On CT scan, hypodense areas and small calcifications inside the seminoma were noted. The right -sided undescended testis was atrophy and was located in the right inguinal canal.

PIG = Par infravaginalis gubernaculi
β-HCG = β-human chorionic gonadotropin

INTRODUCTION

Undescended testis is usually within the inguinal canal but can be anywhere along the path of descent from the retroperitoneum. The two most important complications of undescended testis are infertility and testicular cancer. The most common malignancy of the undescended testes is seminoma. A case presenting with a large retroperitoneal mass that proved to be a seminoma in one of bilateral undescended testes is presented with a review of the radiological features and current literatures.

CASE REPORT

A 53-year-old man presented with progressive enlargement of abdominal mass and weight loss 7 kg in approximately 2 months. He was in good health until this time, and he had not previously undergone surgery. He was HIV negative. He was infertile but had no medical work up.

The initial physical examination revealed body temperature 36.5 °C, BP 120/80 mmHg, pulse rate 80 beats/min, and respiratory rate 22 /min. The patient was cachectic, mild pale, and no jaundice. The heart and lungs appear normal. The abdominal examination revealed a large palpable mass in the left-upper and mid lower abdomen, size approximately 15x20x20 cm. It was not movable and was firm in consistency. The testes were not palpable in the scrotal sac. The rest of physical examination including neurological examination was within normal limits.

Plain KUB revealed a large soft tissue mass in left-sided and mid lower abdomen. The mass had neither calcification nor fat density (Figure 1). Chest radiograph appeared normal.

[1] Phuvitoo Sungtong, MD.
Division of Radiology Hatyai Hospital Songkhla Thailand 90110.
E mail addresses : **phuvitoo@hotmail.com, Phuvitoo@yahoo.com**

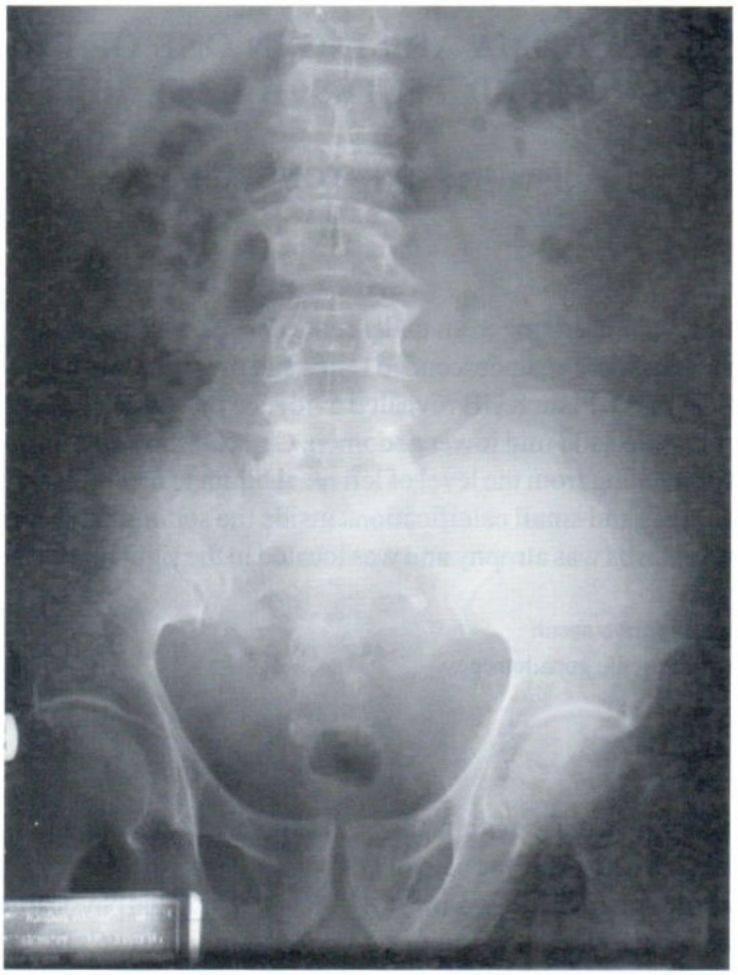

Fig. 1 Plain KUB revealed a large soft tissue mass in left -sided and mid lower abdomen. The mass had neither calcification nor fat density.

Abdominal CT scan showed a large, well circumscribed soft tissue mass extending from deep retroperitoneum space to anterior abdominal wall, left side. Hypodense areas and small calcifications inside the mass were noted. It measured approximately 13x20x22 cm in size. Its most cephalic portion was located at the level of left renal hilum. Its most caudal portion was located in the left inguinal canal. The aorta, IVC, urinary bladder, and sigmoid colon were displaced to the right. The left psoas muscle was compressed. Dilatation of the left pelvio-calyceal system and left proximal ureter was noted. Right kidney appeared normal. An oval-shaped soft tissue mass with central hypodensity was visualized in right inguinal canal, size 1.5x2x2 cm. It was located superomedially to the right inguinal ligament. There was no other right-sided soft tissue mass along the path of testicular descent. Neither ascites nor enlarged lymph node was observed. By CT scan, no evidence of other associated anomaly of the genitourinary system was demonstrated (Figure 2).

The initial tumor markers were measured. The serum level of α-fetoprotein was 2.9 IU/ml (normal value < 4.6 IU/ml) and β-human chorionic gonadotropin (β-HCG) was less than 1.0 mIU/ml.

Fig. 2 Transverse CT scan obtained after administration of oral contrast material.

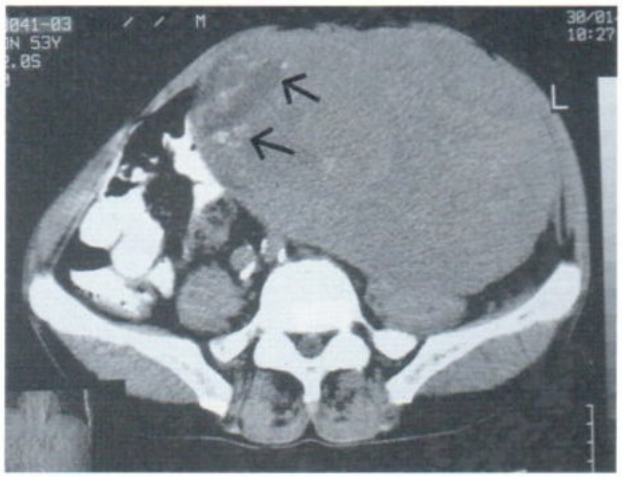

Fig. 2A CT scan obtained before I.V. contrast administration showed a large soft tissue tumor in left-sided retroperitoneum with small calcifications and hypodense areas (arrows).

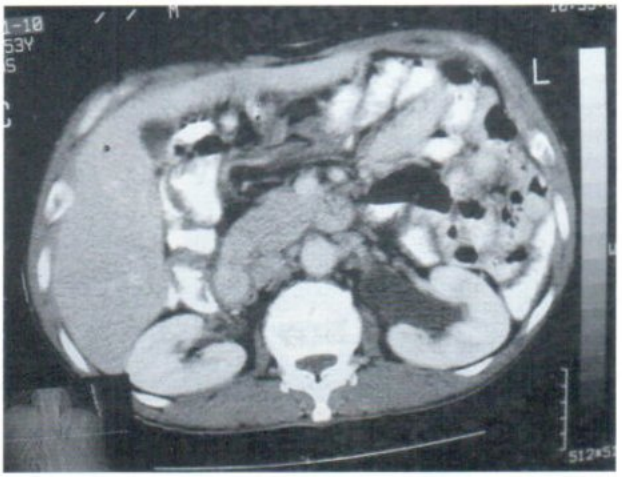

Fig. 2B CT scan obtained after I.V. contrast administration through the level of the kidneys showed hydronephrosis of left kidney.

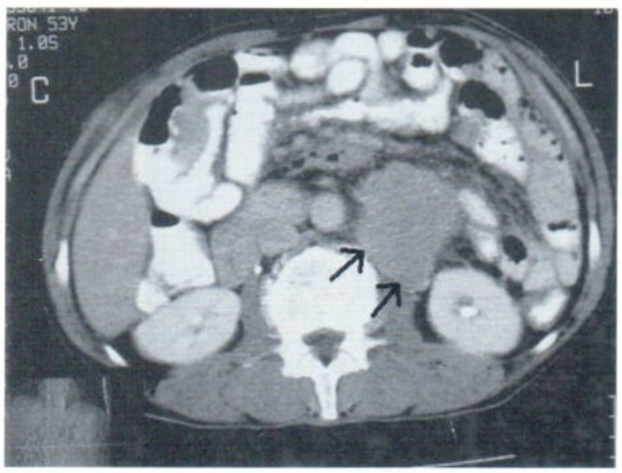

Fig. 2C The CT section caudad to 2B showed a homogeneous retroperitoneal soft tissue mass located between the lower pole of left kidney and aorta (arrows).

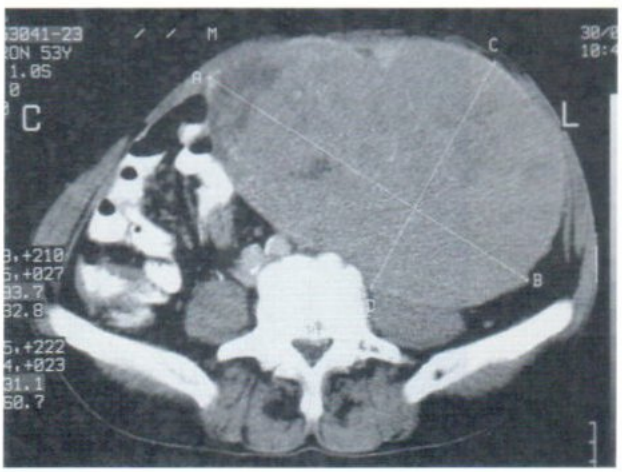

Fig. 2D CT scan post I.V. contrast at the same level of 2A showed that most of the mass enhanced homogeneously except the hypodense areas which could be due to tumor necrosis.

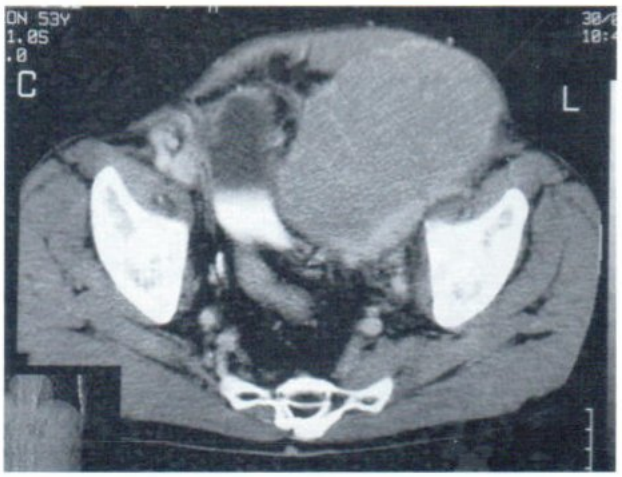

Fig. 2E The mass displaced the urinary bladder and sigmoid colon to the right side.

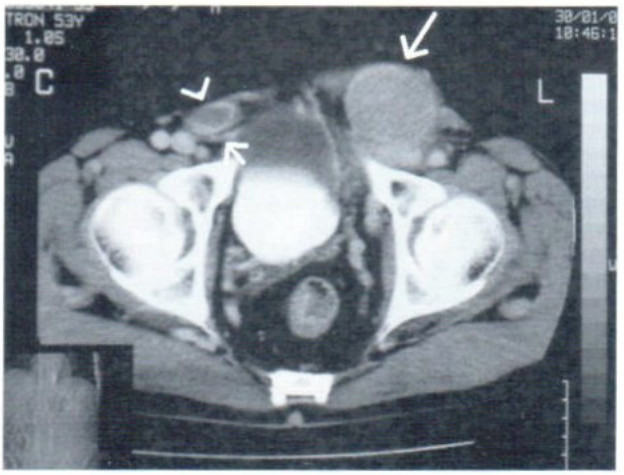

Fig. 2F The tumor extended inferiorly to the left inguinal canal with evidence of left external iliac vein invasion(long arrow). There was a 2 cm mass with central hypodensity in right inguinal canal (arrow head). It was located superomedially to the inguinal ligament (short arrow).

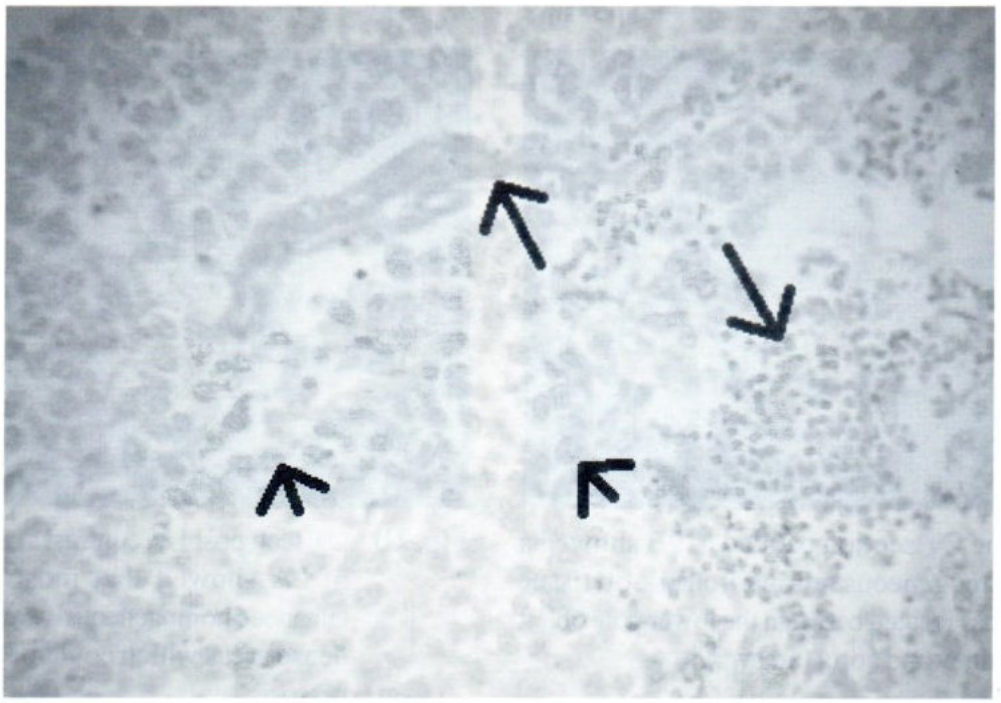

Fig. 3 High-power photomicrograph (Original magnification, x200) revealed lobules of seminoma cells with abundant clear cytoplasm (short arrows) which were separated by fibrous septa that contained numerous lymphocytes (long arrows).

The operation showed a large tumor, measuring 14x17x22 cm. It extended from left renal hilum to the left inguinal canal. The urinary bladder and sigmoid colon were displaced to the right. The left ureter and left external iliac vein were wrapped around by the tumor. External surface was adherent to surrounding tissue. Histological examination of the tumor revealed lobules of seminoma cells with abundant clear cytoplasm. Tumor cells were separated by fibrous septa that contained numerous lymphocytes (Figure 3). The right testis was located in the right inguinal canal near the external inguinal ring. Right orchidectomy was also performed. Histopathology of right testis was atrophic testes.

Seminoma arising in an undescended testis was diagnosed. Postoperative radiotherapy was the additional treatment. Unfortunately, the patient died after incomplete course of radiration due to multiple medical complications.

DISCUSSION AND REVIEW OF LITERATURES

Cryptorchidism results from the abnormal formation and descent of the testes. The testes form from genital ridge, which lie on both sides of the midline and extend from T6 through S2 vertebrae in the developing embryo. Between the 7th and 12th weeks of gestation, the testes contract and become more ovoid as they begin their descent into the pelvis. They remain near the deep inguinal ring until the 7th month of gestation.[1,2] The testes usually descend into the scrotum at approximately 8th month of fetal life.[3-5] About 33% of premature and 3% of full-term male neonates have unilateral undescended testes.[4] It can be bilateral in 10% of patients.[6,7] Most of undescended testes will descend spontaneously around the age of 1 year, but 0.8% of boys continue to have undescended testes. Spontaneous descent after 1 year of age is unlikely.[5]

Factors causing testicular undescended include[1] hormonal factors, especially dihydrotestosterone;[2] the development of the abdominal muscles, which increases the intraabdominal pressure, forcing the testes down (this is the reason that testes are undescended in the absent abdominal muscles syndrome and in some patients with congenital abdominal wall defects;[3] swelling of the gubernaculum, which distends the scrotum and the inguinal canal allows the epididymis, and then the testis, to pass through the inguinal canal.[6]

An incompletely descended testis may be located anywhere from renal hilum to the inguinal canal or along the course of the normal spermatic cord.[8] Sixty-six percent of undescended testes are ectopic (pass through the external ring but not reaching the scrotum), 16% are intracanalicular (within the inguinal canal), 10% are intraabdominal, and 3% are surgically absent.[9]

Because of its association with other urinary tract abnormalities, cryptorchidism is thought to be one manifestation of a generalized defect in genitourinary embryogenesis. Other associated malformations include renal agenesis or ectopias, ureteral duplications, seminal vesical agenesis or cysts, and hypospadias.[10-14]

Undescended testes tend to be more atrophic or dysplastic. They can be associated with significant complications such as cancer, infertility, torsion with infarction, and indirect inguinal hernia.[15-20] Therefore, early diagnosis and management of an undescended testis are required to preserve the patient's fertility and allow early detection of testicular malignancy. Orchiopexy should follow diagnosis of an ectopic testis in a child. Because of the risk of cancer, close observation or surgical removal of the undescended testis is recommended if it is first detected in an adult. Orchiopexy does not prevent the development of cancer; regular self-exmination and medical follow-up are needed.[21]

The pathophysiology of malignant transformation in undescended testes is not completely understood. One hypothesis is that cryptorchidism is not merely incomplete descent of the testis, but that reflects a

generalized defect in embryogenesis and results in bilateral dysgenetic gonads.[14] An embryologic defect in testicular formation is supported by the observation that risk for testicular carcinoma is not limited to the undes- cended testis but extends to the contralateral testis, even if it is normally descended. The defective embryogene- sis hypothesis is further supported by the observation that orchiopexy, even at early age, does not appreciably decrease the risk of developing a tumor.[13]

Malignancy occurs 12-40 times more commonly in the undescended than in the descended testis.[22] The peak age for cancer in undescended testis is similar to that in scrotal testes, generally the third and fourth decades of life. The distribution of histologic types of tumors in undescended testes are similar to that in scrotal testes: pure seminoma, 43% ; embryonal cell carcinoma, 28%; Teratocarcinoma, 27% ; and chorio- carcinoma, 2%.[23] With appropriate management, the prognosis for seminomas arising in undescended testes is similar to that for seminomas arising in scrotal testes, i.e. excellent.[24]

Radiologic methods have been used in the preoperative localization of an undescended testis. The previously available imaging methods, such as testicular arteriography and venography are not only invasive but also technically difficult. They are also associated with high radiation dose and some morbidity.[25,26]

Ultrasonography has been used in the localization of an undescended testis within the inguinal canal but not within the pelvis or abdomen. An undescended testis will appear hypoechoic with ultrasonography. A bright echogenic band inside the testis, the medias- tinum testis must be identified for confident diagnosis. This is necessary because an enlarged lymph node can simulate an undescended testis but lacks this structure.[6] More importantly, agenesis cannot be discriminated from atrophy with US.[6,7]

Computed tomography scanning is easily reproducible and does not depend on operator skill. Detection of an undescended testis by CT is based upon the recognition of a mass, which is of soft tissue density and is oval in shape, along the expected course of testicular descending. In the inguinal area and lower pelvis where normal structures are usually bilaterally symmetrical, an extra soft tissue mass, even as small as 1 cm, can be detected. Higher in the pelvis or lower abdomen where bowel loops, vascular structures, and lymph nodes are more abundant, detection of such an atrophic testis and differentiation from adjacent structures may be more difficult. In young children, examination of the abdomen and upper pelvic struc- tures by CT may also be difficult due to lack of body fat.[8] CT cannot show the mediastinum testis and also lacks the specificity and sensitivity that are needed to diagnose agenesis.[14,27]

Magnetic resonance imaging has advantage of improved soft tissue contrast and can be used to detect undescended testis in both transaxial and coronal planes, but reports have varied as to its usefulness. [28,29] On MR imaging, the testis is typically of low signal on T1-weighted and of high signal on T2-weighted images. Undescended testes that are atrophic may not be of high intensity on T2-weighted scans.[27] The mediastinum testis is a band along the posterior margin of the testis. It is hypointense relative to the testicular parenchyma in both T1-weighted and T2 -weighted images.[30] The results of a study by Lam et al[31] showed that gadolinium-enhanced MR veno- graphy performed in conjunction with routine pelvic MR imaging increased sensitivity for differentiation of agenesis from ectopia.

There is an important potential pitfall that can cause confusion with the undescended testis. The par infravaginalis gubernaculi (PIG) can be similar to the undescended testis on any imaging study. It is a distal bulbous segment of the gubernaculum which is a cordlike structure that extends from the lower end of the testis to the scrotum and guides the testis in its descent. In early fetal development, the gubernaculum is soft and jellylike. When descent is completed, the

gubernaculum and par infravaginalis gubernaculi normally atrophy. If the testis fails to descend to the scrotum, the gubernaculum frequently persists as a fibrotic rather than gelatinous remnant. The PIG is always located distal to the undescended testis, usually in the scrotum but sometimes craniad to the scrotum. It is the latter case that the PIG and undescended testis may be confused. More importantly, cases with the PIG in the high scrotum or in the inguinal canal with surgically absent of the testes had been reported.[27]

Sonographically, the PIG appears as a hypoechoic mass with a cordlike structure of similar echogenicity led into it. The mediastinum testis, which can be identified in the normally descended and in some undescended testes, is absent in the PIG.[27]

The CT appearance of the gubernaculum and PIG is indistinguishable from that of the spermatic cord and testis. In the patient in whom the PIG is present distal to a normal testis, CT identifies two structures, allowing the correct diagnosis. Therefore, if scanning is started at the scrotum, it is important to continue to the renal hila, because the initial structure identified could be the PIG.[27]

On MR imaging, the PIG appears as a mass, which is isointesnse on T1-weighted and hypointense relative to the normal testis on T2-weighted images. These findings could not be reliably distinguished from an atrophic ectopic testis. The spermatic cord leading to the testis and gubernaculum leading to the PIG have identical properties on MR imaging. The mediastinum testis, which sometimes can be seen on MR studies, is the only finding that clearly identifies a structure as a testis.[27]

Diagnosing malignancy in an undescended testis can be difficult. The clinical presentation varies considerably and, when the tumor is in certain locations, often includes secondary symptoms from mass effect. Most commonly, patients seek medical attention for symptoms simulating appendicitis or retroperitoneal mass, urinary frequency or dysuria from mass effect on the bladder, or acute abdominal pain from tortion of the malignant growth.[20]

Tumor markers have a well-established role in the diagnosis of germ cell tumors. The two most clinically useful tumor markers are α-fetoprotein and β-human chorionic gonadotropin (**β-HCG**). α-fetoprotein is a protein produced early in gestation by the fetal liver, gastrointestinal tract, and yolk sac. It is a marker for hepatocellular carcinoma and germ cell tumors (nonseminoma with yolk sac elements). **β-HCG** is a glycoprotein produced by syncytiotrophoblasts of the developing placenta during pregnancy. Its level is elevated in tumors containing the syncytiotrophoblasts such as gestational trophoblastic disease and germ cell tumors, especially teratocarcinomas and choriocarcinomas. Both α-fetoprotein and β-human chorionic gonadotropin play crucial roles in the management of patients with nonseminomatous germ cell tumors. α-fetoprotein or **β-HCG** is elevated in 85% of nonseminomatous tumors. α-fetoprotein does not elevate in seminoma and dysgerminoma. **β-HCG** is occasionally elevated in seminoma and dysgerminoma.[30,32] These two tumor markers were not elevated in this reported case of seminomatous carcinoma.

The imaging findings of cancerous intraabdominal testes have not been well described. Sonography has been advocated to detect malignancy in undescended testes. It can be a solid slightly heterogeneous echoic mass anywhere along the path of descent from renal hilum to the inguinal canal. On CT examination, it can be a well circumscribed, homogeneous soft-tissue density mass without obvious evidence of necrosis or calcification.[20] However, areas of necrosis and small calcifications in a seminoma arising in the intraabdominal testes were also reported.[14,18] MR findings can show the mass as isointense to muscle on T1-weighted images, of relatively high signal intensity on T2-weighted and short inversion time inversion recovery images, and markedly enhanced on T1-weighted images after I.V. gadolinium

administration.[20]

The seminoma of this reported case is a large retroperitoneal mass, extending from the left renal hilum to the inguinal canal. It is located between the aorta and left psoas muscle. It is a well circumscribed mass with CT evidence of small calcifications and hypodense areas, which possible to be necrotic areas. No adjacent enlarged lymph node is noted. Although the differential diagnosis of a retroperitoneal mass might have included retroperitoneal fibrosis, lymphoma, metastatic adenopathy, paraganglioma, liposarcoma, leiomyosarcoma, and malignant fibrous histiocytoma. None of the previously mentioned diagnoses could reveal as a large mass extending from renal hilum to the ipsilateral inguinal canal. The only clue that makes the most likely diagnosis carcinoma arising in an undescended testis is a single mass locating within the nearly entire path of testicular descent.

Therefore, when a retroperitoneal or pelvic mass is detected in a male patient, tumor arising in an undescended testis might be included in the differential diagnosis. The helpful information is history taking about the lack of a testis in the scrotum. Past history of infertility is also helpful in the diagnosis, in a patient with bilateral undescended testes. Tumor markers may useful in the diagnosis of nonseminomatous germ cell tumors but they show no benefit in seminoma.

A small mass with central hypodensity in the right groin of this patient was detected by CT scan. This mass was located in the right inguinal canal, just proximal to the external inguinal ring (Fig 3F). It can be distinguished from an enlarged lymph node because an enlarged groin lymph node is located inferolateral to the inguinal ligament or adjacent to the femoral and iliac vessels.[33]

The differential diagnosis of a right-sided inguinal canal mass in this patient might have included atrophic testis and par infravaginalis gubernaculi. These two conditions cannot be distinguished by imaging. Although, there is no soft tissue mass in the more craniad sections along the path of right testicular descent, the PIG is still possible, because this may be due to small atrophic right testis which could not be demonstrated by imaging or due to agenesis of right testis.

CONCLUSION

An undescended testis can be found any where along the path of testicular descent from renal hilum to the upper part of scrotum. Atrophic undescended testis has similar radiologic features with the par infravaginalis gubernaculi. An important CT feature of a seminoma arising in an undescended testis is a retroperitoneal or pelvic soft tissue mass with or without internal calcifications and necrotic areas.

ACKNOWLEDGEMENT

Thanks to Dr. Lek Charoenkijkajorn for assistance with the photomicrography of the pathological specimen.

REFERENCES

1. Lasen WJ. Human embryology. New York, NY: Churchill Livingstone, 1993; 235-280.
2. Moore KL, Persaud TV. The developnig human: Clinically oriented embryology. 5th ed. Philadelphia, Pa: Saunders, 1993; 281-303.
3. Cooper ERA. History of retrained testis in the human subject at different ages and its comparison with scrotal testis. J Anat 1929; 64: 5-27.
4. Kogan SJ. Cryptorchidism. In: Kelalis PP, King LR, Gelman AB, eds. Clinical pediatric urology. 2nd ed. Philadelphia: Saunders, 1985; 864-887.

5. Scorer CG, farrington GH. Congenital anomalies of the testes: cryptorchidism, testicular tortion, and inguinal hernia and hydrocele. In: Harrison WS, Gittes RJ, Perlmutter AD, eds. Campbell's urology. 4th ed. Vol 2. Philadelphia: Saunders, 1978; 1549-1565.
6. Friedland GW, Chang P. The role of imaging in the management of the impalpable undescended testis. AJR Am J Roentgenol 1988; 151: 1107-1111.
7. Frush DP, Sheldon CA. Diagnostic imaging for pediatric scrotal disorders. Radiographics 1998; 18:51-53.
8. Lee JKT, McClennan B, Stamley RJ, Sagel SS. Utility of computed tomography in the localization of the undescended testis. Radiology 1980; 135: 121-125.
9. Moul JW, Belman AB. A review of surgical treatment of undescended testes with emphasis on anatomic position. J Urol 1988; 140: 125-128.
10. Pappis CH, Argianas SA, Bousgas D, Athanasiades E. Unsuspected urological anomalies in asymtomatic cryptorchid boys. Pediatr Radiol 1988; 18:51-53.
11. Schlegel PN, Shin D, Goldstein M. Urogenital anomalies in men with congenital absence of the vas deferens. J Urol 1996; 155: 1644-1648.
12. Flageat J, Vicens JL, Metges PJ. Seminoma on ectopic testis associated with renal agenesis. J Radiol 1982; 63: 763-765.
13. Ulbright TM, Amin MB, Young RH. Tumors of the testis, adnexa, spermatic cord, and scrotum. Atlas of tumor pathology, fasc 25, ser 3. Washington, DC: Armed Forces Institute of pathology, 1999, 1-290.
14. Woodward PJ. Seminoma in an undescended testis. Radiology 2004; 231: 388-392.
15. Fonkalsrud EW, Mengel W, eds. The undescended testis. Chicago: Year book Medical, 1981.
16. Allan WR, Brown RB. Torsion of the testis: a review of 58 cases. Br Med J 1966; 1: 1396-1397.
17. Wilbur AC, Mostowfi K. Heydemann J Daza RC. Infarcted undescended testis appearing as a calcified abdominal mass in an adult. AJR 1990; 155: 547-548.
18. Pak K, Sakaguchi N, Takeuchi H, Tomoyoshi T. Computed tomography of carcinoma of the intraabdominal testis: A case report. J Urol 1981; 125: 253-254.
19. Dosimo SG, Silver RI, Cromie W. The undescended testicle: diagnosis and management. Am Fam Physician 2000; 62: 2037-2044.
20. Miller FH, Whiteney WS, Fitzgerald SW, Miller EI. Seminomas complicating undescended intraabdominal testes in patients with prior negative findings from surgical exploration. AJR Am J Roentgenol 1999; 172: 425-428.
21. Fonkalsrud EW. Current management of the undescended testis. Semin Pediatr Surg 1996; 5: 2-7.
22. Pinch L, Aceto T Jr, Meyer-Bahlburg HFL. Cryptorchidism: A pediatric review. Urol Clin North Am 1974; 1: 573-592.
23. Batata MA, Whitmore WF Jr, Chu FCH, et al. Cryptorchidism and testicular cancer J Urol 1980; 124: 382-387.
24. Gauwitz MD, Zagars GK. Treatment of seminoma arising in cryptorchid testes. Int J Radiat Oncol Biol Phys 1992; 24: 153-159.
25. Diamond AB, Meng CH, Kodroff M. Testicular venography in the nonpalpable testis. Am J Roentgenol 1977; 129: 71-75.
26. Jacobs JB. Selective gonadal venography. Radiology 1969; 92: 885-888.
27. Rosenfield AT, Blair DN, McCarthy S, Glickman MG, Rosenfield NS, Weiss R. Society of Uroradiology Award paper: The pars infravaginalis gubernaculi: importance in the identification of the undescended testis. AJR Am J Roentgenol 1989; 153:775-778.

28. Kier R, McCarthy S, Rosenfield AT, Rosenfield NS, Rapoport S, Weiss RM. Nonpalpable testes in young boys: evaluation with MR imaging. Radiology 1988; 169:429-433.
29. Fritzsche PJ, Hricak H, Kogan BA, Winkler ML, Tanagho EA. Undescended testis: value of MR imaging. Radiology 1987; 164: 169-173.
30. Woodward PJ, Sohaey R, O'Donoghue MJ, Green DE. Tumors and tumorlike lesions of the testis : Radiologic-pathologic correlation. Ragiographic 2002; 22: 189-216.
31. Lam WW, Tam PK, Ai VH, Chan KL, Chan FL, Leong L. Using gadolinium-infusion MR venography to show the impalpable testis in pediatric patients. AJR Am J Roentgenol 2001; 176:1221-1226.
32. Johnson PJ. The role of serum alpha-fetoprotein estimation in the diagnosis and management of hepatocellular carcinoma. Clin Liver disease 2001; 5: 145-159.
33. Clair LS, Stefan BJH, Rosalind BD. Imaging of groin masses : Inguinal anatomy and pathologic conditions revisited. Radiographic 2001; 21:261-271.

A COMPARISON OF BONE SPECT IMAGE QUALITIES OBTAINED FROM OSEM AND FBP ALGORITHMS

Chiraporn TOCHAROENCHAI[1] PhD (Biomedical Engineering),
Surachai NGAMRATANAPAIBOON[2] ME (Biomedical Engineering),
Chulaluk KOMOLTRI DrPH (Biostatistics)[3]

ABSTRACT

The aim of the study was to compare the image qualities of bone SPECT obtained from ordered subset expectation maximization (OSEM) and filtered-backprojection (FBP) image reconstruction algorithms for bone SPECT imaging. This study was divided into two parts; the optimal numbers of subset and iteration of OSEM using a Zubal brain phantom were firstly determined. The projection datasets of the phantom were generated with 128x128 matrix sizes and 120 views over 360 degrees. Poisson noise and collimator-detector blur were added to the projection data for simulating the clinical condition. Then OSEM image reconstruction was performed with various numbers of subset and iteration. The minimum mean square error (MSE) was used as an index of the optimal parameter. The second part was to evaluate the image qualities of bone SPECT images obtained from OSEM compared to that from FBP. Thirty-two patients with lower back pain requested for bone SPECT imaging were used. A pilot study was conducted to find the preferable algorithm using a preference study. Two nuclear medicine physicians with experiences in bone SPECT images were participated. The frequencies of the scores and the agreement between readers were investigated. The results showed that the combination of the 6th subset and 2nd iteration gave the minimum MSE and less time-consuming. For preference study, two readers preferred OSEM to FBP with the agreement of 65.6%. In conclusion, the optimal numbers of subset and iteration of OSEM were 6 and 2 respectively. The OSEM algorithm gave better image quality of bone SPECT than FBP.

Key Words: OSEM, iterative method, image quality, Bone SPECT

INTRODUCTION

In nuclear medicine, single photon emission tomography (SPECT) is performed to obtain tomographic images. SPECT camera(s) has to rotate around the patient and the pictures of radioactivity distribution inside the patient are taken at different angles. The procedure, called image reconstruction, is done afterward by mathematically putting all the pictures together to obtain SPECT images. Two methods of image reconstruction; analytical and iterative, are commonly used in nuclear medicine. The most popular algorithm of analytical method is filtered backprojection (FBP) which is fast but its streak artifacts is a drawback, especially when a small region of interest contains high activity.[1,2] Iterative

[1] Department of Radiological Technology, Faculty of Medical Technology, Mahidol University.
[2] Biomedical Engineering Program, Faculty of Engneering, Mahidol University
[3] The Department of Research and Development, Faculty of medicine Siriraj Hospital, Mahidol University.

image reconstruction has been becoming popular for many reasons. Firstly, image noise is easily modeled and handled, especially low count imaging. Secondly, poor spatial resolution due to depth-dependant blurring can be recovered. Thirdly, the quantitative capability can be improved because of easily incorporating a model of the physical factors influencing the absolute quantitation, such as photon attenuation and scatter in organs. The ordered-subset expectation maximization (OSEM) algorithm is one of the most popular iterative methods because it produces better image quality than that of FBP. It also shortens the reconstruction time compared with other iterative algorithms.[3-5]

In nuclear medicine, bone SPECT imaging is useful because it provides three-dimensional data resulting in improving image contrast and the location of abnormal lesions. Moreover, the accurate sites of abnormalities may help to differentiate between degenerative bone and bone metastases leading the appropriate treatments. The image quality obtained from FBP is mostly poor due to streak artifacts. Therefore, to improve the image quality of bone SPECT is of interest. The aim of this study was to compare the image qualities of bone SPECT images obtained from OSEM and FBP algorithms.

MATERIALS AND METHODS

This study was divided into two parts, the first part was to determine the optimal numbers of subset and iteration of OSEM algorithm. The second one was a pilot study to compare the image qualities between images obtained from OSEM and FBP using a preference study.

Determination of the optimal numbers of subset and iteration of OSEM algorithm

Anthropomorphic Phantom

A Zubal brain phantom[6] was used to mimic a human brain. This phantom allows users to flexibly assign the activities in the brain. In this study we experimented the activities that gave the projection data similar to the patients' data. Then the emission data of the phantom was created as shown in Fig.1.

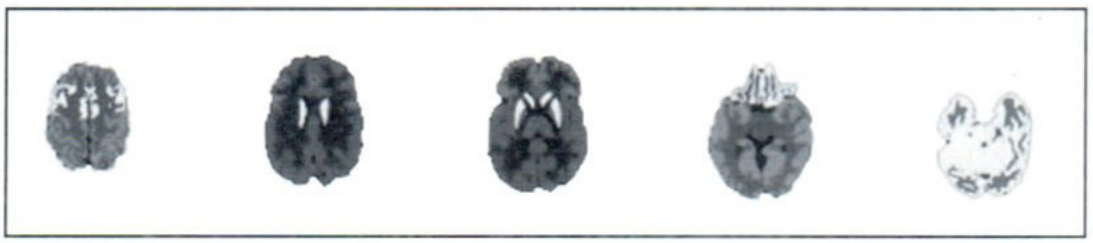

Fig. 1 A Zubal brain phantom (emission data) at different slices.

The 128x128 matrix size with 120 views of projection data of the phantom were generated. Poisson noise and collimator-detector blur (with 5 pixels width of gaussian distribution) were added to projection data for making noisy data similar to clinical studies. Then OSEM image reconstruction was performed with various numbers of subset and iteration. The number of subset ranged from 2 to 30 with the increment of 2 and the number of iteration ranged from 1 to 20 with the increment of 1 were used. No compensations for image degrading factors such as attenuation, detector response, or scatter, were applied. Fig 2 showed the reconstructed images of the brain phantom obtained from OSEM using 6 subsets and different numbers of iteration. The image reconstruction software was developed using Interactive data language (IDL) version 5 on window platform. It consumed less than 3.25 sec/slice for image reconstruction using OSEM.

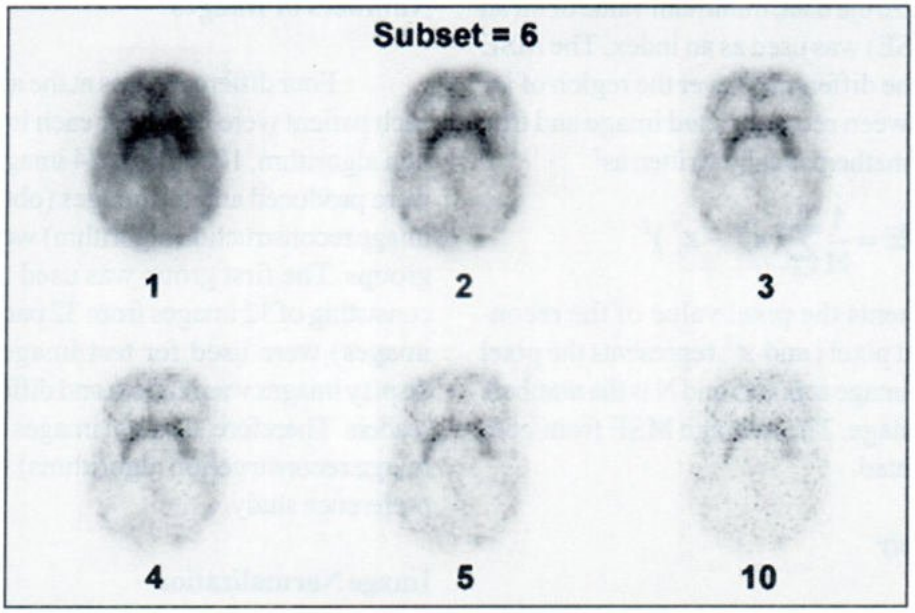

Fig. 2 The reconstructed images of the brain phantom using OSEM algorithm using 6 subsets with different numbers of iteration.

Data Analysis

A reconstructed image of each condition was analyzed. Two 5x5 pixel ROIs were drawn over the image (one for the left and one for the right) as shown in Fig 3. The pixel count within each ROI was recorded and then the average pixel count was calculated. Similarly, the average pixel count of true image was determined.

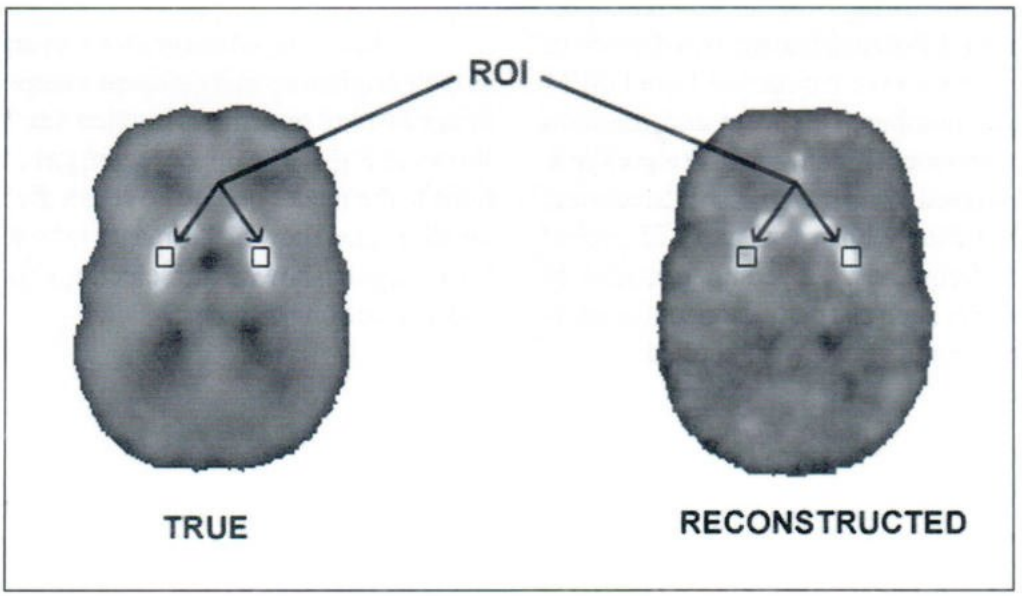

Fig. 3 The ROIs over the OSEM reconstructed and true images.

To analyze the data, minimum value of mean square error (MSE) was used as an index. The MSE was defined as the differences over the region of interest (ROI) between reconstructed image and true image. It can be mathematically written as[7]

$$MSE = \frac{1}{N}\sum_{i=1}^{N}(x_i^R - x_i^T)^2$$

where x_i^R represents the pixel value of the reconstructed image at pixel i and x_i^T represents the pixel value of the true image at pixel i and N is the numbers of pixel in the image. The average MSE from both sides was calculated.

Preference Study

In this part, a comparison between the image qualities obtained from OSEM and FBP algorithms were conducted. Due to the limitation in recruiting nuclear medicine physician, a preference study was performed instead of an human observer study.

Data Acquisition and Processing

Thirty-two patients with lower back pain and underwent bone SPECT imaging at Division of Nuclear Medicine, Department of Radiology, Faculty of Medicine Siriraj Hospital were retrospectively investigated. For each patient, two datasets of reconstructed images were obtained from OSEM (using optimal numbers of subset and iteration obtained from previous section) and FBP algorithms. All the reconstructed images were post-filtered using 2D Butterworth filter with order 5 and 0.25 cycles/pixel cut-off frequency. No compensations of degrading factors such as attenuation, collimator-detector response and scatter were applied.

Numbers of Images

Four different slices at the areas of suspect of each patient were used. For each image reconstruction algorithm, 128 images (4 images x 32 patients) were produced and the images (obtained from each image reconstruction algorithm) were divided into 2 groups. The first group was used for a training set consisting of 32 images from 32 patient. The rest (96 images) were used for test images. The order of display images was random and different for different readers. Therefore, the total images of 256 (from two image reconstruction algorithms) were used in this preference study.

Image Normalization

For maximizing the image contrast on the monitor display using a 256-level grayscale, all reconstructed images were normalized such that the pixel values of the display images ranged from 0 to 255. In normalization scheme, the maximum count in the image was determined and then scaled to 255. Negative values in the image will be normalized to zero.

Image Display

The displayed images were enlarged as twice as their original sizes by bilinear interpolation. The image display screen was divided into 3 regions as shown in Fig 4. The upper region gave the instructions to the reader on how to select the image. The middle region showed the images to be selected. The lower region showed the selections for readers to make by clicking on them.

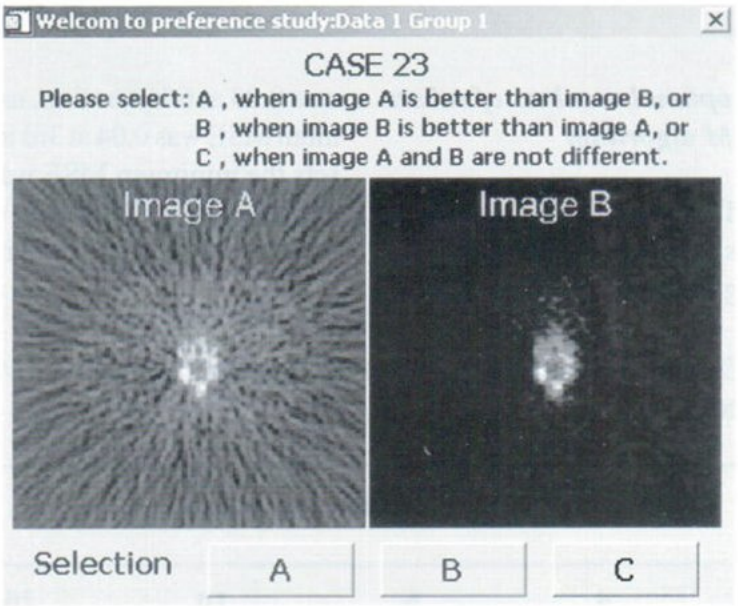

Fig. 4 Image display format used in the preference study. The instruction on how to select the image is shown in the upper part, The test images are displayed in the middle and the lower part shows the options to be selected.

Readers

Two readers were participated in this study. They are nuclear medicine physicians and familiar to bone SPECT images for more than 3 years.

Reader's Task

The readers were given full training in the preference study at the beginning to acquaint them. They were asked to carefully read the instruction of the study and were shown a demonstration of how to select the images. The readers were not told the details of the test condition of the images to avoid bias that might affect the results. Due to reader fatigue and time-consuming used for single session in the preference study, the 96 test images were split into 3 blocks and each block consisted of 32 different images (one image from each patient). The order of images was random. The readers were told to take their times and they could have a short break between each block of images. Two images of the same patient with different image reconstruction algorithms were displayed at the same time. The task of a reader was to select the best image quality which gave the best localization of hot lesion. Without streak artifacts was another criterion if both images were not different in localization. There were three options for readers to select. The reader was asked to select one of the three options; "A" represented the superiority of image A to image B and "B" represented the superiority of image B to image A. If the image qualities of both images were not different, the reader was asked to click "C".

Data Analysis

The frequencies of the scores obtained from each reader were determined. Individual preference was also evaluated and the agreement between readers was studied.

RESULTS

Determination of the optimal numbers of subset and iteration of OSEM algorithm

Table 1 showed the average MSEs obtained from different numbers of subset and iteration. The results showed that using 2 subsets the minimum MSE was 0.03 at 6th iteration, using 4 subsets the minimum MSE was 0.04 at 3rd iteration and using 6 subsets the minimum MSE was 0.01 at 2nd iteration. When using 10, 20 and 30 subsets the MSEs were increased as the number of iteration increased.

Table 1. Average MSEs at different numbers of subset and iteration. The minimum MSE of each combination was underlined.

Iteration Number	Number of Subset					
	2	4	6	10	20	30
1	22.90	7.35	2.34	0.25	0.80	0.88
2	7.35	0.80	0.01	0.25	0.95	0.51
3	2.48	0.04	0.20	0.50	1.13	0.51
4	0.78	0.13	0.42	0.61	1.35	0.83
5	0.19	0.32	0.55	0.70	1.55	0.93
6	0.03	0.45	0.62	0.77	1.72	0.99
7	0.05	0.55	0.68	0.85	1.86	1.03
8	0.14	0.62	0.72	0.91	1.96	1.07
9	0.24	0.66	0.77	0.98	2.06	1.10
10	0.33	0.71	0.81	1.04	2.15	1.13
11	0.41	0.75	0.86	1.10	2.23	1.16
12	0.48	0.79	0.89	1.15	2.29	1.20
13	0.53	0.83	0.94	1.19	2.35	1.22
14	0.57	0.86	0.98	1.24	2.38	1.24
15	0.61	0.90	1.03	1.28	2.43	1.27
16	0.64	0.93	1.06	1.31	2.48	1.30
17	0.67	0.97	1.10	1.35	2.51	1.32
18	0.68	1.00	1.14	1.39	2.56	1.34
19	0.71	1.04	1.18	1.41	2.60	1.37
20	0.73	1.07	1.21	1.44	2.63	1.38
21	0.74	1.12	1.16	1.44	2.50	1.60
22	0.77	1.16	1.22	1.48	2.60	1.63
23	0.78	1.19	1.26	1.50	2.69	1.80
24	0.80	1.14	1.30	1.67	2.95	1.85
25	0.82	1.17	1.25	1.71	2.89	1.87
26	0.79	1.21	1.26	1.73	2.96	1.89
27	0.77	1.15	1.35	1.76	3.03	1.92
28	0.78	1.15	1.38	1.79	3.10	1.88
29	0.80	1.19	1.41	1.85	3.03	2.03
30	0.82	1.13	1.44	1.87	3.10	2.53

Preference Study

Table 2 reported the frequencies of the scored from two readers. The results showed that reader 1 preferred image B (OSEM algorithm) to image A (FBP algorithm) with 65.6% (63 of 96 images) and image A to image B with 18.8% (18 of 96 images). There was no difference between image A and B with 15.6% (15 of 96 images). While reader 2 absolutely preferred image B to image A with 100%.

Table 2 Frequencies of scores from a preference study

	Score		
Number of Reader	**Image A better than Image B**	**Image B better than Image A**	**Image A equal to Image B**
1	18 images (18.8%)	63 images (65.6%)	15 images (15.6%)
2	none	96 images (100%)	none

DISCUSSION AND CONCLUSION

In this study, we found that using Zubal brain phantom the numbers of subset and iteration that gave small MSEs were 2 subsets with 6 iterations (0.03), 4 subsets with 3 iterations (0.04) and 6 subsets with 2 iteartions (0.01). Those three MSEs from three combination sets were quite similar and actually the numbers of image updates were the same (12 updates). Then we studied the computational time for each set and we found that 2 subsets with 6 iterations consumed 1.42 sec/slice, 4 subsets with 3 iterations consumed 0.73 sec/slice and 6 subsets with 2 iterations consumed 0.503 sec/slice. Therefore, the combination of 6 subsets and 2 iterations was optimal because it gave minimal MSE and less computational time. Although this number obtained from a Zubal brain phantom but it could be used as a guideline for any SPECT imaging. We implemented this number for bone SPECT imaging to compare the image qualities between OSEM and FBP algorithms. And we found that there were differences between two readers. Reader 1 undoubtedly preferred OSEM with 65.6%; however for large hot lesions these two algorithms provided similar information (with 15.6%). The performances of these two algorithms were not different with 18.8% because the reader was doubted with the image quality of OSEM even though it was superior. That means the numbers of training images are not sufficient for readers to get familiar to OSEM images. For reader 2 there was no doubted that the image quality obtained from OSEM was superior to that from FBP. Therefore, the agreement between these two readers was 65.6%. Although this study cannot recruit as many physicians as it should be, the numbers of test images are sufficient to conduct the study. However, more patient data and more readers will minimize the error and make a reliable result. Moreover, this study agrees with the superiority of OSEM to FBP algorithms and shows the optimal parameters of OSEM algorithm to be used.

In conclusion, the optimal numbers of subset and iteration of OSEM are 6 and 2 respectively. The image quality obtained from OSEM is superior to that from FBP in hot lesion localization and without streak artifacts.

ACKNOWLEDGEMENTS

The author would like to thank the Faculty of Medical Technology for supporting IDL software and the Division of Nuclear Medicine, Department of Radiology, Faculty of Medicine Siriraj Hospital for patients' data. The author also would like to thank generous readers for their co-operations and the Medical Imaging Research Group (MIRL) at the University of North Carolina, USA for the softwares.

REFERENCES

1. Philippe P. Bruyant, Jacques Sau, and Jean -Jacques Mallet. Streak Artifact Reduction in FilteredBackprojection Using a Level Line -Based Interpolation Method. J Nucl Med 2000; 41:1913-1919
2. Didier Blocklet, Alain Seret, Niculaie Popa and Andre? Schoutens. Maximum-Likelihood Reconstruction with Ordered Subsets in Bone SPECT. J Nucl Med 1999; 40:1978-1984
3. Hudson HM, Larkin RS. Accelerated image reconstruction using ordered subsets of projection data. I-EEE Trans Med Imaging. 1994; 13:601-609.
4. G.L. Zeng. Image reconstruction-a tutorial. Computerized Medical Imaging and Graphics 25 (2001) 97-103.
5 David S. Lalush and Benjamin M. W. Tsui. Performance of Ordered-Subset Reconstruction Algorithms Under Conditions of Extreme Attenuation and Truncation in Myocardial SPECT. J Nucl Med 2000; 41:737-744
6. http://noodle.med.yale.edu
7. Cliff X. Wang, Wesley E. Snyder, Griff Bilbro, Pete Santago. Performance evaluation of filtered backprojection reconstruction and iterative reconstruction methods for PET images. Computer in Biology and Medicine 1998 ;28: 13-25.